9. PRIMARY AND SECONDARY $PM_{2.5}$ SOURCE CONTRIBUTIONS

This section addresses Objective 3, the apportionment of secondary sulfate, secondary nitrate, and suspended dust aerosol to their primary emitters. Three independent approaches are taken to this apportionment.

Transport simulations integrate the NFRAQS meteorological measurements to determine the transport and dispersion of SO_2 and its reaction products. These simulations were not intended to precisely reproduce the measured sulfur concentrations, though comparisons were made between simulated and measured concentrations to evaluate the simulations (Fujita et al., 1998). They were intended to approximate the relative contributions from large point sources with emissions aloft and from surface sources to the ambient concentrations of SO_2 and its reaction products at the Welby, Brighton, Evans, and CAMP receptors. These simulations identified the largest potential contributors to sulfur arriving at these sites, contributors that were of moderate importance, and sources that probably contributed little to sulfur concentrations at the receptors.

The CMB simulation applied in Section 7 to the apportionment of carbonaceous particles was also applied to $PM_{2.5}$ mass, sulfur dioxide, and oxides of nitrogen. While the $PM_{2.5}$ apportionments are quantitative, within stated uncertainty intervals, the gas apportionments are not. Owing to different deposition and transformation rates during transport, the ratios of SO_2 and NO_x to $PM_{2.5}$ change by the time they reach the receptors. These gas apportionments indicate how much of these gases could have arrived at the receptors along with the primary particles, within large propagated uncertainty intervals.

Finally, diurnal cycles of carbon monoxide, elemental carbon, sulfur dioxide, sulfate, nitrogen oxides, and nitrate are examined. These cycles indicate which pollutant concentrations are most closely linked to the morning and evening rush hour traffic and which appear to be linked to the maximum in vertical mixing that occurs during midday. Also, the relative amounts of nitrogen and sulfur species in the atmosphere are compared with the relative amounts in the emissions of surface and major point sources. It is found that the atmosphere does not contain the amount of sulfur that would have to be there if the major elevated point sources made more than minor contributions to ambient NO_x and its reaction products.

The analyses in this section rank the major sources of SO_2 according to their contribution to ambient sulfur species at the receptor sites and place an upper limit on the contribution of the major elevated point sources to nitrate concentrations. These analyses do not quantitatively apportion secondary ammonium sulfate and secondary ammonium nitrate directly to sources of precursor gases. As explained in Section 8, these secondary particle compounds are formed in the atmosphere and markers were not measured that indicate specific origins of their SO_2 and NO_x precursors.

9.1 Emissions Transport from Surface and Elevated Sources

Transport simulations were undertaken to integrate the large quantities of meteorological and emissions data acquired during the NFRAQS Winter 97 intensive operation period. Details on simulation methods are described by Fujita et al. (1998). These simulations were completed for the 01/12/97 to 01/21/97 and 01/27/97 to 01/31/97 episodes to determine the times and places that sulfur dioxide from large elevated point sources and surface emitter sources might arrive at receptors in the NFRAQS domain. Simulated SO_2 concentrations were compared with monitoring data at the CAMP, Welby, Brighton, and Evans sites at which hourly concentrations were measured. Simulated transport was evaluated by comparing results from a grid and a puff simulation and by meteorological analysis of portions of the episodes.

9.1.1 Simulation Methods

Transport did not include chemical reactions, so the calculated SO_2 concentrations provide an estimate of the combined concentrations of sulfur dioxide and its reaction product, ammonium sulfate. The quantitative data presented later in this section show that the Cherokee coal-fired power station and surface sources made large contributions to ambient sulfur concentrations. The Valmont, Arapahoe, and Trigen coal-fired power stations, and the Diamond Shamrock and Conoco refineries were minor sulfur contributors, and the Rawhide and Pawnee coal-fired power stations were negligible sulfur contributors to NFRAQS receptors during the simulated episodes. Fujita et al. (1998) describe how the transport simulations were carried out and the extent to which they estimated measured concentrations. These simulations were found to qualitatively estimate the movement of pollutants between source and receptor, but their results do not always correspond with measured ambient sulfur concentrations at a given time and location.

Gridded, hourly wind fields were calculated for the NFRAQS domain shown in Figure 2.1-3. This domain extends 220 km (137 mi) from the Wyoming border on the north to the Palmer Divide on the south, and 312 km (194 mi) from the crest of the Front Range on the west nearly to the Nebraska border on the east. The grid cells were 4 by 4 km, and there were 26 vertical levels. The first vertical cell thickness was 20 m agl and the second was 30 m. Above that, a vertical cell thickness of 50 m was used to a height of 1 km, 250 m cells were used between 1 and 2 km, and the top cell had a thickness of 800 m. The top of the wind field grid had a height of 2800 m (9186 ft) agl, which is above the height of the Northern Front Range. The wind field calculation method combined interpolation between measurements with the superposition of terrain effects. Examples of terrain effects considered include blocking of flows by elevated terrain and upslope or downslope flows generated by surface heating or cooling, respectively.

Wind fields were evaluated by: 1) viewing computer displays in which vectors representing measured surface winds were superimposed on a grid of vectors representing the calculated surface winds; and 2) qualitatively comparing calculated winds aloft with time-lapse video images of plume motion to see if the direction of transport and phenomena such as slope flows and flow reversals were properly simulated. Satisfactory agreement was observed

in these comparisons. The simulation properly captured the spatial and temporal variability in the winds caused by large-scale meteorological features and by nighttime drainage and afternoon upslope flows induced by local terrain.

A puff (CALPUFF or SCIPUFF) or gridded (UAM-IV) simulation moves emissions from one point to another in response to the wind fields. Puff simulations more accurately represent emissions transport and dispersion from elevated sources during the first few hours, but wind shear is not well represented by puff simulations. In CALPUFF, for example, unless puff splitting is enabled, each puff is transported as a unit at all downwind distances using winds at the puff center, even when the puff has diffused into vertical layers with different wind speeds and directions. Enabling puff splitting can greatly increase the number of puffs to be simulated and thus increase the execution times for the simulation. Gridded simulations allow portions of a plume to be mixed vertically and then transported according to winds at each height above ground level. A disadvantage of gridded simulations is that emissions from a point source are immediately mixed throughout the 4 by 4 km grid cell in the vertical layer in which they are released, then almost immediately begin diffusing into the neighboring cells. As a result, gridded simulations mix elevated emissions to the ground too rapidly. The gridded approach was used for most NFRAQS transport simulations because there is substantial variation of wind speed and direction with height along the Northern Front Range. A few puff simulations were executed for comparison with the gridded UAM.

SO_2 emissions from the following sources were separately identified in the simulations: 1) Arapahoe coal-fired power station; 2) Cherokee coal-fired power station; 3) Pawnee coal-fired power station; 4) Valmont coal-fired power station; 5) Rawhide coal-fired power stations; 6) Trigen coal-fired power station; 7) Diamond Shamrock and Conoco refineries combined; 8) other elevated emitters combined; and 9) all surface emitters combined. Section 2.2 shows where these large sources are located and provides perspective on their relative emission rates. The first five coal-fired power station emission rates were obtained from hourly continuous emissions monitors. All other emissions were obtained from the Colorado Department of Health and the Environment (CDPHE) point source inventory. Elevated emissions are those with a stack height greater than 30 m (100 ft). Surface sources include point sources with a stack height less than 30 m as well as mobile, area, and wood burning emissions. Airport SO_2 emissions were not included owing to their small magnitude. Table 9.1-1 summarizes the emission rates used in the transport simulations, where the CEM data are the hourly rates during the 60-day Winter 97 study and the remainder are daily averages from the CDPHE inventory.

Simulations were carried out without SO_2 dry deposition and with a deposition velocity of 1.5 cm/s. These represent lower and upper bounds of feasible rates for Northern Front Range land uses; the 1.5 cm/s is much larger than the deposition velocity for particulate sulfur. The results of the simulations with and without dry deposition bracket concentrations that would be obtained from a more precise representation of dry deposition.

Simulations did not include chemical reactions; calculated SO_2 concentrations estimate the combined concentrations of sulfur dioxide and particulate sulfur. Simulated SO_2 is

therefore compared with the sum of measured SO_2 and particulate sulfur concentrations. The hourly particulate sulfur concentrations were obtained from the PIXE analysis of streaker samples (Chow et al., 1998). When hourly PIXE data were not available, the average particulate sulfur concentration from the six- and twelve-hour SFS filter samples was used. The simulated SO_2 concentrations for each hour were displayed in: 1) computer animations; 2) time series plots; and 3) cumulative frequency distributions.

At the Brighton and Evans sites, the mean bias and mean error in the calculated hourly SO_2 concentrations on most days were between 50% and 100% of the observed total ambient sulfur concentrations (Fujita et al., 1998). At the Welby site, the simulated hourly SO_2 concentrations were more than 10 times the measured total sulfur concentrations for many hours.

Forty animations, which are part of the NFRAQS data base, display gridded simulated plume transport with dry deposition; three additional animations display the results of the puff transport simulations. Separate animations simulate transport for each of the nine sources and for all sources combined during two January episodes. Separate displays show SO_2 concentrations in the surface layer and the vertical integral of the SO_2 concentrations at all heights in a grid cell.

As is typically the case for simulations of the transport and dispersion of point source plumes, the detailed correspondence between simulated and measured SO_2 pulses in space, time, and intensity is not very good. More often than not, high simulated SO_2 concentrations were not accompanied by high measured concentrations, and high measured concentrations were not accompanied by high simulated concentrations. These discrepancies were sometimes due to small displacements in the time or location of the high SO_2 concentrations.

9.1.2 Simulated SO_2 Contributions from Elevated and Surface Emitters

Cumulative frequency distributions (CFDs) of the calculated SO_2 concentrations provide information that is directly useful for source attribution. CFDs highlight the intensities of calculated SO_2 contributions. They do not identify when these contributions occur, nor the possibility of SO_2 interaction with fogs or clouds that enhance its conversion to ammonium sulfate.

Table 9.1-2 shows CFDs of simulated SO_2 concentrations at Brighton during the 01/12/97 to 01/21/97 episode. Concentrations calculated with and without dry deposition are compared. Each block of data was sorted separately, so concentrations at the same percentile level in Table 9.1-2 probably did not occur during the same hour. The final value reported in each block of data is the average SO_2 concentration, which was used to determine the ranking of the sources in the table.

Fujita et al. (1998) report CFDs for all of the simulations. The results for the 01/12/97 to 01/21/97 episode from simulations that included dry deposition are briefly summarized in Figure 9.1-1 and Table 9.1-3. Figure 9.1-1 shows the average concentrations attributed to each source at each site. The sites are in the same order as their location along the South

Platte River, and the sources are ranked in decreasing average simulated SO_2 concentrations at Welby. These simulations show that the Cherokee coal-fired power station and combined SO_2 emissions from many surface sources were the largest contributors to atmospheric sulfur at NFRAQS receptors during these episodes. The Arapahoe and Trigen coal-fired power stations were moderate contributors, and the Valmont power station was a minor contributor. The contributions attributed to the Pawnee and Rawhide coal-fired power stations, and other elevated sulfur emitters, were negligible. It is shown below that the average SO_2 concentrations at Welby attributed to Cherokee and surface sources by these simulations are too large.

Table 9.1-3 shows the highest, tenth percentile, and average simulated SO_2 concentrations for the simulations in Figure 9.1-1. The results for each monitoring site are in a column, and the sources are ranked in descending order of the average SO_2 concentrations at that site. These data indicate that, on average, surface sources and the Cherokee power station accounted for 71% to 93% of the simulated SO_2 concentrations. These source contributions are overestimated by the gridded simulations, as shown below, but this overestimation does not change the conclusion that they are the largest sulfur contributors to NFRAQS receptors for the episodes examined.

Figure 9.1-2 shows the average simulated concentrations for the 01/27/97 to 01/31/97 episode; these contributions are similar to those for the 01/12/97 to 01/21/97 episode. The main difference is that, except for the Arapahoe power station, the SO_2 concentrations attributed to each source are lower during the second episode.

9.1.3 Puff Transport Simulations

Biases introduced by the gridded approach to transport and dispersion were evaluated with the SCIPUFF puff simulation applied without deposition to emissions from Cherokee, Pawnee, and Valmont coal-fired power stations during the 01/13/97 to 01/21/97 episode. The 01/12/97 portion of this episode was excluded because upper-air data were not available at the time the simulations were performed. The SCIPUFF simulation and its implementation are described in detail by Fujita et al. (1998). Table 9.1-4 compares the results of the puff transport simulation with those from the gridded transport simulation at Brighton and shows that the gridded simulation yields higher concentrations than the puff simulation.

Puff-simulated SO_2 concentrations are compared with grid-simulated SO_2 and measured total ambient sulfur at the bottom of Table 9.1-4. In the "hybrid" total, the SO_2 contributions from the Cherokee, Pawnee, and Valmont power stations were determined by the puff transport simulations and the remaining source contributions were determined by the gridded simulations. CFDs of the measured total ambient sulfur are shown at the bottom right of the table. The percentile values from the two simulation methods and the measurements generally differ by no more than a factor of two.

All of the results from the puff simulations and comparisons with those from the gridded simulations at CAMP, Welby, and Evans are summarized in Fujita et al. (1998). The largest differences between the gridded and puff transport simulations are for the sulfur at

Welby attributed to the nearby Cherokee power station. The maximum value and the 5 to 30 percentiles in the grid-simulated CFDs are 20 to 40 times larger than corresponding percentiles for the puff-simulated CFDs. As noted above, gridded transport simulations overestimate SO_2 concentrations and the puff transport simulations underestimate SO_2 concentrations when distances are short between source and receptor, as is the case for the Cherokee/Welby relationship. At greater distances from point sources, SO_2 CFDs calculated by the two simulation methods are within a factor of two or three of each other at all percentile points for simulated SO_2 concentrations that exceed 0.5 ppbv.

9.1.4 Transport Simulation Uncertainties

The comparison between grid and puff simulations and measurements shows that 1) the gridded transport simulations overestimate SO_2 concentrations at the surface near a large source; 2) the puff transport simulations underestimate the concentrations at the surface near a large source; and 3) the SO_2 concentrations attributed to surface sources appear to be too large. The discrepancies are most apparent at Welby, where portions of the CFDs for the separate contributions of the Cherokee station and surface sources to SO_2 concentrations calculated by the gridded transport simulations are larger than the corresponding values determined from the measured ambient concentrations.

Fujita et al. (1998) show that for the emissions from the Cherokee station alone, the maximum and average simulated hourly SO_2 concentrations and the percentile values for 5% through 40% were approximately twice the measured ambient sulfur concentrations during the 01/12/97 to 01/21/97 episode. For surface emissions, Fujita et al., (1998) show that the average and all percentile values (except the maximum) were larger than the measured ambient concentrations. When the simulated concentrations from one source alone are larger than the measured concentrations from all sources, it is certain that the simulated concentrations are excessive and do not represent the real world.

Fujita et al. (1998) also show that the puff simulations underestimate the peak SO_2 concentrations. The maximum hourly SO_2 concentration measured at Welby during the 01/12/97 to 01/21/97 episode was 72 ppbv and 5% of the measured hourly SO_2 concentrations exceeded 17 ppbv. According to the puff simulations, the maximum hourly SO_2 contribution from the Cherokee station to Welby was 5 ppbv; 5% of the hourly concentrations attributable to the Cherokee station exceeded 2 ppbv. The puff simulations estimated a maximum hourly SO_2 concentration at Welby from the Valmont station of 6 ppbv and 5% of the hourly concentrations attributed to the Valmont station exceeded 0.5 ppbv. Meteorological analyses indicate that the occasional high SO_2 concentrations observed at Welby are due to coal-fired power station plumes. Puff simulations do not contain SO_2 peaks like those observed. Since the same emissions and meteorological data were used for the gridded and puff transport simulations, the major differences between the CFDs for the SO_2 peaks at Welby attributed to the Cherokee station result from differences in the simulation methods.

Fujita et al., (1998) show that the results from the two simulation methods tend to converge as the distance from the elevated sources increases. With the exception of the

simulated SO_2 concentrations due to Cherokee at Welby and Brighton, the CFDs of SO_2 concentrations calculated by the gridded and puff simulation methods were within a factor of two or three of each other at all percentile points for which the predicted SO_2 concentration is greater than 0.5 ppbv. The simulated concentrations at Brighton and Evans also agree with the measurements to within a factor of two.

It is not known why the grid-simulated attribution of SO_2 concentrations at Welby to surface sources exceeded measured sulfur concentrations. It is possible that the surface emissions rates are uncertain. It is also possible that the wind fields do not adequately simulate transport in layers near ground level. In any case, the overestimation of surface source SO_2 attribution at Welby decreases confidence in the simulated surface source attribution for other sites. The diurnal profiles of ambient sulfur concentrations discussed in Section 9.3 show the effects of surface SO_2 emissions, but they are smaller than the effects of SO_2 mixed down from aloft during midday. These diurnal patterns support the hypothesis that the contribution of surface sources to ambient sulfur concentrations is overestimated at all monitoring sites by the gridded transport simulations.

With consideration for these discrepancies and uncertainties, transport simulations demonstrate that the Cherokee power station contributes more sulfur at the monitoring sites than any other power station. Surface sources are the next largest contributors. The following four point sources are moderate to minor contributors: the Diamond Shamrock and Conoco refineries, the Arapahoe power station, Valmont power station, and the Trigen power station. These five point sources collectively contributed more sulfur at the monitoring sites than the surface sources.

The Pawnee and Rawhide power stations contributed negligible amounts of sulfur, mostly owing to winds that transported their emissions away from receptors during the simulated episodes. The sulfur contributions from other elevated point sources in the emissions inventories of Section 2 were small because of their small emissions.

9.1.5 Sulfur Dioxide Transport Meteorology

Meteorological and five-minute to hourly air quality measurements were examined to better understand the atmospheric mechanisms responsible for the mid-morning SO_2 pulses measured at Welby and Brighton. These analyses also determined the potential for sulfur dioxide plumes to pass through clouds or fogs, near ground-level or aloft, that could enhance the conversion of sulfur dioxide to sulfate.

The conceptual model of the atmospheric processes that cause the midmorning SO_2 pulses is shown in Figure 9.1-4. On the day prior to an SO_2 pulse, daytime convection mixes surface emissions, including CO, NO_x, SO_2, and elemental carbon (which is mostly emitted by motor vehicles), into the daytime convective boundary layer. As the ground cools in the evening and throughout the night, a nocturnal inversion forms near the surface, and this decouples the daytime mixed layer from the surface. The aged daytime mixed layer, above the nocturnal boundary layer and below an aloft inversion, is called the residual layer.

Because of the increased stability, elevated emissions are injected into the residual layer during the overnight hours as indicated in Figure 9.1-4. These elevated emissions mix with the prior day's surface emissions during the night. On the following day, as daytime convection begins, the boundary layer grows into the residual layer and mixes the air in the residual layer down to the surface. The nighttime elevated SO_2 emissions and the surface emissions from the prior day impact the monitoring site together. Under some conditions, surface emissions may not be mixed aloft during the prior day or they may mix aloft and be transported in a way such that they do not mix with elevated SO_2. When either of these conditions occurs, SO_2 from elevated sources can be mixed to the surface without being accompanied by surface emissions from the prior day.

SO_2 pulses may also arrive at receptors as a result of horizontal transport within the surface layer from upwind surface sources. This surface emission transport pathway would contribute most when the atmosphere is stable with minimal vertical mixing. SO_2 from surface sources is likely transported with other surface emissions, specifically CO, elemental carbon, and NO_x. As explained in Section 8, SO_2 is rapidly oxidized to sulfate when mixed into clouds or fog that contain oxidizing agents. As a result, when an increase in particulate sulfur accompanies an SO_2 pulse, it is likely that clouds or fogs were present in the region during the hours preceding the SO_2 and particulate sulfur pulse.

The following days were analyzed to identify these associations: 12/15/96, 12/26/96, 12/31/96, 01/02/97, 01/07/97, 01/14/97, and 01/20/97. These days were selected because SO_2 pulses exceeding 25 ppbv were observed and other meteorological data were readily available. Because 01/14/97 and 01/20/97 had the highest observed SO_2 concentrations, they were analyzed in greater detail than the other days. Also, 12/26/96, 01/02/97, and 01/14/97 were the only days of this selected group on which the SO_2 pulse was accompanied by a particulate sulfur pulse.

Five-minute average SO_2, CO, NO_x, NO, and elemental carbon and hourly particulate sulfur measurements from the Welby and Brighton sites were examined for pulses. It was suspected that SO_2 pulses were caused by the mixing of SO_2 to the surface, so meteorological data were examined for evidence of this mixing. Sodar, wind profiler reflectivity data, and RASS temperature data collected at Welby and Brighton were reviewed for evidence of vertical mixing. Time-lapse video looking east toward the Pawnee Power Plant and time-lapse video from Thornton looking south toward Denver were also viewed for evidence of mixing and for liquid water in clouds or fog. Effective stack heights were calculated for Cherokee and Pawnee to determine if the aloft layers that mix down to the surface could contain SO_2 emitted from elevated sources. Winds collected at several stations throughout the study area were analyzed to address the hypothesis that the SO_2 pulses were caused by surface transport. Table 9.1-5 summarizes the relevant air quality and meteorological features associated with the SO_2 pulses.

Analysis of the upper-air data showed that convective daytime mixing was probably the cause of the SO_2 pulse on four of the seven days analyzed. Data from one additional day were inconclusive. Analysis of the effective stack heights showed that that SO_2 emitted from major point sources at night typically rose to heights of 250 to 400 magl. During most days,

surface emissions were also mixed upward to this height, then trapped there by the nocturnal boundary layer to form a residual layer. The result was that surface emissions from the previous day and point source emissions during the night were commingled in the residual layer. When the plumes in the residual layer were mixed to the surface on the following day, the CO, NO_x, and elemental carbon in the residual layer were probably mixed to the surface at the same time. In some cases, this caused the concentrations of CO and elemental carbon to increase by as much as a factor of two when the plume SO_2 and NO_x was mixed to the surface.

Analysis of upper-air data showed no evidence of mixing associated with the SO_2 pulse on two of the days. In one case, this was probably caused by transport of surface SO_2 emissions by surface winds on one of these days. In the other case, the SO_2 pulse was probably from an elevated source.

Of the four SO_2 pulses attributable to mixing, there were at times large, but not consistent changes in the concentration of CO, NO_x, NO, and elemental carbon; therefore, apportioning SO_2 between elevated and surface sources based upon their relative concentrations is not possible. On each of the four days, vertical mixing resulted in different changes in air quality: 1) NO_x increased while CO remained unchanged; 2) NO_x increased and CO increased; 3) NO_x decreased and CO remained unchanged; and 4) NO_x decreased and CO decreased.

On the two days when the SO_2 pulses were not clearly attributable to mixing, there was also no consistent change in the concentration of CO, NO_x, NO, and elemental carbon. On these days: 1) NO_x increased while CO remained unchanged; and 2) NO_x and CO decreased. Although the meteorological data do not show mixing, the decrease in CO and NO_x is consistent with an SO_2 pulse from elevated sources.

On two of the three days when particulate sulfur accompanied an SO_2 pulse, clouds (liquid water) were observed at 200 to 300 m agl during some of the hours just prior to the SO_2 and particulate sulfur pulse. The highest five-minute SO_2 concentrations were measured at Brighton (80 ppbv) and Welby (102 ppbv) on 01/14/97 and the second highest SO_2 concentration was measured at Welby (94 ppbv) on 01/20/97. The analysis provided below details the physical mechanisms causing the SO_2 pulses on these days. Events on 01/14/97 and 01/20/97 are examined in greater detail to elucidate these observations.

9.1.5.1 January 14, 1997 Case Study

Figure 9.1-5 shows that during the midmorning hours on 01/14/97, the SO_2 concentration at Brighton increased from ~5 ppbv at 0900 MST to 80 ppbv at 1000 MST. From 1000 MST to 1100 MST, SO_2 decreased to 42 ppbv followed by another rapid rise in the SO_2 concentration to 52 ppbv at 1105 MST. During the initial 1000 MST pulse, the NO_x, NO, CO, and elemental carbon concentrations also increased, but not as much as the SO_2 concentration. During the second SO_2 pulse the NO_x, NO, CO, and elemental carbon concentrations did not change.

As at Brighton, rapid increases in SO_2, NO, NO_x, CO, and elemental carbon concentrations were measured at the Welby site on the morning of 01/14/97. However, as shown in Figure 9.1-5, the concentration increases at Welby started at 1000 MST rather than at 0900 MST, and most of this pulse occurred between 1030 MST and 1100 MST. The SO_2 concentration increased from 7 ppbv at 0955 MST to 100 ppbv at 1105 MST, while CO, NO, and NO_x concentrations doubled. The first observed SO_2 pulse at Brighton probably resulted from elevated emissions in the residual layer mixing down through the surface inversion and impacting the Brighton monitoring site.

Although the RASS vertical temperature measurements indicate that there was strong atmospheric stability on 01/14/97, mixing resulting from an atmospheric disturbance was likely. Sodar reflectivity, wind profiler reflectivity, and videos were examined to detect the extent of vertical mixing between the surface and aloft at the time of the first Brighton SO_2 pulse. On 01/14/97, sodar reflectivity (Figure 9.1-6) showed three layers: 1) a nocturnal surface layer at ~50 m agl; 2) a second inversion at ~175 m agl; and 3) an inversion at ~250 to 300 m agl. The temperature structure, mixing heights, and effective stack heights indicate that the surface emissions from the prior day's and overnight elevated emissions resided in an aloft layer at ~200 m as depicted in Figure 9.1-4. At ~0900 MST on 01/14/97, the sodar reflectivity data and video showed the existence of a gravity wave at ~400 m agl (Figure 9.1-6). At Brighton, from 0900 MST to 0940 MST, the gravity wave appears to mix or inject residual-layer air containing the pollutants to the surface (see Figures 9.1-4, 9.1-6, and 9.1-7). The SO_2 pulse was observed at 0900 MST, corresponding to the mixing of aloft air to the surface; the SO_2 concentration increased from 0900 MST until 1000 MST (see Figure 9.1-5).

The second pulse measured at Brighton at 1100 MST resulted from daytime convective mixing to the surface of residual layer air containing overnight elevated emissions and the prior day's surface emissions; this differs from mixing or injection of aloft air to the surface due to a gravity wave. As shown in Figures 9.1-6 and 9.1-8, sodar reflectivity data showed the surface layer (formally the nocturnal boundary layer) developing into the mixed layer at 1100 MST. Shortly after, at 1120 MST, a weak SO_2 pulse was observed.

In contrast to the situation at Brighton, sodar reflectivity and wind profiler reflectivity measurements at Welby did not show mixing of the residual layer to the surface at 0900 MST, and Welby did not measure an SO_2 pulse at 0900 MST. At 1000 MST, the sodar reflectivity showed weak mixing of residual-layer air to the surface, and the SO_2 concentration increased slightly. At 1100 MST, as at Brighton, sodar reflectivity showed the surface layer (formally the nocturnal boundary layer) growing into the mixed layer (Figure 9.1-9). In response, the SO_2 concentration increased from ~10 ppbv to 102 ppbv.

An alternative explanation for the SO_2 pulses at Welby and Brighton on 01/14/97 is that surface winds transported surface pollution to the Brighton site and then an hour later to the Welby site. The temporal offset between the SO_2 pulse at Brighton (0900 MST) and the SO_2 pulse at Welby (1000 MST), combined with the relatively high concentrations of surface emissions, including elemental carbon and CO, accompanying the SO_2 pulse is consistent with this theory. However, examination of morning winds showed southwesterly to westerly winds at the surface until ~1100 MST. A southwesterly to westerly surface flow would cause an

SO_2 pulse to be measured first at Welby and later at Brighton. Given that the majority of SO_2 emissions are from elevated sources, it is unlikely that such high SO_2 concentrations would impact both sites if only surface transport was a factor. Furthermore, it is also unlikely that the SO_2 concentrations would increase by a factor of 16 during the pulse while CO, NO_x, NO, and elemental carbon increase only by factors of 1 to 6, if no elevated emissions were involved in the pulse.

9.1.5.2 January 20, 1997 Case Study

The 01/20/97 event differed from the 01/14/97 event because Brighton did not measure a SO_2 pulse and no gravity wave assisted the mixing of elevated pollutants to the surface. As shown in Figure 9.1-10, on 01/20/97 the SO_2 concentration at Welby increased from ~7 ppbv at 1000 MST to ~92 ppbv at 1030 MST. From 1030 MST to 1200 MST, SO_2 decreased to 3 ppbv followed by another rapid rise in the SO_2 concentration to 46 ppbv at 1215 MST. During the first pulse, between 1000 MST and 1030 MST, NO_x, NO, and CO concentrations decreased by a factor of two. During the second pulse, the NO_x and NO concentrations doubled, while the CO concentrations did not appreciably change. No pulse was observed at Brighton.

As in the 01/14/97 event, the initial pulse observed at Welby on 01/20/97 appeared to result from elevated emissions in the residual layer mixing down as the daytime boundary layer convectively mixed into the aloft layer. The temperature structure, mixing heights, and effective stack heights indicate that overnight elevated emissions remained the residual layer at ~200 m agl. As shown in Figure 9.1-11, the surface and aloft layers coupled on the morning of January 20 at ~1015 MST and an SO_2 pulse of 92 ppbv was measured at 1030 MST (Figure 9.1-10). By 1200 MST the surface layer was well mixed with the residual layer, and the second SO_2 pulse could have resulted from elevated emissions mixing to the surface or from upwind surface sources transported over the site.

9.2 Chemical Mass Balance $PM_{2.5}$ and Precursor Apportionment

CMB source contributions are presented for primary $PM_{2.5}$ and precursor SO_2 and NO_x. As noted in the introduction to this section, the $PM_{2.5}$ source contribution estimates have a high degree of confidence. The gas apportionments represent possible contributions with higher uncertainties, owing to the reactive nature of SO_2 and NO_x and the presence of SO_2 emitters that do not have distinctive $PM_{2.5}$ profiles.

9.2.1 $PM_{2.5}$ Source Contributions

Tables 9.2-1 and 9.2-2 show the average $PM_{2.5}$ source contributions at Welby and Brighton for the extended (including organic species) and conventional (including only elements, ions, elemental carbon, and organic carbon) CMB. For these apportionments, R^2 typically exceed 0.9 and χ^2 values are mostly between 0.3 and 0.5. The percent mass values are within one standard deviation of 100% for most of the samples. Figure 9.2-1 compares the 24-hour $PM_{2.5}$ source contributions from conventional CMB for the three core and six satellite sites during the Winter 97 NFRAQS. The areas of the pies are proportional to the

average $PM_{2.5}$ concentrations, which reflect the observations in Section 6 that $PM_{2.5}$ are largest in the Denver urban core and at sites along the South Platte River (Evans and Masters). Figures 9.2-2 and 9.2-3 show time-series plots of the 6-hr and 12-hr $PM_{2.5}$ source contributions from the extended CMB for Welby and Brighton, respectively.

On average, vehicle-related emissions that are characteristics of gasoline exhaust, diesel exhaust, and road dust contribute 55% of the $PM_{2.5}$ in Denver. Light-duty gasoline vehicle exhaust is 29.7 ± 2.6% of the $PM_{2.5}$ at Highlands, 30.5 ± 2.1% at CAMP, and 31.3 ± 3.2% at Welby. Diesel exhaust contributes 5.3 ± 1.2%, 10.6 ± 1.3%, and 9.0 ± 1.2% of the $PM_{2.5}$ at the three Denver sites, respectively, and road and geologic dust contributes 18.9 ± 2.9%, 12.2 ± 2.9%, and 16.7 ± 2.9%, respectively. The fractional contributions of vehicle-related $PM_{2.5}$ are twice as high in Denver than in the non-urban locations of Brighton, Evans, and east of Longmont. Source contributions at Ft. Collins reflect higher influence of motor vehicle exhaust. Source contributions at Chatfield and Masters, which are located at the extremes of the NFRAQS network, show less urban influence with vehicle exhaust contributions of 17% and 8%, respectively.

The 24-hour average gasoline vehicle exhaust contributions from extended CMB for LDGV cold starts, LDGV hot stabilized, and LDGV high particle emitters are 11.9 ± 2.3%, 3.2 ± 0.8%, and 12.7 ± 2.2%, respectively, at Welby and 3.6 ± 0.9%, 1.5 ± 0.5%, and 18.8 ± 2.0%, respectively, at Brighton. The sums of the gasoline vehicle exhaust contributions are comparable to corresponding contributions from conventional CMB. Contributions of LDGV cold start emissions at Welby are nearly twice as high in the overnight and morning samples than in the afternoon samples. In comparison, there is little diurnal variation in contribution of LDGV cold start emissions at Brighton. Contributions from non-smoking hot stabilized emissions and high particle emitters do not show significant diurnal variation. Contributions of diesel exhaust to $PM_{2.5}$ are about 10 ± 2% at both Welby and Brighton. Although absolute contributions of diesel exhaust are lowest during the overnight sampling period, relative contributions show no diurnal variation.

In contrast to urban locations, secondary particles (i.e., ammonium nitrate and ammonium sulfate) are often the largest contributors to $PM_{2.5}$ (about 50% on average) at the non-urban sites of Brighton, Evans, and Masters. Ammonium nitrate is three to four times higher than ammonium sulfate at sites north of Denver, and twice the ammonium sulfate contributions at the Denver sites. Nitrate concentrations have a greater effect on the relative importance of sulfate and nitrate within the NFRAQS domain as sulfate concentrations are more spatially uniform. Diurnal variations of ammonium nitrate and ammonium sulfate contributions were minor at both Welby and Brighton with slightly higher values during the afternoon and overnight periods.

Meat cooking and wood combustion were commonly minor or moderate contributors, but there were many periods during which their contributions were not detected. The 24-hour average contributions of meat cooking to $PM_{2.5}$ at Welby and Brighton are 3.7 ± 1.2% and 1.9 ± 0.9%, respectively. Meat cooking contributions are highest in the 1800-0600 samples at Welby. The 24-hour average contributions of wood combustion to $PM_{2.5}$ at Welby and Brighton are 4.8 ± 1.1% and 2.1 ± 0.03%, respectively. Emissions from softwood and

hardwood are split 40/60. Contributions of wood combustion are higher in the overnight samples with softwood emissions showing greater diurnal variations.

Primary particle contributions from coal-fired power stations contributed no more than minor fractions of $PM_{2.5}$ at any of the measurement locations. $PM_{2.5}$ unexplained by the CMB apportionments was within propagated uncertainties most of the time. On average, the unexplained fraction was largest at the Chatfield and Masters sites.

9.2.2 Sulfur Dioxide and Nitrogen Oxides Source Contributions

Tables 9.2-3 and 9.2-4 show the potential SO_2 and NO_x contributions at the Welby and Brighton sites. These contributions were determined from the extended CMB 6-hour, 12-hour, and 24-hour intervals. Contributions to individual samples are shown in Figures 9.2-4 through 9.2-7. The R^2 and χ^2 values in the tables apply to the $PM_{2.5}$ apportionment. The Percent Mass measures, however, are specific to the apportioned gases. Neither SO_2 nor NO_x were used as fitting species, so the apportionments are totally independent of the gas concentrations measured at receptors. Samples with low measured values (less than 1 ug/m^3 for SO_2 and less than 25 ug/m^3 for NO_X) were removed from the averages.

The CMB-calculated SO_2 concentrations exceeded measured concentrations by 40% to 90% for daytime samples at both sites. CMB-calculated SO_2 concentrations for the nighttime samples underestimated measured values by about 34% at Brighton and overestimate measured values by 24% at Welby. CMB-calculated NO_x concentrations overestimate measured values at Brighton and generally agreed with measured concentrations at Welby. These discrepancies are consistent with the expectation that gases emitted with primary particles react and deposit more rapidly than the particles, thereby depleting their ratio to $PM_{2.5}$ mass during transport between source and receptor.

Figures 9.2-4 and 9.2-5 show that the CMB estimated zero coal-fired power station contributions for ~30% of the samples. This does not necessarily imply that there were no power station contributions during these periods, but that these contributions did not exceed their propagated standard errors. The detectable contributions were also associated with large standard errors, often in the range of 30% to 60% of the CMB-calculated contribution. Furthermore, the profile used for coal-fired power stations was derived from a 1987-88 test of the Cherokee generating station, and this may not reflect the relationships between gases and particles for that station, or any of the other power stations, during the Winter 97 period. The CMB gas apportionments are not definitive, but they are included for comparison with the other SO_2 and NO_x apportionments discussed in this section.

The CMB apportionments estimate that 51 ± 9% of 24-hour average SO_2 at Welby and 41 ± 9 % of 24-hour average SO_2 at Brighton were contributed by coal-fired power stations. The CMB attributed 21% of 24-hour average SO_2 to motor vehicle exhaust at Welby and 16% to motor vehicle exhaust at Brighton. The contributions from this source are twice as high during the overnight periods than during the afternoon. This is consistent with more traffic during the morning and overnight periods and shallow surface layers that allow surface emissions to accumulate.

An important caveat to the SO_2 apportionment is that the CMB does not detect industrial source contributions other than those from coal-fired power stations. About a quarter of the SO_2 at Welby and half at Brighton are unexplained. With the profiles available and the particulate species measured at source and receptor, contributions from refineries, grain elevators, natural gas boilers, and other point sources identified in Section 2 do not have unique chemical markers that allow them to be distinguished by $PM_{2.5}$ apportionment. This is not important for the $PM_{2.5}$ apportionment, since most of the mass is explained by other contributors and the primary particle emissions from these sources are negligible compared to those from the apportioned source types. This is not the case for sulfur dioxide, for which Section 2 showed several other emitters other than coal-fired power stations. Of particular importance are the Conoco and Diamond Shamrock refineries, the wastewater treatment plant, and the Rocky Flats emissions that must certainly contribute to the Welby site measurements along with contributions from the nearby Cherokee coal-fired power station.

The CMB shows that ~50% of the NO_x is contributed by motor vehicles at Welby and 73% at Brighton. Consistent with the carbon apportionment, diesel exhaust is a larger source of NO_x at Brighton, while gasoline vehicle exhaust is the largest contributor at Welby. Coal-fired power stations contribute 7.4 ± 2.9% at Welby and 9.4 ± 3.6% of the NO_x at Brighton. Diurnal changes in NO_x contributions are consistent with larger contributions from surface motor vehicle emitters to nighttime and morning samples, with larger but not dominant contributions from coal-fired power stations during afternoon samples. The Welby site experiences a 42% portion of NO_x that is unexplained by the $PM_{2.5}$ sources, consistent with potential contributions from other nearby point sources that were not included in the $PM_{2.5}$ apportionment.

9.3 Diurnal Variations in Atmospheric Composition

The Winter 97 NFRAQS monitoring network obtained five-minute to one-hour average concentrations of particle sulfur and sulfur dioxide, nitrogen oxides, and ammonia precursor gases. The source apportionment approach for secondary species and their precursors intended to apply a simple, semi-quantitative CMB to the time variation of the atmospheric constituents to infer the origin of those constituents. For example, if a pulse of SO_2 accompanied by particulate sulfur and NO_x arrived at a monitoring site without any increase in CO or elemental carbon concentrations, it would be inferred that the particulate sulfur was due primarily to the emissions of elevated point source emitters of these components rather than to surface motor vehicle emitters. This inference was to be justified by the fact that elevated sources emit large amounts of SO_2 and NO_x, and very little CO and elemental carbon. In contrast, SO_2 and NO_x from mobile emissions are accompanied by CO and elemental carbon. This approach worked well in the Mt. Zirkel Visibility Study (Watson et al., 1996) where nearby sulfur dioxide emitters and populated areas were fewer in number and clustered in specific locations with channeled flows.

Application of this approach to NFRAQS measurements, however, revealed that the more numerous and diverse locations of area and point sources, coupled with complex meteorology and atmospheric processes, yielded too many transport and chemical pathways

for this approach to definitively differentiate among contributors. At night, emissions from elevated sources become mixed aloft with surface emissions from the prior day. On the next day, the combined emissions are mixed to the ground after having been commingled for many hours. Sulfate and nitrate can be formed in these emissions both before and after they are mixed. Because of the possibility that all components of the mixture arrive at the monitoring station with approximately the same time history, time series analysis does not provide the information necessary to apportion the sulfate and nitrate to sources.

The short-time measurements did, however, allow the diurnal variations in atmospheric composition to be studied. "Box and whisker" plots similar to the ones in Figure 9.3-1 show the distribution of concentrations measured each hour during the day. The methods for generating and interpreting these plots are illustrated by describing the methods for calculating the upper left panel in Figure 9.3-1. For the symbol appearing at hour zero (midnight), all data for hour zero during the winter study were collected in one group and sorted to determine the median, the values at the 25^{th} and 75^{th} percentiles, etc. This process was repeated for each hour of the day and the results are shown by the symbols for each hour.

The line through the box indicates the median value; half of the data points have a higher value and half have a lower value. The top and bottom of the box indicate the concentrations at the 25^{th} and 75^{th} percentiles. One quarter of the data points have a lower concentration than the value at the bottom of the box and one quarter have a value higher than the value at the top of the box. The whiskers always end on a data point, and have a maximum length equal to 1.5 times the length of the box. Concentrations exceeding the maximum range allowed for the whiskers are plotted individually, and the whisker ends on the data point farthest from the median that is within the allowed range of the whisker. Outliers that are beyond the range of the whisker and within three times the length of the box from the nearest end of the box are shown with an asterisk. Outliers that are farther from the end of the box are shown with an open circle. If there are no data points outside the allowed range of the whisker, the whisker ends on the data point farthest from the end of the box.

Plots labeled "filter days" include only data from the episodic days for which particle chemical composition was determined on the filter samples. Plots labeled "non-filter days" include only data from the days the filter samples were not analyzed. Plots labeled "all days" are based on data from the entire 60-day measurement period of the winter study.

The variation in the composition of the atmosphere as a function of the time of day shows that NO_x and CO followed the same diurnal pattern, consistent with their having a common origin. Both of these gases have maximum concentrations during the morning and evening rush hours, indicating that they are mostly attributable to nearby mobile sources. SO_2 had a different diurnal pattern. SO_2 concentrations were highest during midday, when elevated emissions can reach the ground owing to daytime mixing. The diurnal patterns of SO_2 concentrations also show the contributions of nearby mobile sources.

Sulfate changed little during the day at most sites. The diurnal pattern of sulfate at Welby showed the effects of nearby mobile sulfur emissions. Nitrate concentrations increased most rapidly during the day, when photochemical oxidation of NO_2 and mixing with ammonia

from rural areas can occur. Only a small fraction of the ambient NO_x oxidized to nitrate (nitric acid plus particulate nitrate).

Most emitted NO_x remained in the atmosphere as NO and NO_2. The median values for the fraction converted to nitrate are less than 4% at Welby and 8% at Brighton, and the maximum conversion observed was 20%. Nearly all of the SO_2 either deposited or oxidized to particulate sulfur, especially in the hours before dawn. Complete conversion of non-deposited sulfur dioxide was observed on more than 25% of the days between the hours of 0200 and 0800 MST at Welby and the hours of 1900 and 0900 MST at Evans. Complete conversion of non-deposited SO_2 was observed on more than half of the days at 0600 MST at Welby and at 0600 and 0700 MST at Evans. Complete conversion of non-deposited SO_2 was less common at Brighton.

9.3.1 CO, NO_x, and SO_2 Diurnal Variations

Figures 9.3-1 and 9.3-2 show the diurnal variations at the CAMP monitoring station in downtown Denver. Figure 9.3-1 shows measurements during the Winter 97 period while Figure 9.3-2 shows the longer period including 11/96 and 02/97 because the NO_x data from CAMP were not valid for much of the Winter 97 period. Many heavily traveled roads surround the CAMP site, and CO concentrations were high during the morning andevening rush hours. The NO_x concentrations follow the same diurnal profiles, indicating that most NO_x also comes from nearby mobile sources. CO concentrations were larger on the filter days than on non-filter days, and the differences are greatest in the afternoon and evening. This pattern is observed in all cases where ambient concentrations were similarly compared. CO is directly emitted from sources, so this pattern is caused by less transport and mixing of the emissions during the days selected for the chemical analysis of filter samples than during other days. The higher concentrations during the evening rush hour and night increase the pollutant concentrations that can be carried over to the following day.

The diurnal patterns for SO_2 at CAMP are mixed. Figure 9.3-1 shows that SO_2 concentrations were highest at midday on the filter days. In Figure 9.3-2 and the non-filter days in Figure 9.3-1, the highest median occurred during the morning rush hour instead of at noon. In all cases, the effects of mobile sources are evident in the 25th percentile concentrations, shown by the bottoms of the boxes. SO_2 concentrations increase on most mornings during the rush hour. In all SO_2 plots in Figure 9.3-1, the highest whiskers occur during midday when SO_2 from elevated plumes is most likely to mix to the surface. This vertical mixing explains the occasional high SO_2 concentrations indicated by the whiskers.

Similar diurnal patterns for CO, NO_x, and SO_2 at Welby, Brighton, and Evans are shown in Figures 9.3-3 through 9.3-5. CO concentrations were omitted from Figure 9.3-3 because the CO data from Welby were rounded to the nearest 1 ppmv, and this rounding obscured the diurnal variations in the CO concentrations. The Welby data show a strong midday peak in SO_2 concentrations, especially on filter days. The transport analyses in Section 9.1 indicate that this peak is mostly attributable to the Cherokee station emissions. The persistence of the NO_x concentrations at Welby into the evening and past midnight on filter days also stands out.

At the less urban Brighton site the CO and NO_x concentrations do not show as distinct changes with time of day as at CAMP and Welby. As at CAMP, the diurnal SO_2 variations show the effects of both mobile and elevated emissions. It is likely that the increase in the 25th percentile concentrations during the morning rush hour on all days and the high median and 75th percentile values during the morning rush hour on the non-filter days are caused by nearby mobile emissions. Mixing of elevated SO_2 emissions to the surface is the likely cause of the high 75th percentile values, high whiskers, and high values in the outliers during the middle of the day on filter days in Figure 9.3-4. These results are consistent with those from the transport simulations in Section 9.1.

Higher nearby emissions in the Evans area than at Brighton are evidenced by CO and NO_x concentrations with more distinct diurnal variation. Median NO_x concentrations at Evans on filter days are exceeded those at Brighton, and were comparable to or greater than those at Welby. The diurnal profiles of SO_2 concentrations on all days indicate that daytime mixing of SO_2 from aloft is much more important than local mobile contributions.

In summary, the diurnal profiles of CO and NO_x concentrations are always consistent with the hypothesis that their concentrations are dominated by nearby mobile emissions. The concentrations of CO and NO_x are larger during the evening rush hours and in the early part of the night on filter days than on non-filter days. This is consistent with less transport and dispersion of emissions on filter days than on non-filter days. The diurnal variations of the SO_2 concentrations are consistent with contributions from nearby mobile emissions during morning rush hours and midday mixing of elevated emissions to the surface. The diurnal profiles indicate that mixing of elevated emissions contributes more SO_2 than nearby mobile emissions.

The analyses in Section 9.1.5 indicate that mobile emissions can be mixed aloft, reside there for some time, and then be mixed to the surface during the following day. As a result, some of the SO_2 mixed to the surface during the day accompanies that emitted by major point sources.

9.3.2 Light-Absorbing Particles Diurnal Variations

Figure 9.3-6 shows the diurnal variation of particle light absorption measured with the aethalometer at Welby, Brighton, and Evans. These variations are similar to those for CO and are consistent with the hypothesis that light-absorbing particles are primarily due to nearby mobile emissions. These data show that transport and dispersion are more effective on non-filter days than on days when filter samples were analyzed.

9.3.3 Sulfate and Nitrate Diurnal Variations

Figure 9.3-7 shows the hourly variation in sulfur concentrations for the filter days on which both gas and particle sulfur concentrations were available at the Welby, Brighton and Evans sites. Particulate sulfur was primarily in the form of ammonium sulfate. To facilitate the stoichiometric calculations, the particulate sulfur concentrations are reported in units of

ppbv, the gas concentration that would result if the particulate sulfur were vaporized into sulfur atoms.

The hourly particulate sulfur concentrations do not exhibit a consistent diurnal variation; the concentrations remain nearly constant. There is a slight tendency for the median particulate sulfur concentrations to increase at Brighton during the day. At Welby, particulate sulfur concentrations increased during the morning and evening rush hours, consistent with contributions from nearby mobile sources. At Evans, the median concentrations were nearly constant during the day, but the 75th percentile concentrations increased slightly during the day and the 25th percentile concentrations increased slightly during the morning and evening rush hours and during the first part of the night.

Ambient sulfur concentrations, i.e., the sum of the SO_2 and particulate sulfur concentrations, follow the diurnal variations for SO_2. The fraction of the ambient sulfur that is in the form of particulate sulfur is shown by the sulfur conversion plots. At Welby and Evans, the tops of many box symbols have a value of 1. During these hours, the ambient sulfur is either deposited or fully converted to sulfate on more than 25% of the days that measurements were made. At 0600 MST at Welby and at 0600 and 0700 MST at Evans, the median value is 1.0, indicating that the ambient sulfur is fully converted to sulfate on more than 50% of the days at these hours. The decrease in the sulfur conversion during midday indicates that the SO_2 mixed to the surface during this time of day was typically accompanied by a relatively small amount of sulfate.

The value at the bottom of the boxes in the sulfur conversion plots indicates the fraction of the ambient sulfur converted to particulate sulfur on at least 25% of the days. These values are typically small, indicating that on one-quarter of the days, only 5 to ~20% of the SO_2 converted to sulfate. In the early morning hours at Evans, at least 30% of the sulfur converted to particulate sulfur on the 75% of the days with the greatest conversion.

Hourly particulate sulfur measurements were averaged over the three-hour periods corresponding to the SGS nitrate measurements at Welby and Brighton and are shown in Figures 9.3-8 and 9.3-9. Labels are the same as those for Figure 9.3-7 and the diurnal patterns in the three-hour data are consistent with those in the hourly data discussed above. In Figure 9.3-9 "Nitrate" includes both particulate nitrate and nitric acid, "Ambient N+O Species" is the sum of NO_x, nitric acid, and particulate nitrate, and "Nitrogen Conversion" is the fraction of these species as nitrate. The numerator in this ratio is nitric acid plus particulate nitrate and the denominator is the sum of NO_x, nitric acid, and particulate nitrate. The three-hour average NO_x concentrations show the effects of nearby mobile sources evident in the hourly data but are not displayed.

Figure 9.3-9 indicates that nitrate concentrations increase during the daytime, while the Figures 9.3-3 and 9.3-4 indicate that NO_x concentrations decrease during this time period. NO_x concentrations are much larger than nitrate concentrations, so the ambient N+O species concentrations decrease during the daytime. The opposite trends in nitrate and NO_x cause the fraction of the nitrogen converted to nitrate to increase rapidly during the day. Even so, the median nitrogen conversions never exceeded 8% at Brighton and 4% at Welby. The 75th

percentile conversions were less than 12% at Brighton and 5% at Welby. The largest conversions measured were ~20%. These data indicate that most of the measured "N+O" species is in the form of NO_x.

The increase in the fraction of the "ambient N+O species" as nitrate that occurs during the day is due to some combination of: 1) photochemical oxidation during the daytime; 2) nighttime oxidation via the NO_3 radical; and 3) mixing down during the day of pollutants aged aloft. Of these, daytime photochemical oxidation is believed to be the most important. There is good evidence that coherent plumes aloft are not the dominant cause of the observations: 1) the same diurnal profiles and distribution among chemical species are observed for nitrogen compounds in the San Joaquin Valley (SJV) in California during the winter (Kumar et al., 1998); 2) the SJV does have large point sources that cause plumes aloft like those in the NFRAQS area; and 3) elevated point source plumes typically contain NO, which inhibits nitrate formation, and are relatively deficient in VOC (volatile organic compounds) and O_3, which enhance nitrate formation.

If any nitrate were formed via the nighttime NO_3 reaction pathway, this would most likely occur aloft because surface NO emissions would quench the NO_3 radical concentration. NO and O_3 concentrations aloft at night were not measured during NFRAQS, so the possibility of some nighttime nitrate formation aloft via the NO_3 radical cannot be ruled out. However, it is known that the daytime photochemical oxidation of NO_2 to nitrate does occur both at the surface and aloft, and that this chemical reaction pathway provides an adequate explanation of the observations.

Figure 9.3-10 shows data from 6- and 12-hour SFS sampling periods at Welby, Brighton, and Evans. The longer sample times provide less time resolution. The large fractions of sulfur converted to particulate sulfur before dawn at Welby, shown in the hourly data in Figure 9.3-7, are not apparent in Figure 9.3-10. The large fractions of sulfur converted to particulate sulfur during the night show only in the data for Evans.

The average data during the 6- and 12-hour filter sampling periods show only a few percent of the NO_x converted to nitrate at Welby and Brighton. At Evans, the fraction of the nitrogen species converted to nitrate is larger than at the other two sites, and is ~10% or more on 25% of the days during the afternoon (1200 to 1800 MST) filter samples.

9.4 Particulate Sulfate and Nitrate from Coal and Other Fuel Combustion

Nitrate and sulfate are formed in the atmosphere from NO_x and SO_2 emissions, and they have the same chemical composition regardless of the emissions source. As indicated in Tables 9.2-1 and 9.2-2, the CMB does not apportion these species to precursor gas emitters. In this section, data for the relative amounts of nitrogen and sulfur species in the atmosphere are used to obtain information about the relative importance of surface and major point source contributions to particulate ammonium nitrate. It is found that the atmosphere typically does not contain enough sulfur for the major point sources to have contributed more than a small fraction of the NO_x emissions that are converted to nitrate.

Table 9.1-1 summarizes the average SO_2 and NO_x emissions rates and their ratios that were used in the transport simulations described in Section 9.1. The ratio (on a mole basis) of NO_x to SO_2 in the emissions from the major point sources that influence ambient concentrations at the NFRAQS core monitoring sites is in the range from 0.6 to 1.5 when these sources are burning coal. Mobile sources, or point sources that burn gas, emit much higher ratios of NO_x to SO_2. The average ratio of NO_x to SO_2 in the emissions from surface sources in Table 9.1-1 (identified by a source flag value of nine) is 27. These ratios are so different that the relative amounts of nitrogen and sulfur species in the atmosphere can give information on the relative contributions of coal-burning sources with tall stack emissions and surface sources to the concentrations of these species. Because ambient concentrations are altered by chemical reactions and by dry deposition, the effects of these processes on ambient concentrations are evaluated before the data for the ratios of nitrogen and sulfur species are presented.

When all sources are nearby so there is little time for dry deposition and chemical reactions in the atmosphere, the relative concentrations of sulfur and nitrogen species can be determined by comparing SO_2 and NO_x concentrations. However, the data in Section 9.3 show that all of the sulfur in the atmosphere is, at times, completely converted to particulate sulfur. If not accounted for, this conversion of SO_2 to sulfate could distort the calculations. The effect of chemical reactions in the atmosphere on the calculated ratios of nitrogen to sulfur species was removed, as much as possible, in the analyses below by comparing the sum of the concentrations of NO_x and its reaction products with the sum of the concentrations of SO_2 and its reaction products. Some reaction products of NO_x, such as PAN (peroxyacetyl nitrate), were not measured.

Ambient sulfur and nitrogen species concentrations are also altered by dry deposition. An upper limit for the effect of dry deposition of SO_2 on ambient sulfur concentrations can be obtained from the results of the gridded transport simulations performed with and without dry deposition of SO_2 as described in Sections 9.1.2 and 9.1.3 and reported in Fujita et al. (1998). The effects of dry deposition are briefly summarized in Table 9.4-1, which shows the ratio of the average SO_2 concentrations calculated with and without deposition at each of four receptor sites for both of the episodes simulated. Chemical reactions were not included in these simulations; it was assumed all ambient sulfur remained in the form of SO_2, which is deposited much more rapidly than particulate sulfur. Also, an SO_2 deposition velocity of 1.5 cm/sec was used, and this is an upper limit for most types of land use in the NFRAQS area during the daytime, and is much larger than the expected nighttime value (Wesely, 1989). The calculated effect of dry deposition of SO_2 on ambient sulfur concentrations would have been significantly smaller than in Table 9.4-1 if the slower deposition of sulfate and SO_2 at night had been accounted for.

Additional information on the effects of dry deposition on sulfur concentrations is summarized in Table 9.4-2. The average SO_2 concentrations during the 01/13/97 to 01/21/97 episode calculated by both the gridded and puff simulations with no dry deposition are compared with the average measured total ambient sulfur concentrations. These data are from Tables C.3-13 through C.3-16 of Fujita et al. (1998). The simulations and observations are in reasonable agreement at all sites, except Welby, where the simulations overestimate

sulfur concentrations. The disagreement at Welby could be due to uncertainties in: 1) data for nearby emissions; 2) the simulation methods; and 3) ambient measurements. The approximate agreement at other sites could be fortuitous. Even so, the data in Table 9.4-2 provide some support for the above analyses indicating that the results in Table 9.4-1 overestimate the effects of SO_2 dry deposition on ambient sulfur concentrations.

Nitrogen species are also deposited. NO is deposited quite slowly, but the deposition velocity for NO_2 is approximately the same as for SO_2 (Wesely, 1989). Nitric acid is deposited very rapidly. The data in Section 8 indicate that only a small fraction of the ambient nitrate is in the form of nitric acid, but when it is removed by deposition, ammonium nitrate may evaporate to replenish the removed nitric acid. Calculations have not been done to estimate the effect of dry deposition on the ambient concentrations of nitrogen species, but they are not negligible. As with sulfur, removal of nitrogen species by deposition would be greatest at Evans, where the pollutant age and conversion to oxidized forms is greatest. All of the above considerations indicate that on average, dry deposition would increase the ratio of nitrogen to sulfur species by less than a factor of ~2 at Evans, and by less than ~20% at Welby.

Table 9.4-3 shows data for the dependence of the fraction F of the ambient "N+O species" attributable to the emissions of coal-fired point sources on: 1) the ratio of NO_x to SO_2 in point source emissions; 2) the ratio of NO_x to SO_2 in surface emissions; and 3) the measured ratio r of "N+O species" to total ambient sulfur at a monitoring site. Effects of dry deposition were ignored. The first column is the value of the measured ambient ratio r, which appears in the plots presented below. The second column is the fraction F calculated for the emission ratios from Table 9.1-1 discussed at the beginning of this section. In this case, when the ambient "N+O species" concentrations exceed eight times the ambient sulfur concentrations, less than 10% of the "N+O species" are attributable to coal-fired point sources. The third column shows values for the fraction F when the ratio of NO_x to SO_2 in the surface emissions is doubled to 54. This doubling could be caused either by: 1) smaller SO_2 emissions by surface sources than in the emission inventory; or 2) preferential deposition of SO_2 from surface sources. The fourth column shows the effect of doubling the NO_x to SO_2 ratio in only the point source emissions, and the fifth column shows the effect of doubling both. As indicated above, the data in the fourth and fifth columns probably overestimate the effects of dry deposition on the emissions from major point sources. The data in Table 9.4-3 are used in the interpretation of the ambient data presented below.

Figure 9.3-10 shows data from the 6- and 12-hour SFS sampling periods for the ratios of the concentrations of sulfur species (SO_2 plus particulate sulfur) to "N+O species" (NO_x plus particulate nitrate). Nitric acid was not measured with this time resolution. The ratio of sulfur "N+O species" shown at the bottom of Figure 9.3-10 is the reciprocal of the ratio in the first column of Table 9.4-3. The reason for inverting the data is to better display the data points for relatively high sulfur concentrations, which correspond to larger contributions of coal-fired point sources. Numerical values for these ratios also appear in Table 9.4-4, where the data have not been inverted. The values on the y-axis at the bottom of Figure 9.3-10 are the reciprocals of the data in Table 9.4-4.

Figure 9.4-1 shows data for the ratios of sulfur to "N+O species" calculated from the three-hour filter samples collected at Welby and Brighton. Nitric acid was measured with this time resolution and was added to the particulate nitrate and NO_x concentrations to determine the "N+O species" concentrations. Numerical data for the three-hour samples are in Table 9.4-5. This figure and table follow the same conventions as Figure 9.3-10 and Table 9.4-4; the data in the figure are inverted. These three-hour ratios are consistent with the 6- and 12-hour results, except that the shorter sampling interval shows more times when the effects of major point sources are significant. This is expected, because point-source plumes typically do not impact a monitoring site for more than a few hours at a time.

With the exception of the three-hour samples beginning at noon, the median ratios from both filter averaging times are 9 or greater. This ratio indicates that for the medians, less than 10% of the ambient "N+O species" is due to coal-fired point sources. The nitrate concentrations were typically higher at Evans than at other sites. At Evans, the median ratio is 19 or greater, indicating less than 10% of the ambient "N+O species" due to coal-fired sources even when the emission ratios in Table 9.4-3 are adjusted to 54 and 2. Most of the time, emissions from coal-fired sources contribute less than 10% of the ambient "N+O species."

The data in Figure 9.4-1 show that there are times when contributions from coal-fired sources are dominant, especially at Welby. Events in which elevated plumes are mixed to the surface are described in Section 9.1.5. The ratios show that the effects of coal-fired sources are greatest during the filter sample times starting at noon. The discussion of these data continues in Section 9.4.3.

Figure 9.4-2 shows the same three-hour data as Figure 9.4-1. The y-axis is the sum of the concentrations of sulfur species and the x-axis is the sum of the concentrations of "N+O species." Logarithmic scales are used to simplify the presentation of data for concentration ratios, and the values of the ratios are indicated by the diagonal grid lines. Low ambient concentrations are at the lower left, and high concentrations at the upper right. The dotted lines in the upper panel of Figure 9.4-1 show the ratios from Table 9.1-1 of nitrogen to sulfur emissions from sources that make the greatest contribution to sulfur and nitrogen species concentrations at these sites.

These figures show that the ratios of the concentrations of nitrogen to sulfur species do not depend on whether the concentrations are high or low. Few data points have a concentration ratio similar to that for coal-burning point sources. Most data points have a ratio closer to that for surface sources than for coal-burning sources. Many data points have a ratio of nitrogen to sulfur species larger than the ratio for the combined emissions from the surface sources in Table 9.1-1.

Tables 9.4-4 and 9.4-5 show that the ratios of "N+O" to sulfur species larger than 100 occur mostly during the night and early morning hours. Ten percent of the 12-hour nighttime samples have a ratio larger than 156 at Evans and larger than 131 at Welby. Since dry deposition is highest during daytime and lowest at night, this observation indicates that some significant sources of NO_x emit very little SO_2. This explanation of the high nitrogen to sulfur

ratios is supported by the fact that SO_2 concentrations at Welby from surface emissions from transport simulations exceeded the measured ambient sulfur concentrations. (The possible role of meteorology, e.g., deposition by rain or snow, has not been investigated. Dense fogs can selectively remove soluble species by droplet settling.)

The 6- and 12-hour SFS measurements in Figure 9.3-10 were also plotted in this logarithmic format, but are not shown. The results for Welby and Brighton were similar to those for the same sites in Figure 9.4-2. The results for Evans were similar to those for Welby, except that there were no data points close to the 1:1 line.

The data presented above and in Section 9.3 indicate that during most of the filter sampling time periods, less than 10% of the ambient "N+O species" were attributable to the emissions from coal-fired power stations. These data also show a few events during which power station emissions were clearly dominant. The following discussion focuses on the smaller values in the distribution of ratios of "N+O" to sulfur species, where the contribution of the emissions of major coal-fired sources is greatest. It also comments on the changes in nitrate concentrations likely to result from decreases in NO_x emissions.

Nitrate concentrations were higher at Evans than at any other core site most of the time. It was shown above that for the median ambient ratios of "N+O" to sulfur species, the contribution of coal-fired sources to "N+O species" was less than 10%. The data in Table 9.4-4 show that the 10^{th} percentile values of the ratio of "N+O" to sulfur species range from 7 to 12. For emission ratios at the left of Table 9.4-3, these ratios correspond to contributions of coal-fired sources to "N+O species" concentrations between 5% and 11%. If the emission ratios are doubled, the right column of Table 9.4-3 shows contributions ranging from 13% to 26%. The contributions of coal-fired sources to ambient "N+O species" are estimated to be less than 15%, and probably not more than 20%, for 90% of the filter samples, and less than 10% for more than 50% of the filter samples.

Table 9.4-5 shows a three-hour ambient ratio as small as 4 to 6 about 10% of the time at Welby, and at Brighton the ambient ratios are this small about 20% of the time. These ratios correspond to coal-fired sources contributing approximately 10% to 20% of the ambient "N+O species."

Figures 9.3-9 and 9.3-10 show that more than 90% of the ambient nitrogen species that were measured were NO_x (either NO or NO_2) for most samples. Less than 10% of the ambient "N+O species" were converted to inorganic nitrate (nitric acid plus particulate nitrate). The possibility that the efficiency of conversion of NO_x to nitrate could depend on the source of the NO_x should be evaluated. Also, when designing control strategies, the effects of changes in emissions on nitrate concentrations should be considered.

The wintertime photochemistry of urban areas is generally sunlight- and VOC-limited, rather than NO_x-limited. According to the current understanding of VOC/NO_x systems, a 10% decrease in NO_x concentrations would result in less than a 10% decrease in inorganic nitrate (nitric acid plus particulate nitrate) if other variables such as sunlight, temperature, VOC concentrations, VOC composition, CO, and ozone concentration remain constant

(Carter, 1990). The reason for the less than 1:1 response is that the efficiency of nitric acid production from NO_2 increases as the VOC to NO_x ratio increases. Given the same background ozone levels, lower NO_x levels will increase the relative rate of NO to NO_2 conversion because of the higher HO radical concentrations associated with higher VOC to NO_x ratios.

It is also estimated that a decrease in NO_x emissions from major coal-fired point sources will result in a smaller decrease in nitrate than a similar reduction in NO_x from surface sources. One reason is that under stable conditions, plumes contain relatively high concentrations of NO, which inhibit all oxidation reactions. Another is that major point sources do not emit large amounts of VOC, so that nitrate formation in the plume is VOC limited. When the plumes are mixed to the ground in rural areas, the oxidation is still VOC limited. It is only when the plume is mixed to the ground in urban areas that the fraction of the NO_x oxidized to nitrate would become comparable to that for surface emissions.

Ammonia does not play a significant role in the reactions that convert NO_x into nitrate (nitric acid plus particulate nitrate). As shown in Section 8, ammonia reacts with nitric acid, an invisible gas, to convert it to particulate nitrate, which contributes to $PM_{2.5}$ and to perceptible haze. Section 8 also shows that ammonia is typically present in excess for the formation of ammonium nitrate from nitric acid. Most of the nitrate is in the form of particulate ammonium nitrate under present conditions, and this would continue to be the case if ammonia emissions remained unchanged and NO_x emissions decreased.

In summary, it is estimated that a 10% decrease in NO_x emissions in the NFRAQS domain would decrease nitrate concentrations by less than 10%. Before it becomes mixed with other pollutants, NO_x from major point sources is less rapidly oxidized to nitrate than NO_x from surface sources. During ~90% of the filter samples, less than 10% to 15% of the ambient "N+O species" were due to the emissions from major coal-fired power plants. A major decrease in these NO_x emissions would decrease particulate nitrate concentrations by less than 10% to 15%. This limit to the contribution of major point sources to nitrate was based on the ratios of nitrogen to sulfur species observed in the atmosphere. The atmosphere does not contain the amount of sulfur that would have to be there if the major elevated point sources made a larger contribution to nitrogen species than estimated here.

A complex computer simulation containing physical meteorological representations and explicit chemical transformation mechanisms can be applied to these data to obtain more quantitative representations of source contributions and relationships to changes in specific precursor emissions. These may or may not be more accurate that the estimates presented here. At a lower level of effort, NFRAQS measurements could be stratified according to the particulate nitrate concentration and the composition of the atmosphere examined to estimate the relative contributions of surface and elevated sources during time periods with high particulate nitrate concentrations.

Table 9.1-1
Summary of the Emission Rates Used in the Transport Simulations

Source	Data Source	Source Flag	Emission Rate (tons/day) Sulfur Dioxide	Nitrogen Oxides	NO_x/SO_2 Mole Ratio
Arapahoe	CEM	1	16.82	18.60	1.54
Cherokee	CEM	2	43.74	41.03	1.31
Pawnee	CEM	3	33.47	9.67	0.40
Valmont	CEM	4	15.03	6.16	0.57
Rawhide	CEM	5	1.69	6.94	5.71
Trigen	CDPHE	6	6.26	4.14	0.92
Refineries	CDPHE	7	1.58	2.32	2.04
Other Elevated Pt	CDPHE	8	5.48	8.2	2.08
Low Point	CDPHE	9	6.9	62.0	12.50
Mobile	CDPHE	9	7.3	207.5	39.55
Area	CDPHE	9	2.3	58.5	35.39
Wood Comb.	CDPHE	9	0.2	1.2	8.35
Airport	CDPHE	Omitted	0.06	6.3	
Total Modeled			140.8	426.3	4.21
Total with Source Flag 9 (See column 3)			16.7	329.2	27.43
Surface sources in CMB			7.5	208.7	38.72
Surface sources not in CMB			9.2	120.5	18.22

Table 9.1-2
Cumulative Frequency Distributions of SO_2 Concentrations at Brighton during the 01/12/97 to 01/21/97 Episode Calculated by the Gridded Transport Simulations with and without Dry Deposition

	SO2 Concentrations (ppbv)			SO2 Concentrations (ppbv)			SO2 Concentrations (ppbv)		
	No Dry Deposition	With Dry Deposition	Concent-ration Ratios	No Dry Deposition	With Dry Deposition	Concent-ration Ratios	No Dry Deposition	With Dry Deposition	Concent-ration Ratios
	Surface Sources			**Valmont**			**Rawhide**		
max	33.05	8.71	0.263	6.33	1.94	0.306	0.013	0.009	0.692
5%	15.66	5.47	0.349	1.63	1.05	0.646	0.002	0.001	0.250
10%	9.38	3.09	0.330	1.06	0.74	0.699	0.000	0.000	
20%	4.08	1.90	0.467	0.424	0.261	0.616			
30%	1.82	0.89	0.490	0.248	0.154	0.622			
40%	0.98	0.56	0.573	0.086	0.057	0.663			
50%	0.73	0.42	0.573	0.013	0.007	0.511			
60%	0.50	0.30	0.587	0.005	0.000	0.085			
Avg	2.97	1.10	0.369	0.34	0.18	0.547	0.000	0.000	
	Cherokee			**Trigen**			**Total SO2 Predicted**		
max	28.12	15.54	0.552	1.89	0.79	0.419	56.98	18.69	0.328
5%	8.49	4.79	0.564	0.59	0.28	0.469	26.18	9.79	0.374
10%	5.00	2.36	0.472	0.34	0.17	0.513	14.79	7.38	0.499
20%	1.81	0.87	0.478	0.16	0.068	0.436	9.01	4.04	0.449
30%	0.69	0.44	0.642	0.065	0.028	0.427	5.97	3.04	0.510
40%	0.16	0.074	0.462	0.029	0.010	0.346	4.01	1.96	0.487
50%	0.022	0.011	0.502	0.006	0.002	0.379	1.62	1.07	0.662
60%	0.009	0.004	0.420	0.001	0.000		0.98	0.55	0.563
Avg	1.53	0.79	0.513	0.12	0.053	0.444	5.74	2.52	0.439
	Refineries			**Pawnee**					
max	5.90	2.05	0.348	0.50	0.25	0.501			
5%	2.43	1.21	0.501	0.35	0.14	0.401			
10%	1.50	0.78	0.517	0.15	0.062	0.411			
20%	0.64	0.40	0.629	0.06	0.02	0.338			
30%	0.31	0.19	0.623	0.03	0.009	0.268			
40%	0.12	0.077	0.663	0.015	0.002	0.158			
50%	0.035	0.023	0.647	0.001	0.000				
60%	0.008	0.004	0.461	0.000					
Avg	0.45	0.22	0.499	0.051	0.020	0.397			
	Arapahoe			**Other Point Sources**					
max	3.83	2.39	0.624	0.461	0.193	0.418			
5%	1.68	0.88	0.522	0.187	0.124	0.664			
10%	0.79	0.53	0.672	0.138	0.085	0.615			
20%	0.18	0.093	0.515	0.067	0.043	0.645			
30%	0.054	0.021	0.378	0.052	0.028	0.532			
40%	0.018	0.011	0.583	0.030	0.019	0.625			
50%	0.004	0.001	0.237	0.015	0.010	0.632			
60%	0.001	0.000		0.008	0.006	0.675			
Avg	0.23	0.13	0.562	0.046	0.027	0.582			

Table 9.1-3
Overview of the SO_2 Concentrations Calculated by the Gridded Transport Simulations with Dry Deposition during the 01/12/97 to 01/21/97 Episode

	Simulated Sulfur Dioxide Concentrations (ppbv)			
	CAMP	Welby	Brighton	Evans
	Surface	Cherokee	Surface	Cherokee
maximum	18	106	8.7	2.2
10%	7.3	38	3.1	1.1
average	2.9	10	1.1	0.2
	Cherokee	Surface	Cherokee	Surface
maximum	25	27	15	1.9
10%	6.0	15	2.4	0.5
average	1.6	6.2	0.8	0.3
	Arapahoe	Refineries	Refineries	Valmont
maximum	4.5	6.3	2.1	1.0
10%	2.2	2.0	0.8	0.3
average	0.5	0.8	0.2	0.08
	Refineries	Arapahoe	Arapahoe	Arapahoe
maximum	4.9	6.0	2.4	0.8
10%	0.9	0.9	0.5	0.1
average	0.3	0.3	0.1	0.05
	Trigen	Trigen	Valmont	Refineries
maximum	1.7	1.5	1.9	0.4
10%	0.6	0.7	0.7	0.2
average	0.2	0.2	0.2	0.03
	Pawnee	Valmont	Trigen	Trigen
maximum	0.2	2.3	0.8	0.4
10%	0.05	0.2	0.2	0.09
average	0.01	0.1	0.05	0.02
	Valmont	Pawnee	Pawnee	Other Point Sources
maximum	0.8	0.1	0.3	0.3
10%	0.09	0.05	0.06	0.04
average	0.04	0.01	0.02	0.02
	Other Point Sources	Other Point Sources	Other Point Sources	Pawnee
maximum	0.1	0.2	0.2	0.2
10%	0.04	0.09	0.09	0.03
average	0.01	0.02	0.03	0.01
	Rawhide	Rawhide	Rawhide	Rawhide
maximum	0.00	0.00	0.01	0.06
10%			0.00	0.00
average			0.00	0.00
	Total	Total	Total	Total
maximum	32	116	18	3.5
10%	16	48	7.4	2.3
average	5.5	18	2.5	0.7

Table 9.1-4
Comparison of the Cumulative Frequency Distributions of SO_2 Concentrations at Brighton during 01/13/97 to 01/21/97 Calculated by the Gridded Transport Simulations with and without Dry Deposition and by the Puff Transport Simulations

	UAM With Dry Deposition	UAM No Dry Deposition	SCIPUFF	UAM (No Deposition)/ SCIPUFF
		Cherokee		
max	11.80	28.12	5.45	5.16
5%	5.06	8.66	1.87	4.63
10%	2.65	5.47	1.35	4.06
20%	1.07	2.50	0.83	3.03
30%	0.48	0.93	0.55	1.70
40%	0.13	0.23	0.38	0.60
50%	0.013	0.034	0.26	0.13
60%	0.006	0.009	0.14	0.063
Avg	0.83	1.65	0.51	3.24
		Valmont		
max	1.88	6.03	3.37	1.79
5%	1.13	1.46	0.86	1.71
10%	0.48	0.73	0.61	1.20
20%	0.22	0.41	0.34	1.22
30%	0.11	0.17	0.26	0.640
40%	0.032	0.051	0.20	0.255
50%	0.006	0.012	0.16	0.075
60%	0.000	0.004	0.10	0.038
Avg	0.16	0.30	0.25	1.22
		Pawnee		
max	0.23	0.50	0.15	3.33
5%	0.12	0.39	0.06	6.38
10%	0.041	0.12	0.03	3.83
20%	0.000	0.009	0.009	0.925
30%		0.000	0.002	
40%		0.000	0.000	
50%				
60%				
Avg	0.012	0.036	0.009	4.27

		Totals	
		No Dry Deposition	
	UAM Total	UAM-SCIPUFF Hybrid Total	Measured Ambient Sulfur
max	57.0	36.4	69.5
5%	27.3	20.7	14.7
10%	15.9	11.2	10.5
20%	9.91	6.07	7.36
30%	6.66	3.17	5.48
40%	4.18	1.27	3.62
50%	2.24	0.71	2.71
60%	1.27	0.12	1.80
Avg	6.17	3.58	5.84

Table 9.1-5
Summary of the Air Quality and Meteorological Phenomena Associated with SO_2 Pulses

	Date of SO_2 Pulse Observed At Welby						
	12/15/96	**12/26/96**	**12/31/96**	**1/2/97**	**1/7/97**	**1/14/97**	**1/20/97**
MAXIMUM SO2 (ppbv)	44	59	41	45	52	102	92
OBSERVED MIXING	Y	N	?	Y	N	Y	Y
NOx CHANGE	INCREASED	INCREASED	NOT AVAILABLE	DECREASED	DECREASED	INCREASED	DECREASED
NO CHANGE	INCREASED	INCREASED	NOT AVAILABLE	DECREASED	DECREASED	INCREASED	DECREASED
CO CHANGE	NO CHANGE	NO CHANGE	INCREASED	NO CHANGE	DECREASED	INCREASED	DECREASED
PARTICULATE SULFATE	N	Y	N	Y	N	Y	N
LIQUID WATER	N	Y	N	N	N	Y	N

Table 9.2-1
Contributions to $PM_{2.5}$ at Core Sites – NFRAQS Winter 1996/97, Extended Species CMB

Site	Brighton				Welby			
Start Hour (MST)	06	12	18	06	06	12	18	06
Duration	6	6	12	24	6	6	12	24
Observations	16	14	17		16	15	17	
Concentration (ug/m3)	12.6 ± 1.0	14.0 ± 1.0	10.9 ± 0.7	12.1 ± 0.9	18.6 ± 1.2	17.4 ± 1.1	14.5 ± 0.8	16.3 ± 1.0
R-square	0.93 ± 0.01	0.93 ± 0.01	0.93 ± 0.01	0.93 ± 0.01	0.91 ± 0.01	0.94 ± 0.01	0.93 ± 0.01	0.93 ± 0.01
Chi-square	0.29 ± 0.04	0.28 ± 0.03	0.37 ± 0.04	0.33 ± 0.04	0.45 ± 0.05	0.34 ± 0.04	0.46 ± 0.07	0.43 ± 0.06
Percent Mass Attributed	100.5 ± 3.2	101.0 ± 4.2	103.4 ± 2.4	102.1 ± 3.1	105.1 ± 2.2	105.4 ± 2.7	102.5 ± 1.6	103.9 ± 2.1
Absolute Contributions (ug/m3) [a, b, c]								
LDGV, cold start	0.45 ± 0.53	0.55 ± 0.59	0.36 ± 0.38	0.43 ± 0.48	2.50 ± 1.40	1.33 ± 0.95	1.92 ± 0.94	1.91 ± 1.08
LDGV, hot stabilized	0.17 ± 0.11	0.15 ± 0.13	0.10 ± 0.08	0.13 ± 0.10	0.65 ± 0.27	0.45 ± 0.20	0.40 ± 0.17	0.47 ± 0.21
LDGV, high particle emitter	2.69 ± 0.97	2.18 ± 1.06	2.04 ± 0.64	2.24 ± 0.85	2.51 ± 1.94	2.30 ± 1.53	1.89 ± 1.29	2.15 ± 1.54
Diesel Exhaust	1.19 ± 0.49	1.07 ± 0.50	1.05 ± 0.35	1.09 ± 0.43	2.38 ± 1.13	1.68 ± 0.72	1.48 ± 0.76	1.76 ± 0.86
Meat Cooking	0.24 ± 0.61	0.32 ± 0.69	0.08 ± 0.49	0.18 ± 0.58	0.48 ± 1.23	0.51 ± 1.17	0.69 ± 0.90	0.59 ± 1.06
Wood Combustion (Softwood)	0.11 ± 0.16	0.09 ± 0.17	0.07 ± 0.12	0.09 ± 0.14	0.26 ± 0.28	0.11 ± 0.19	0.47 ± 0.31	0.33 ± 0.28
Wood Combustion (Hardwood)	0.16 ± 0.26	0.15 ± 0.25	0.11 ± 0.16	0.13 ± 0.21	0.37 ± 0.60	0.23 ± 0.36	0.56 ± 0.45	0.43 ± 0.47
Paved Road Dust	1.22 ± 0.50	1.26 ± 0.50	0.96 ± 0.37	1.10 ± 0.44	3.96 ± 1.26	3.53 ± 1.14	2.11 ± 0.67	2.93 ± 0.97
Ammonium Sulfate	1.81 ± 0.30	1.98 ± 0.31	1.65 ± 0.24	1.77 ± 0.28	1.58 ± 0.30	1.91 ± 0.33	1.62 ± 0.26	1.68 ± 0.29
Ammonium Nitrate	4.04 ± 0.53	5.41 ± 0.66	4.26 ± 0.50	4.49 ± 0.55	3.87 ± 0.48	5.26 ± 0.59	3.47 ± 0.41	4.02 ± 0.48
Coal-Fired Powerplant	0.28 ± 0.52	0.27 ± 0.53	0.17 ± 0.36	0.22 ± 0.45	0.55 ± 0.81	0.38 ± 0.75	0.30 ± 0.48	0.39 ± 0.65
Unexplained	0.22	0.61	0.06	0.24	-0.48	-0.29	-0.37	-0.38
Percent Contributions [c, d]								
LDGV, cold start	3.5 ± 1.1	3.7 ± 0.9	3.5 ± 0.7	3.6 ± 0.9	13.1 ± 2.5	7.8 ± 1.7	13.3 ± 2.5	11.9 ± 2.3
LDGV, hot stabilized	2.1 ± 0.7	1.3 ± 0.5	1.3 ± 0.3	1.5 ± 0.5	3.9 ± 1.0	3.0 ± 0.6	2.8 ± 0.7	3.2 ± 0.8
LDGV, high particle emitter	20.5 ± 2.2	16.6 ± 2.1	19.0 ± 1.8	18.8 ± 2.0	13.5 ± 2.8	13.5 ± 2.0	11.8 ± 1.9	12.7 ± 2.2
Diesel Exhaust	9.8 ± 1.5	7.7 ± 1.3	10.2 ± 1.3	9.5 ± 1.3	11.0 ± 1.5	9.3 ± 1.3	9.8 ± 1.3	10.0 ± 1.4
Meat Cooking	2.6 ± 1.1	3.1 ± 1.2	0.9 ± 0.4	1.9 ± 0.9	2.5 ± 0.7	3.0 ± 1.0	4.6 ± 1.4	3.7 ± 1.2
Wood Combustion (Softwood)	1.2 ± 0.5	0.6 ± 0.1	0.8 ± 0.1	0.8 ± 0.3	1.7 ± 0.5	0.9 ± 0.2	2.9 ± 1.0	2.1 ± 0.8
Wood Combustion (Hardwood)	1.5 ± 0.3	1.2 ± 0.3	1.2 ± 0.3	1.3 ± 0.3	1.7 ± 0.3	1.4 ± 0.3	3.8 ± 1.5	2.7 ± 1.1
Paved Road Dust	10.6 ± 1.9	10.3 ± 1.9	9.8 ± 1.7	10.1 ± 1.8	18.1 ± 3.0	18.0 ± 3.2	14.1 ± 1.9	16.1 ± 2.6
Ammonium Sulfate	13.1 ± 1.7	15.0 ± 1.9	15.1 ± 1.7	14.6 ± 1.8	8.3 ± 1.1	11.0 ± 1.8	10.5 ± 1.7	10.1 ± 1.6
Ammonium Nitrate	27.7 ± 3.9	31.6 ± 3.8	33.6 ± 3.4	31.6 ± 3.6	21.4 ± 2.7	27.6 ± 3.1	22.6 ± 3.0	23.5 ± 3.0
Coal-Fired Powerplant	2.6 ± 0.3	2.4 ± 0.4	1.8 ± 0.2	2.1 ± 0.3	2.9 ± 0.4	2.3 ± 0.3	2.0 ± 0.4	2.3 ± 0.4
Unexplained	4.9 ± 2.0	6.5 ± 2.3	2.8 ± 1.0	4.2 ± 1.7	1.8 ± 0.7	2.1 ± 1.3	1.5 ± 0.8	1.7 ± 0.9

a Nonzero concentrations set to minimum of uncertainty/2.
b Uncertainties are root mean squares of the individual 1-sigma error propagations from CMB. Zero uncertainties are excluded from RMS.
c Samples with percent mass attribution > 120 percent are removed from average source contributions.
d Contributions are normalized to sum of contributions including non-negative unexplained contributions. Uncertainties are standard errors of mean percent contributions.

Table 9.2-2
Averages of 24-Hour Contributions to $PM_{2.5}$ at Core and Satellite Sites from Conventional CMB – NFRAQS Winter 1996/97

Site	Chatfield	Highlands	CAMP	Welby	Brighton	Longmont	Fort Collins	Evans	Masters
Start Hour (MST)	0600	0600	0600	0600	0600	0600	0600	0600	0600
Duration	24	24	24	24	24	24	24	24	24
Observations	12	22	17	16	20	18	22	15	18
Concentration (ug/m^3)	8.30 ± 2.35	8.98 ± 0.84	22.06 ± 1.31	14.59 ± 0.96	10.06 ± 0.78	15.38 ± 1.02	14.66 ± 0.96	22.73 ± 1.39	23.01 ± 1.42
R-square	0.88 ± 0.03	0.97 ± 0.00	0.98 ± 0.00	0.97 ± 0.00	0.98 ± 0.00	0.98 ± 0.00	0.97 ± 0.00	0.97 ± 0.00	0.97 ± 0.00
Chi-square	0.20 ± 0.01	0.30 ± 0.04	0.42 ± 0.08	0.43 ± 0.05	0.26 ± 0.03	0.28 ± 0.03	0.40 ± 0.04	0.44 ± 0.07	0.33 ± 0.04
Percent Mass Attributed	83.9 ± 4.9	111.3 ± 5.0	97.6 ± 2.4	103.5 ± 3.2	104.8 ± 3.5	95.1 ± 3.9	100.0 ± 2.2	94.3 ± 1.3	90.4 ± 3.1
Absolute Contributions (ug/m^3) [a]									
Light-Duty Gasoline Vehicle Exhaust	1.19 ± 2.68	2.42 ± 1.79	6.57 ± 3.02	4.61 ± 2.39	2.01 ± 1.32	2.22 ± 1.61	2.77 ± 2.11	3.74 ± 2.00	1.25 ± 2.53
Diesel Exhaust	0.31 ± 1.13	0.52 ± 0.61	2.49 ± 1.15	1.42 ± 0.85	1.09 ± 0.38	1.27 ± 0.36	1.64 ± 0.46	1.63 ± 0.51	0.67 ± 0.36
Paved Road Dust	1.79 ± 0.98	1.40 ± 0.49	2.65 ± 0.99	2.71 ± 0.88	0.71 ± 0.37	0.96 ± 0.48	2.70 ± 0.93	1.13 ± 0.62	5.86 ± 1.83
Meat Cooking and Wood Combustion	1.02 ± 1.73	1.04 ± 1.26	1.45 ± 2.31	0.83 ± 1.82	0.73 ± 1.14	0.92 ± 1.35	1.18 ± 1.97	1.14 ± 1.76	1.43 ± 1.78
Ammonium Sulfate	1.02 ± 0.23	1.21 ± 0.23	2.74 ± 0.41	1.37 ± 0.24	1.48 ± 0.24	1.85 ± 0.30	1.21 ± 0.22	3.01 ± 0.43	2.24 ± 0.42
Ammonium Nitrate	1.52 ± 0.27	2.45 ± 0.38	5.38 ± 0.62	3.64 ± 0.44	3.75 ± 0.45	6.61 ± 0.67	4.74 ± 0.49	10.12 ± 1.08	8.47 ± 0.94
Coal-Fired Power Plant	0.17 ± 1.05	0.10 ± 0.39	0.21 ± 0.75	0.09 ± 0.61	0.24 ± 0.38	0.38 ± 0.46	0.30 ± 0.63	0.52 ± 0.60	0.41 ± 0.92
Unexplained	1.28	-0.15	0.57	-0.08	0.04	1.17	0.12	1.45	2.68
Percent Contributions [b]									
Light-Duty Gasoline Vehicle Exhaust	14.5 ± 3.5	29.7 ± 2.6	30.5 ± 2.1	31.3 ± 3.2	19.7 ± 2.2	13.9 ± 1.8	18.0 ± 1.9	16.3 ± 1.5	5.4 ± 1.6
Diesel Exhaust	2.7 ± 1.4	5.3 ± 1.2	10.6 ± 1.3	9.0 ± 1.2	11.4 ± 1.3	8.6 ± 1.2	10.5 ± 1.2	7.1 ± 0.6	2.7 ± 0.4
Paved Road Dust	21.0 ± 4.5	18.9 ± 2.9	12.2 ± 2.9	16.7 ± 2.9	7.9 ± 1.4	7.5 ± 2.1	19.1 ± 3.4	6.3 ± 2.1	26.9 ± 5.5
Meat Cooking and Wood Combustion	15.6 ± 2.7	11.3 ± 2.2	6.5 ± 1.7	6.0 ± 1.5	8.0 ± 1.0	6.6 ± 0.8	8.3 ± 1.1	6.7 ± 1.5	6.9 ± 0.9
Ammonium Sulfate	10.5 ± 2.4	10.1 ± 1.4	12.0 ± 1.6	9.6 ± 1.5	13.6 ± 1.4	11.8 ± 1.4	8.2 ± 1.2	14.2 ± 1.6	10.7 ± 1.3
Ammonium Nitrate	16.8 ± 2.2	18.9 ± 3.2	22.3 ± 2.4	23.2 ± 2.8	32.5 ± 3.0	40.3 ± 2.5	29.7 ± 2.9	40.2 ± 3.1	34.1 ± 4.3
Coal-Fired Power Plant	1.8 ± 0.5	1.7 ± 0.4	1.1 ± 0.3	0.8 ± 0.3	3.1 ± 0.6	2.7 ± 0.4	2.2 ± 0.5	3.3 ± 1.0	2.1 ± 0.7
Unexplained	17.1 ± 4.5	4.0 ± 1.6	4.8 ± 1.8	3.4 ± 0.9	3.7 ± 1.1	8.7 ± 3.0	4.0 ± 1.1	6.0 ± 1.1	11.4 ± 2.3

[a] Uncertainties are root mean squares of the individual 1-sigma error propagations from CMB.

[b] Contributions are normalized to sum of contributions including non-negative unexplained contributions. Variabilities are standard errors of the mean.

Table 9.2-3
Contributions to Sulfur Dioxide at Core Sites – NFRAQS Winter 1996/97, Extended Species CMB

Site	Brighton				Welby			
Start Hour (MST)	06	12	18	06	06	12	18	06
Duration	6	6	12	24	6	6	12	24
Observations	18	17	16		19	20	18	
Concentration (ug/m3)	14.0 ± 5.4	13.5 ± 5.3	10.9 ± 5.2	12.3 ± 5.3	20.0 ± 5.7	15.1 ± 5.3	9.1 ± 5.1	13.3 ± 5.3
R-square	0.93 ± 0.01	0.93 ± 0.01	0.93 ± 0.01	0.93 ± 0.01	0.92 ± 0.01	0.93 ± 0.01	0.93 ± 0.01	0.93 ± 0.01
Chi-square	0.33 ± 0.03	0.30 ± 0.04	0.38 ± 0.03	0.35 ± 0.03	0.44 ± 0.04	0.37 ± 0.04	0.41 ± 0.05	0.41 ± 0.05
Percent Mass Attributed	144.4 ± 30.8	142.5 ± 41.9	65.9 ± 16.8	104.7 ± 28.6	175.3 ± 33.4	193.3 ± 37.4	123.6 ± 23.3	153.9 ± 30.0
Absolute Contributions (ug/m3) [a, b, c]								
LDGV, cold start	0.22 ± 0.33	0.24 ± 0.43	0.20 ± 0.28	0.21 ± 0.34	1.33 ± 1.92	0.62 ± 0.87	0.98 ± 1.40	0.98 ± 1.45
LDGV, hot stabilized	0.41 ± 0.41	0.37 ± 0.41	0.24 ± 0.23	0.32 ± 0.33	1.62 ± 1.53	1.07 ± 1.01	1.00 ± 1.06	1.18 ± 1.18
LDGV, high particle emitter	0.46 ± 0.30	0.39 ± 0.24	0.31 ± 0.20	0.37 ± 0.24	0.36 ± 0.29	0.38 ± 0.24	0.29 ± 0.26	0.33 ± 0.26
Diesel Exhaust	0.63 ± 0.55	0.60 ± 0.50	0.51 ± 0.43	0.56 ± 0.48	1.01 ± 0.96	0.67 ± 0.57	0.69 ± 0.64	0.77 ± 0.72
Meat Cooking	0.00 ± 0.00	0.00 ± 0.01	0.00 ± 0.00	0.00 ± 0.00	0.00 ± 0.01	0.00 ± 0.01	0.00 ± 0.01	0.00 ± 0.01
Wood Combustion (Softwood)	0.00 ± 0.00	0.00 ± 0.00	0.00 ± 0.00	0.00 ± 0.00	0.00 ± 0.00	0.00 ± 0.00	0.01 ± 0.01	0.01 ± 0.01
Wood Combustion (Hardwood)	0.00 ± 0.00	0.00 ± 0.00	0.00 ± 0.00	0.00 ± 0.00	0.01 ± 0.01	0.00 ± 0.00	0.01 ± 0.01	0.01 ± 0.01
Coal-Fired Powerplant	10.18 ± 3.16	8.82 ± 3.34	3.43 ± 2.57	6.47 ± 2.93	22.64 ± 7.72	17.23 ± 5.65	5.44 ± 3.56	12.69 ± 5.41
Unexplained	2.10	3.09	5.54	4.06	-7.99	-4.90	0.70	-2.87
Percent Contributions [c, d]								
LDGV, cold start	1.3 ± 0.4	2.4 ± 0.6	7.0 ± 1.7	4.4 ± 1.3	5.9 ± 2.0	6.0 ± 1.8	16.6 ± 5.2	11.2 ± 3.9
LDGV, hot stabilized	2.8 ± 0.6	3.4 ± 1.0	12.1 ± 4.3	7.6 ± 3.1	6.5 ± 1.6	9.0 ± 2.7	7.9 ± 3.3	7.8 ± 2.8
LDGV, high particle emitter	3.3 ± 0.9	4.5 ± 1.4	4.6 ± 1.7	4.3 ± 1.5	2.4 ± 0.7	4.0 ± 1.3	2.6 ± 1.2	2.9 ± 1.1
Diesel Exhaust	4.8 ± 1.4	6.3 ± 1.3	6.0 ± 1.4	5.8 ± 1.3	4.7 ± 1.7	6.8 ± 2.2	6.4 ± 1.9	6.1 ± 1.9
Meat Cooking	0.0 ± 0.0	0.0 ± 0.0	0.0 ± 0.0	0.0 ± 0.0	0.0 ± 0.0	0.0 ± 0.0	0.0 ± 0.0	0.0 ± 0.0
Wood Combustion (Softwood)	0.0 ± 0.0	0.0 ± 0.0	0.0 ± 0.0	0.0 ± 0.0	0.0 ± 0.0	0.1 ± 0.0	0.0 ± 0.0	0.0 ± 0.0
Wood Combustion (Hardwood)	0.0 ± 0.0	0.0 ± 0.0	0.0 ± 0.0	0.0 ± 0.0	0.0 ± 0.0	0.0 ± 0.0	0.1 ± 0.1	0.1 ± 0.0
Coal-Fired Powerplant	41.8 ± 10.3	43.5 ± 9.0	38.4 ± 8.8	40.5 ± 9.3	56.2 ± 8.7	45.1 ± 8.3	52.1 ± 10.1	51.4 ± 9.4
Unexplained	45.9 ± 9.5	40.0 ± 8.5	31.7 ± 8.7	37.3 ± 8.8	24.2 ± 7.7	28.9 ± 7.1	14.3 ± 9.9	20.4 ± 8.8

a Nonzero concentrations set to minimum of uncertainty/2.
b Uncertainties are root mean squares of the individual 1-sigma error propagations from CMB. Zero uncertainties are excluded from RMS.
c Samples with percent mass attribution > 120 percent are removed from average source contributions.
d Contributions are normalized to sum of contributions including non-negative unexplained contributions. Uncertainties are standard errors of mean percent contributions.

Table 9.2-4
Contributions to Nitrogen Oxides at Core Sites – NFRAQS Winter 1996/97, Extended Species CMB

Site	Brighton				Welby			
Start Hour (MST)	06	12	18	06	06	12	18	06
Duration	6	6	12	24	6	6	12	24
Observations	20	20	19		17	17	17	
Concentration (ug/m3)	74.3 ± 13.9	59.2 ± 12.4	74.6 ± 13.8	70.7 ± 13.5	265.2 ± 34.2	126.2 ± 18.3	233.8 ± 29.3	214.7 ± 28.3
R-square	0.93 ± 0.01	0.92 ± 0.01	0.93 ± 0.01	0.93 ± 0.01	0.91 ± 0.01	0.94 ± 0.01	0.92 ± 0.01	0.92 ± 0.01
Chi-square	0.31 ± 0.03	0.31 ± 0.03	0.38 ± 0.03	0.34 ± 0.03	0.47 ± 0.05	0.33 ± 0.04	0.45 ± 0.06	0.43 ± 0.06
Percent Mass Attributed	159.4 ± 18.4	165.8 ± 21.7	107.2 ± 13.5	134.9 ± 17.1	101.6 ± 22.1	117.2 ± 16.3	68.2 ± 11.3	88.8 ± 15.9
Absolute Contributions (ug/m3) [a, b, c]								
LDGV, cold start	8.6 ± 17.9	8.1 ± 18.3	5.4 ± 11.4	6.8 ± 15.1	49.6 ± 90.8	19.2 ± 36.8	33.9 ± 66.0	34.1 ± 67.6
LDGV, hot stabilized	9.0 ± 8.3	8.0 ± 7.9	5.6 ± 4.6	7.1 ± 6.6	37.5 ± 30.6	23.1 ± 20.0	21.9 ± 20.2	26.1 ± 23.2
LDGV, high particle emitter	21.5 ± 16.1	18.0 ± 12.8	15.8 ± 11.3	17.8 ± 13.0	16.1 ± 16.4	18.5 ± 13.6	12.0 ± 12.4	14.7 ± 13.8
Diesel Exhaust	32.0 ± 39.0	30.1 ± 36.4	28.0 ± 32.3	29.5 ± 35.1	52.1 ± 72.3	34.7 ± 40.5	32.1 ± 41.4	37.7 ± 50.7
Meat Cooking	0.0 ± 0.0	0.0 ± 0.0	0.0 ± 0.0	0.0 ± 0.0	0.0 ± 0.0	0.0 ± 0.0	0.0 ± 0.0	0.0 ± 0.0
Wood Combustion (Softwood)	0.0 ± 0.0	0.0 ± 0.0	0.0 ± 0.0	0.0 ± 0.0	0.0 ± 0.0	0.0 ± 0.0	0.1 ± 0.1	0.0 ± 0.1
Wood Combustion (Hardwood)	0.0 ± 0.0	0.0 ± 0.0	0.0 ± 0.0	0.0 ± 0.0	0.1 ± 0.1	0.0 ± 0.0	0.1 ± 0.1	0.1 ± 0.1
Coal-Fired Powerplant	12.8 ± 3.7	10.1 ± 3.7	5.3 ± 2.6	8.3 ± 3.2	24.2 ± 8.2	16.1 ± 5.6	12.0 ± 6.1	16.1 ± 6.6
Unexplained	-9.5	-15.0	14.6	1.2	85.6	14.6	121.8	85.9
Percent Contributions [c, d]								
LDGV, cold start	9.0 ± 18.9	9.9 ± 22.6	6.7 ± 14.2	8.1 ± 18.0	18.1 ± 33.2	13.6 ± 26.1	14.3 ± 27.8	15.3 ± 30.4
LDGV, hot stabilized	9.5 ± 8.7	9.8 ± 9.8	7.0 ± 5.8	8.4 ± 7.8	13.7 ± 11.2	16.4 ± 14.2	9.2 ± 8.5	11.7 ± 10.4
LDGV, high particle emitter	22.6 ± 17.0	22.1 ± 15.8	19.7 ± 14.1	21.1 ± 15.5	5.9 ± 6.0	13.1 ± 9.7	5.1 ± 5.2	6.6 ± 6.2
Diesel Exhaust	33.8 ± 41.1	37.1 ± 44.8	34.9 ± 40.2	35.1 ± 41.7	19.0 ± 26.4	24.6 ± 28.7	13.5 ± 17.4	17.0 ± 22.8
Meat Cooking	0.0 ± 0.0	0.0 ± 0.0	0.0 ± 0.0	0.0 ± 0.0	0.0 ± 0.0	0.0 ± 0.0	0.0 ± 0.0	0.0 ± 0.0
Wood Combustion (Softwood)	0.0 ± 0.0	0.0 ± 0.0	0.0 ± 0.0	0.0 ± 0.0	0.0 ± 0.0	0.0 ± 0.0	0.0 ± 0.0	0.0 ± 0.0
Wood Combustion (Hardwood)	0.0 ± 0.0	0.0 ± 0.0	0.0 ± 0.0	0.0 ± 0.0	0.0 ± 0.0	0.0 ± 0.0	0.0 ± 0.0	0.0 ± 0.0
Coal-Fired Powerplant	13.4 ± 3.9	12.4 ± 4.5	6.6 ± 3.2	9.9 ± 3.8	8.9 ± 3.0	11.4 ± 4.0	5.0 ± 2.6	7.2 ± 3.0
Unexplained	11.6	8.7	25.2	17.4	34.3	20.8	52.8	42.1

a Nonzero concentrations set to minimum of uncertainty/2.
b Uncertainties are root mean squares of the individual 1-sigma error propagations from CMB. Zero uncertainties are excluded from RMS.
c Samples with percent mass attribution > 120 percent are removed from average source contributions.
d Contributions are normalized to sum of contributions including non-negative unexplained contributions. Uncertainties are standard errors of mean percent contributions.

Table 9.4-1
Ratio of Average SO_2 Concentrations Calculated by the Gridded Transport Simulations with and without SO_2 Dry Deposition

Episode	CAMP	Welby	Brighton	Evans
01/12-21/97	0.61	0.79	0.44	0.36
01/27-31/97	0.60	0.78	0.42	0.37

Table 9.4-2
Average SO_2 Concentrations (ppbv) Calculated without Dry Deposition by Two Simulation Methods for the 01/13/97 to 01/21/97 Episode Compared with Measured Average Ambient Sulfur Concentrations (ppbv)

Data Source	CAMP	Welby	Brighton	Evans
Gridded Transport Simulations	8.1	22.1	6.2	2.0
Puff Transport Simulations (when available) and Gridded Transport Simulations	6.0	10.6	3.4	1.8
Total Ambient Sulfur	10.6	5.0	5.8	1.4

Table 9.4-3
Fraction of the Ambient "N+O Species" Attributable to Emissions from Coal-Fired Point Sources as a Function of the Ratios of Nitrogen to Sulfur Species in the Surface and Point-Source Emissions and the Measured Ratio of Ambient "N+O Species" to Sulfur Species

Ratio of Nitrogen to Sulfur Species in Surface Emissions	27	54	27	54
Ratio of Nitrogen to Sulfur Species in Point-Source Emissions	1	1	2	2
Ratio of Ambient "N+O Species" to Sulfur Species				
1	1.00	1.00		
2	0.48	0.49	1.00	1.00
3	0.31	0.32	0.64	0.65
4	0.22	0.24	0.46	0.48
5	0.17	0.18	0.35	0.38
6	0.13	0.15	0.28	0.31
7	0.11	0.13	0.23	0.26
8	0.09	0.11	0.19	0.22
9	0.08	0.09	0.16	0.19
10	0.07	0.08	0.14	0.17
12	0.05	0.07	0.10	0.13
14	0.04	0.05	0.07	0.11
16	0.03	0.04	0.06	0.09
18	0.02	0.04	0.04	0.08
20	0.01	0.03	0.03	0.07
22	0.01	0.03	0.02	0.06
24	0.00	0.02	0.01	0.05
26	0.00	0.02	0.00	0.04

Table 9.4-4
Cumulative Frequency Distributions of the Ratio of "N+O Species" to Sulfur Species during 6- and 12-Hour Filter Sampling Periods

Percentile	All Samples	0600 to 1200	1200 to 1800	1800 to 0600
Welby				
10	7	11	6	12
25	14	17	7	23
50	23	22	16	51
75	62	62	23	101
90	101	99	61	131
Brighton				
10	4	4	3	6
25	6	6	4	8
50	11	11	9	15
75	19	17	13	21
90	23	22	21	75
Evans				
10	10	8	7	12
25	18	26	11	33
50	37	45	19	51
75	57	61	32	83
90	99	150	51	156

Table 9.4-5
Cumulative Frequency Distributions of the Ratio of "N+O Species" to Sulfur Species during the 3-Hour Filter Sampling Periods

Percentile	All Samples	0000 to 0300	0300 to 0600	0600 to 0900	0900 to 1200	1200 to 1500	1500 to 1800	1800 to 2100	2100 to 0000
Welby									
10	4	4	5	5	5	4	7	10	5
25	9	17	9	48	10	4	10	11	10
50	27	45	29	95	20	6	23	37	26
75	81	101	47	135	33	10	29	68	142
90	141	161	112	139	42	25	53	102	243
Brighton									
10	4	6	4	5	4	3	4	8	5
25	6	7	5	8	5	4	5	11	10
50	12	14	10	18	11	8	11	15	20
75	20	18	14	24	15	12	19	19	22
90	26	86	19	39	22	20	23	22	27

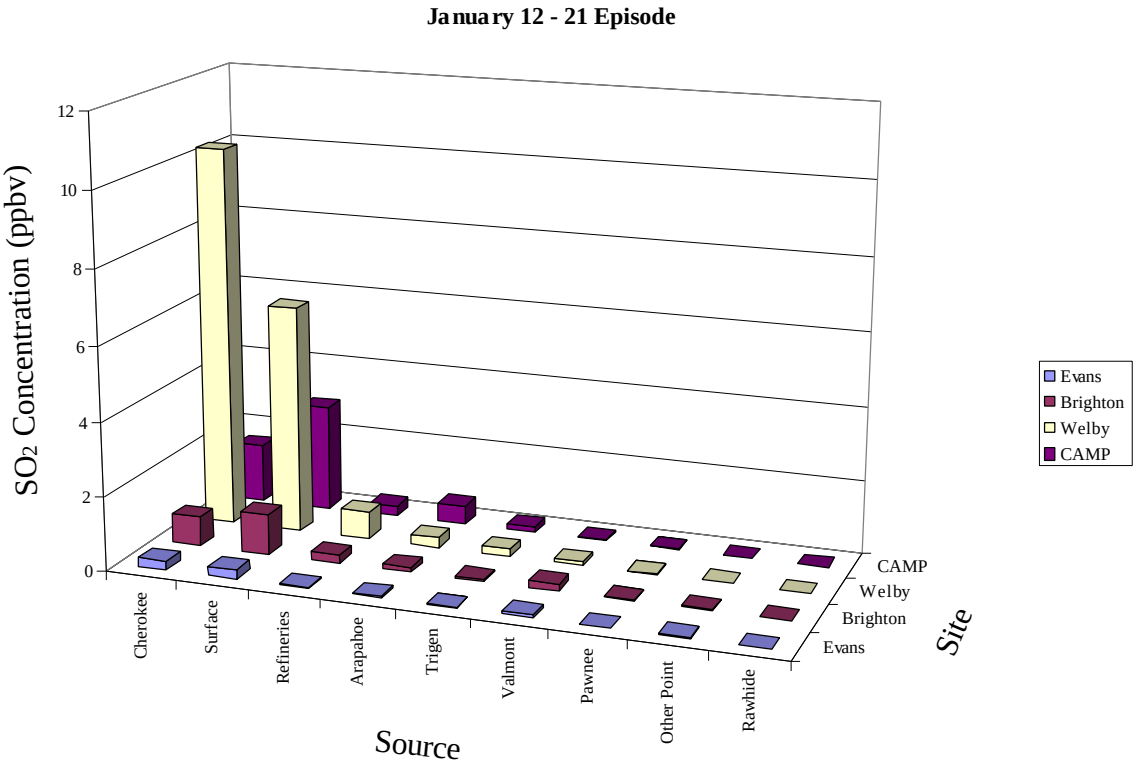

Figure 9.1-1. Average SO_2 concentrations at four monitoring sites attributed to nine sources during the 01/12/97 to 01/21/97 episode calculated by the gridded transport simulations with dry deposition. The calculated values for Cherokee and surface sources are larger than the correct values at Welby.

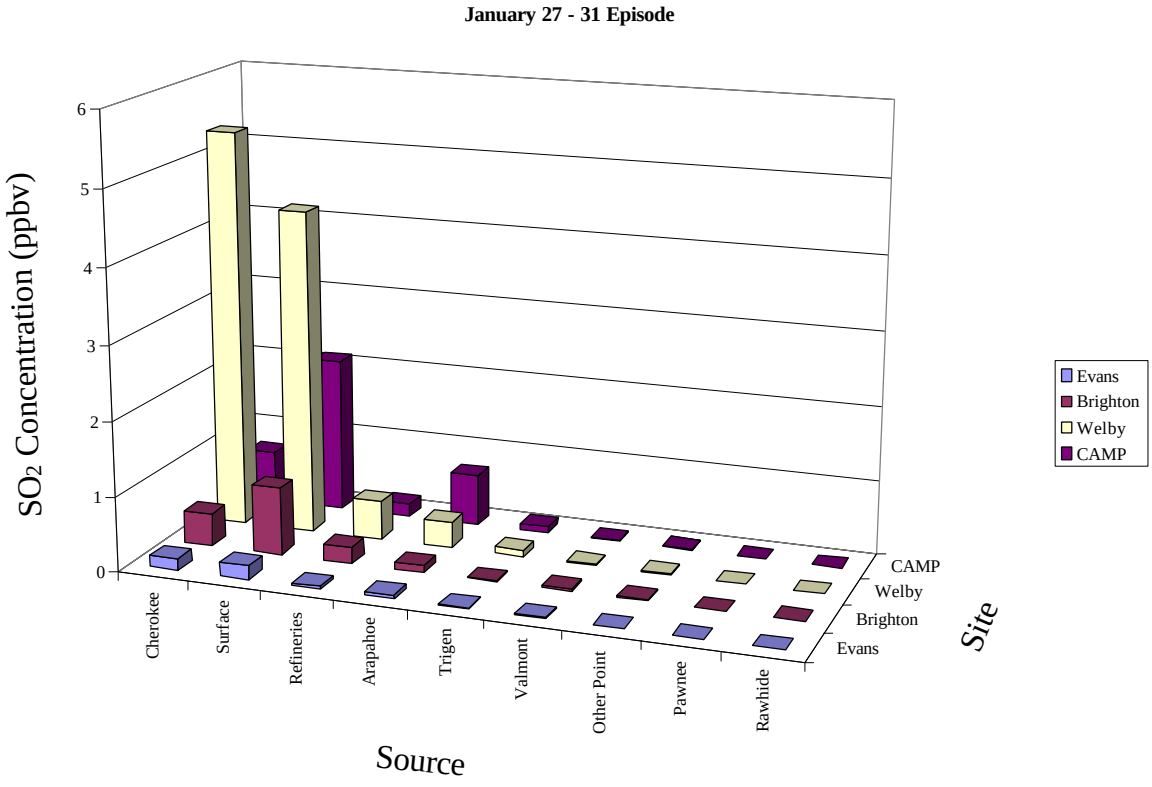

Figure 9.1-2. Average SO_2 concentrations at four monitoring sites attributed to nine sources during the 01/27/97 to 01/31/97 episode calculated by the gridded transport simulations with dry deposition. The calculated values for Cherokee and surface sources are larger than the correct values at Welby.

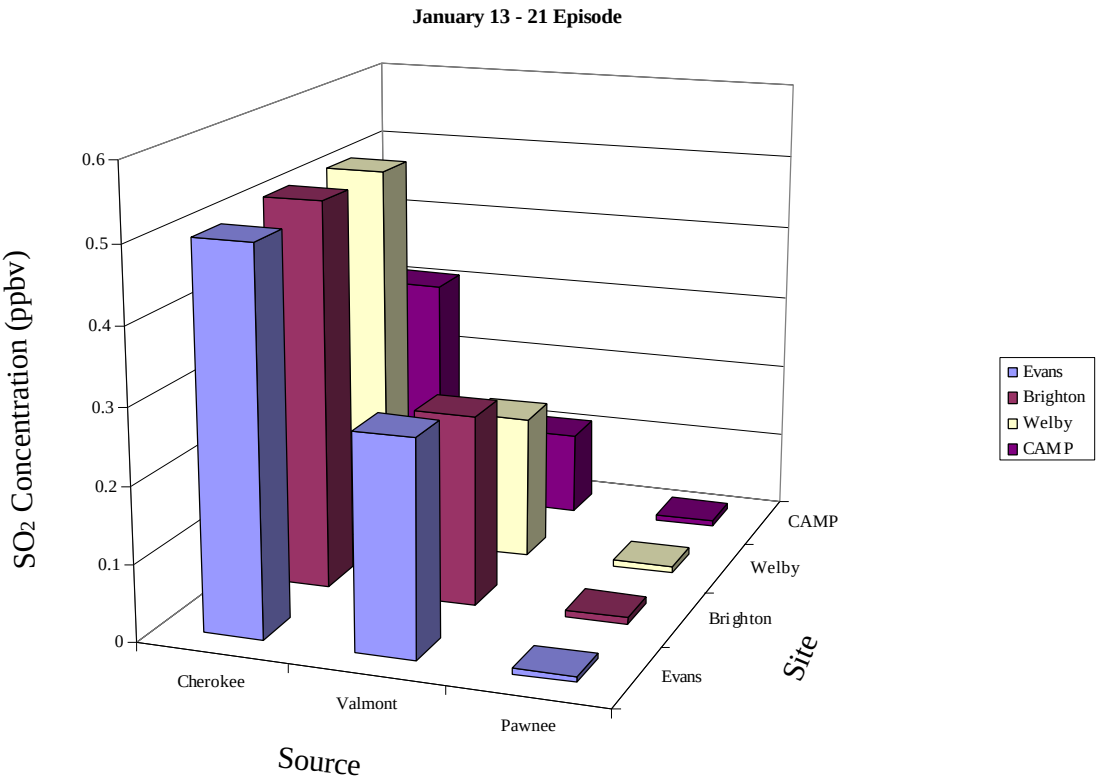

Figure 9.1-3. Average SO_2 concentrations at four monitoring sites attributed to three sources during the 01/13/97 to 01/21/97 episode calculated by the puff transport simulations with no dry deposition. The calculated value for Cherokee is probably smaller than the correct value at Welby.

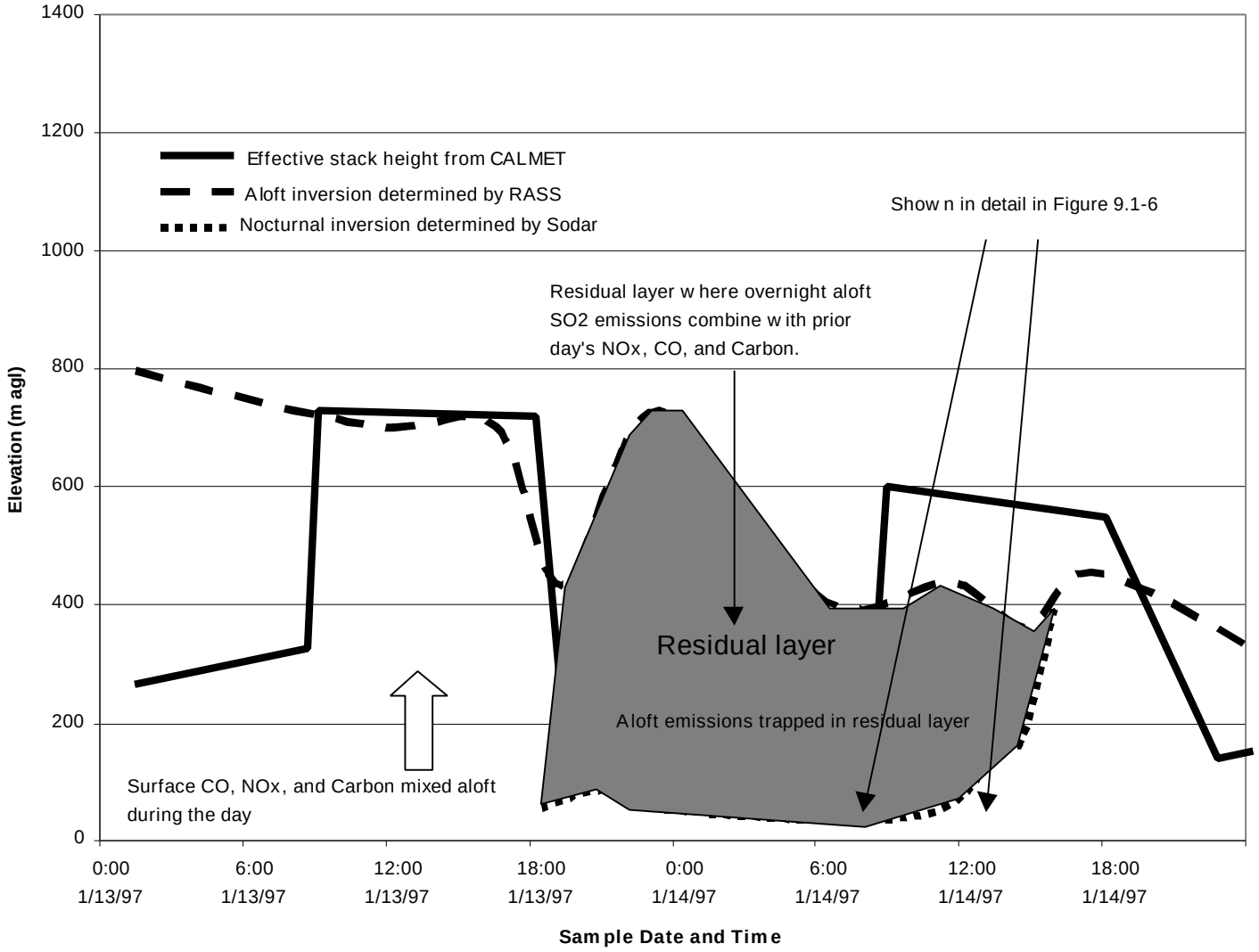

Figure 9.1-4. Time series of inversions at Brighton and effective stack heights for the Cherokee and Pawnee stacks on 01/13/97 and 01/14/97.

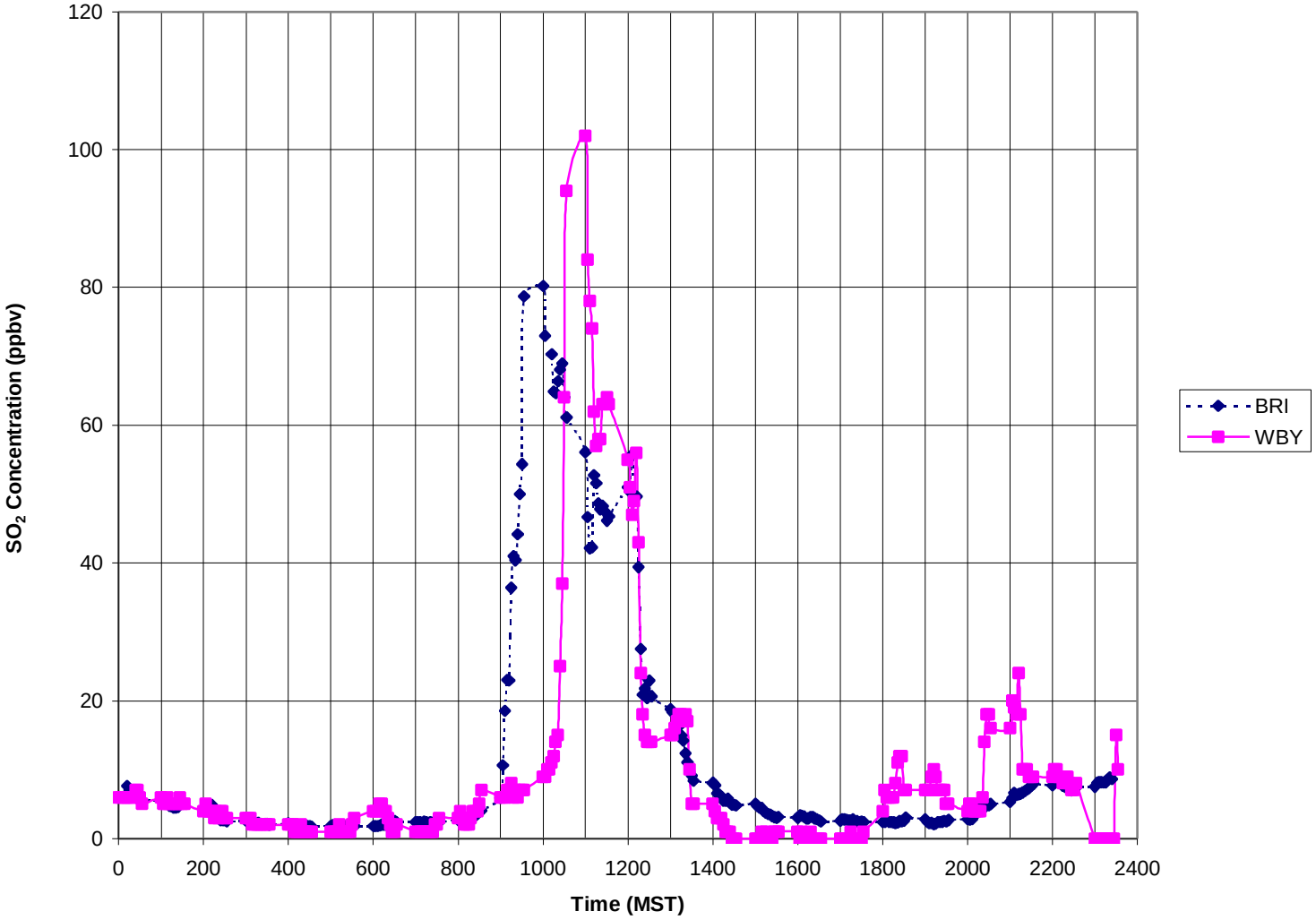

Figure 9.1-5. Observed 5-minute average SO_2 concentrations at Welby and Brighton on 01/14/97.

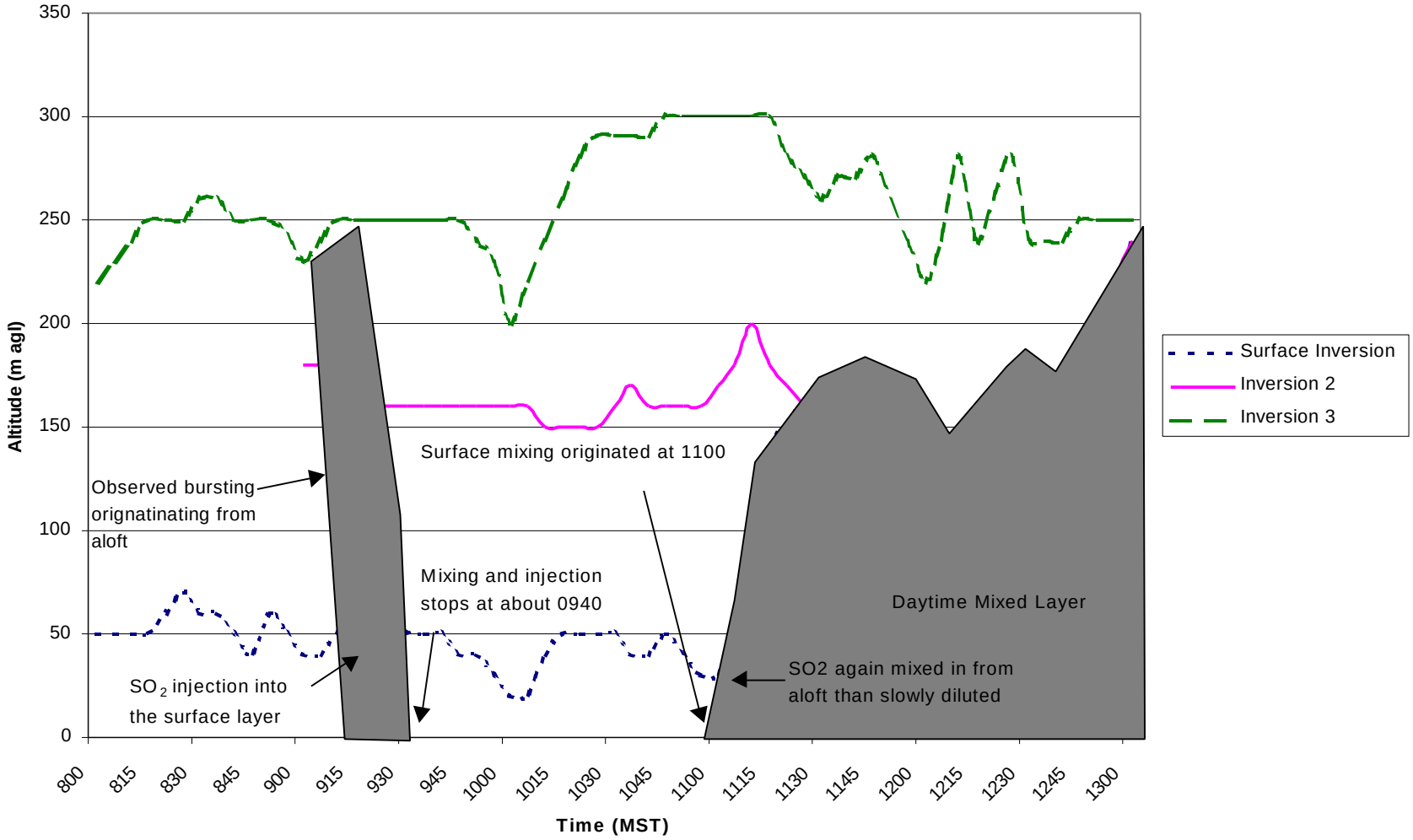

Figure 9.1-6. Evolution and interaction of the multiple inversion layers observed at Brighton on 01/14/97.

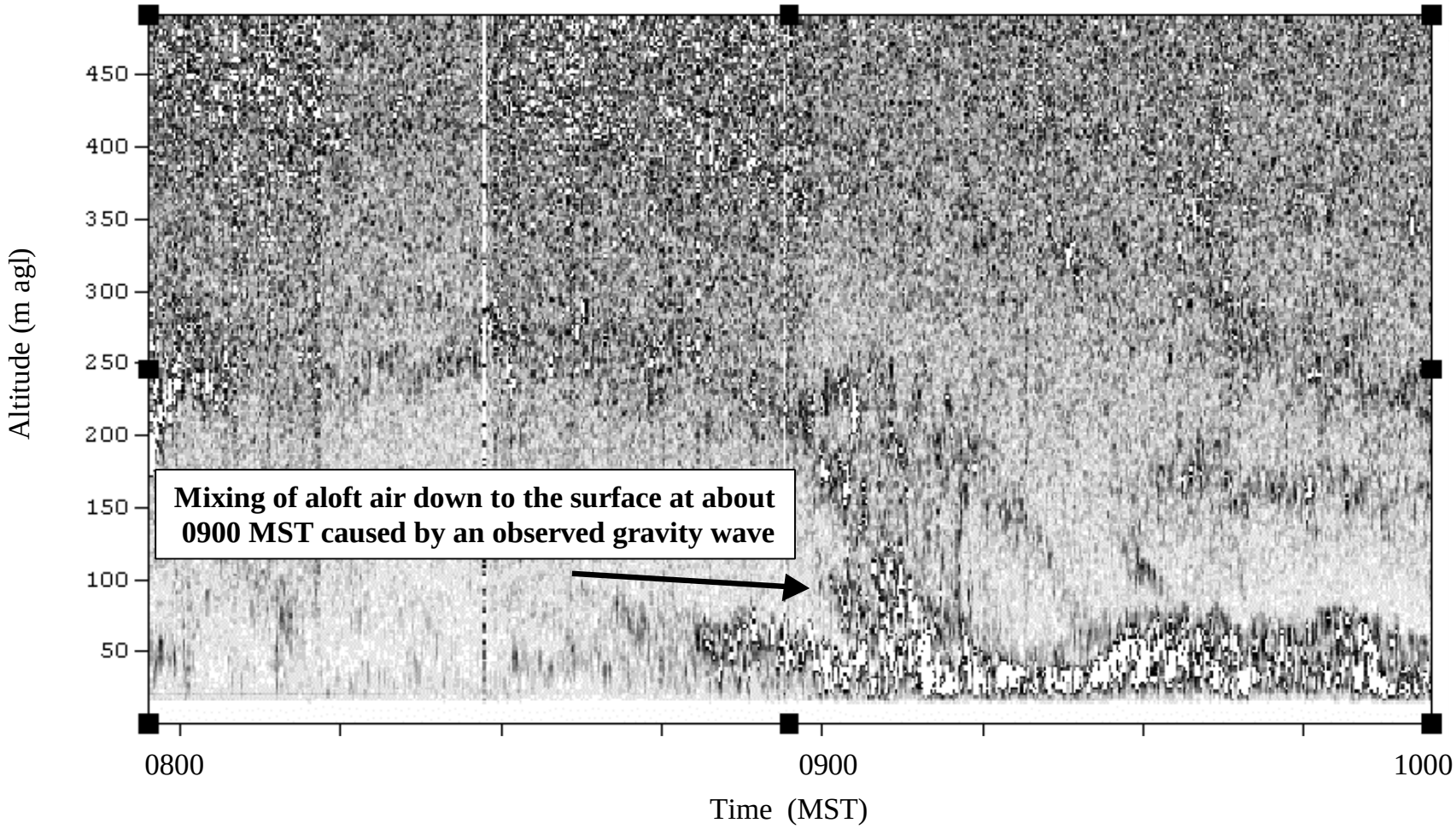

Figure 9.1-7. Sodar reflectivity data at Brighton on 01/14/97 showing the mixing of aloft air down to the surface at 0900 MST.

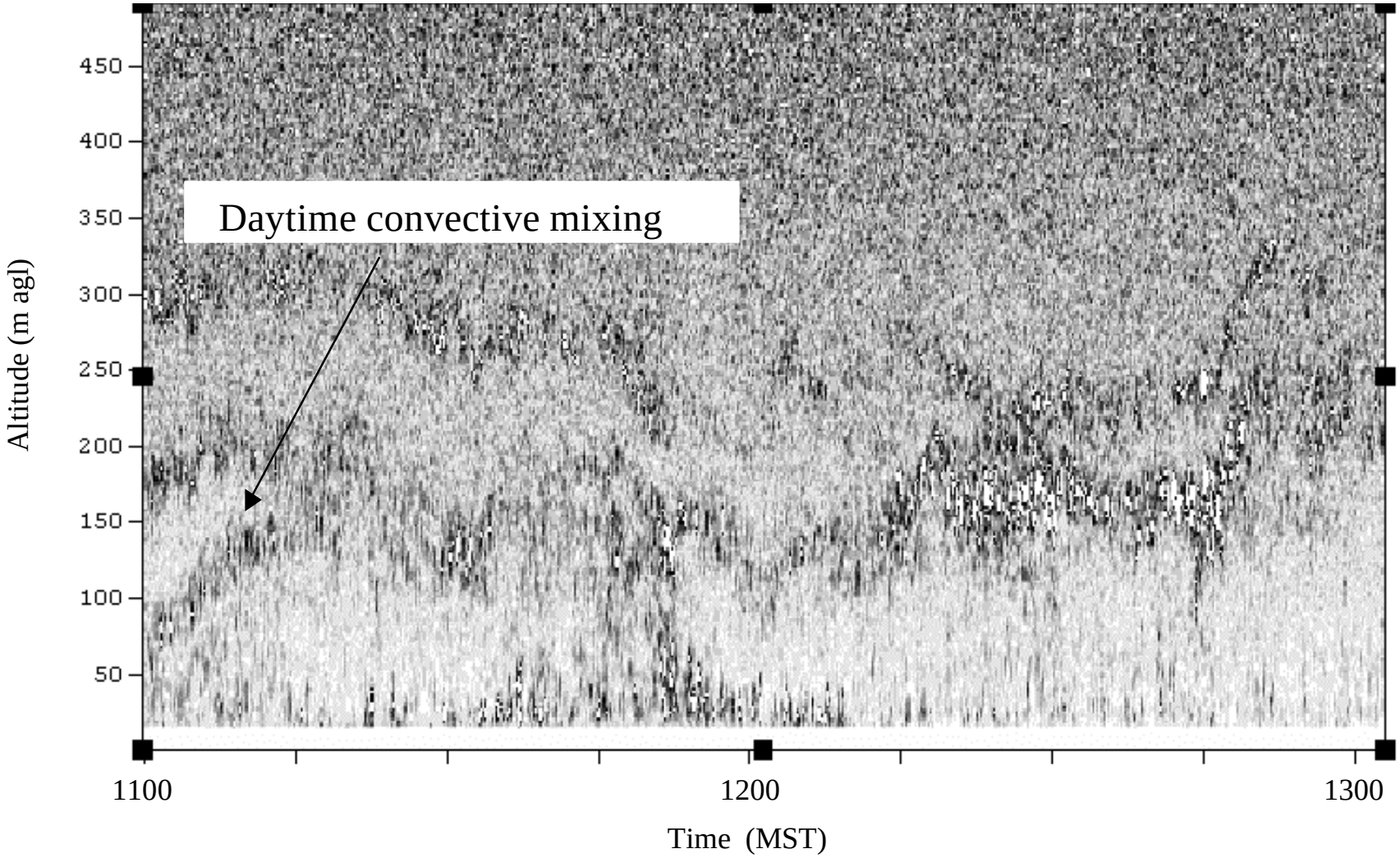

Figure 9.1-8. Sodar reflectivity data at Brighton on 01/14/97 showing the onset of daytime convective mixing.

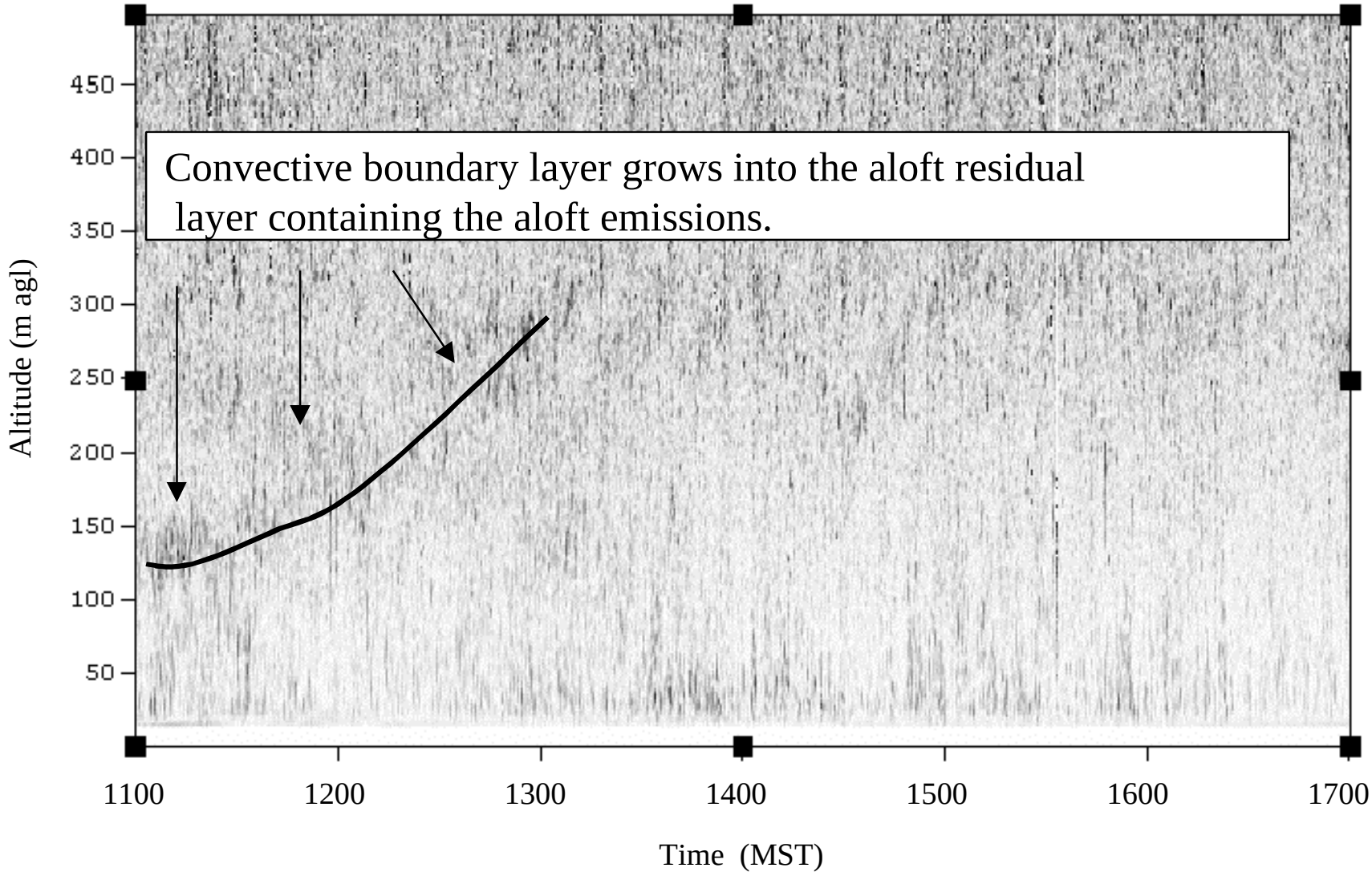

Figure 9.1-9. Sodar reflectivity data at Welby on 01/14/97 showing daytime convective mixing.

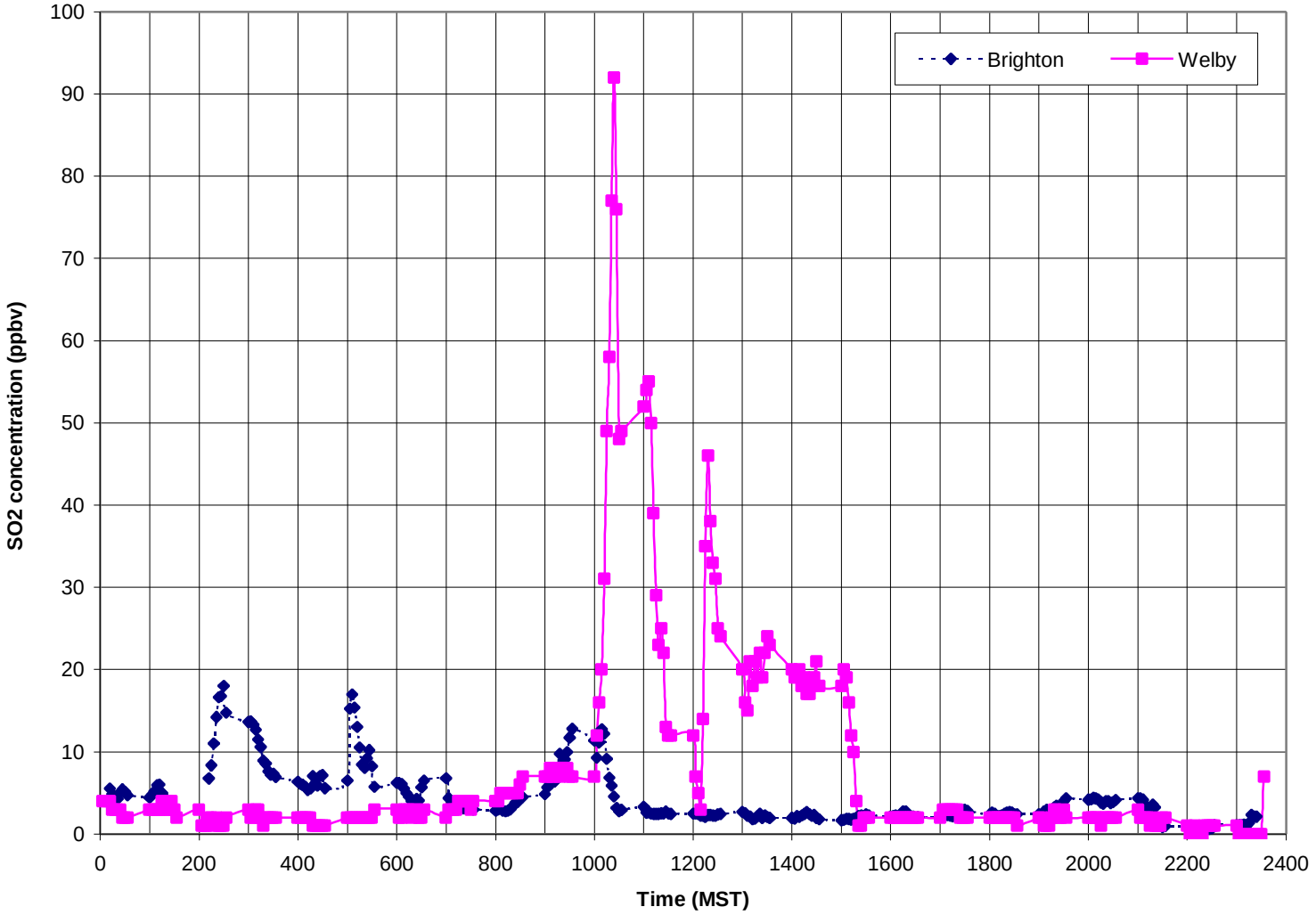

Figure 9.1-10. Observed 5-minute averaged SO_2 concentrations at Welby and Brighton on 01/20/97.

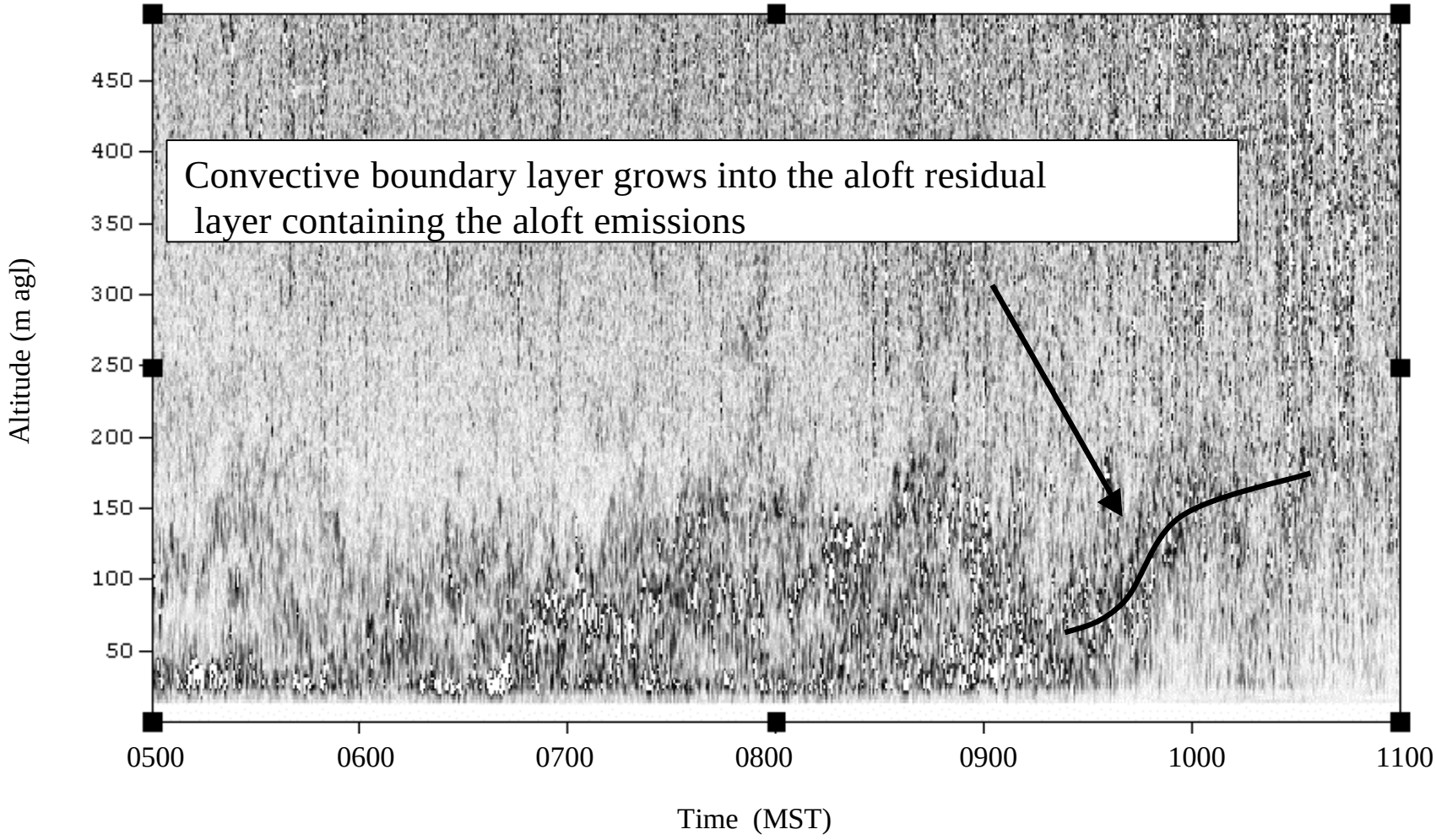

Figure 9.1-11. Sodar reflectivity data at Welby on 01/20/97 showing daytime convective mixing.

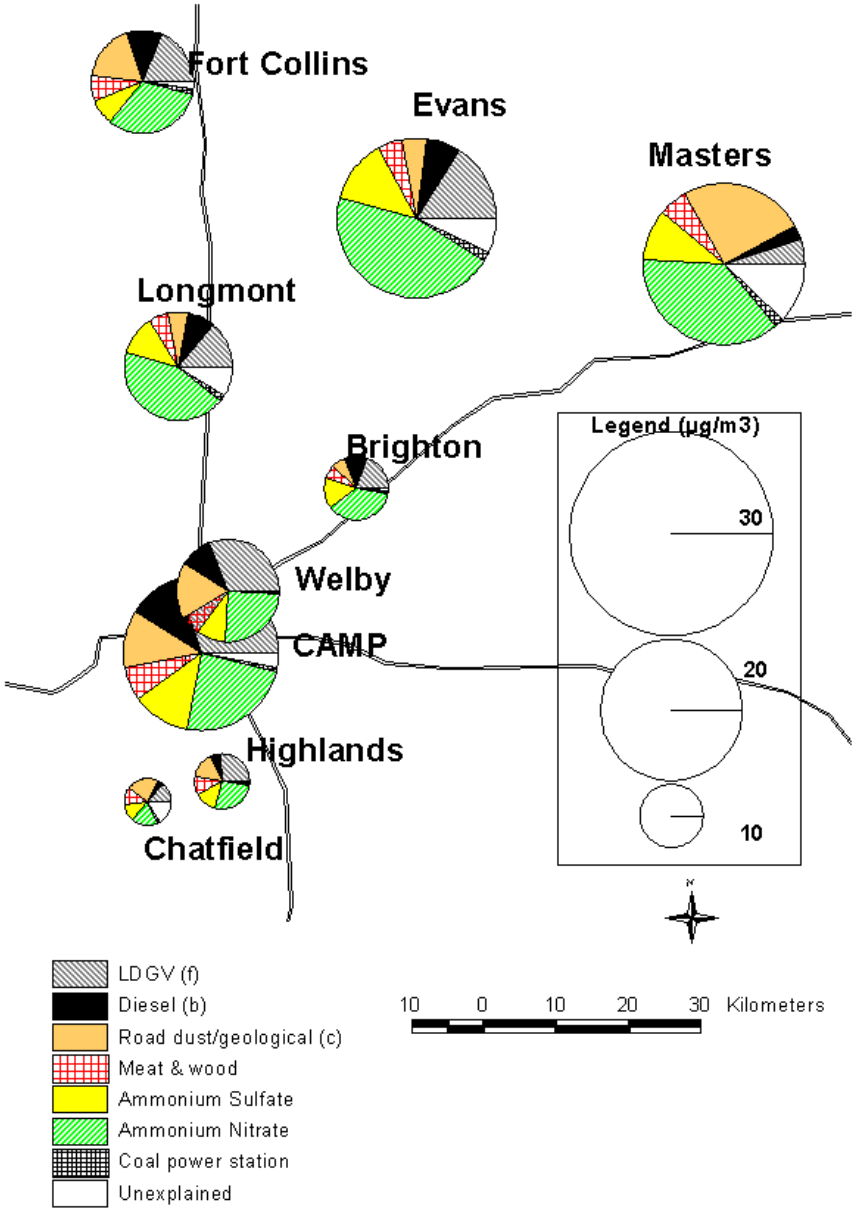

Figure 9.2-1. Spatial variations in apportionment of $PM_{2.5}$ during Winter 1997 NFRAQS.

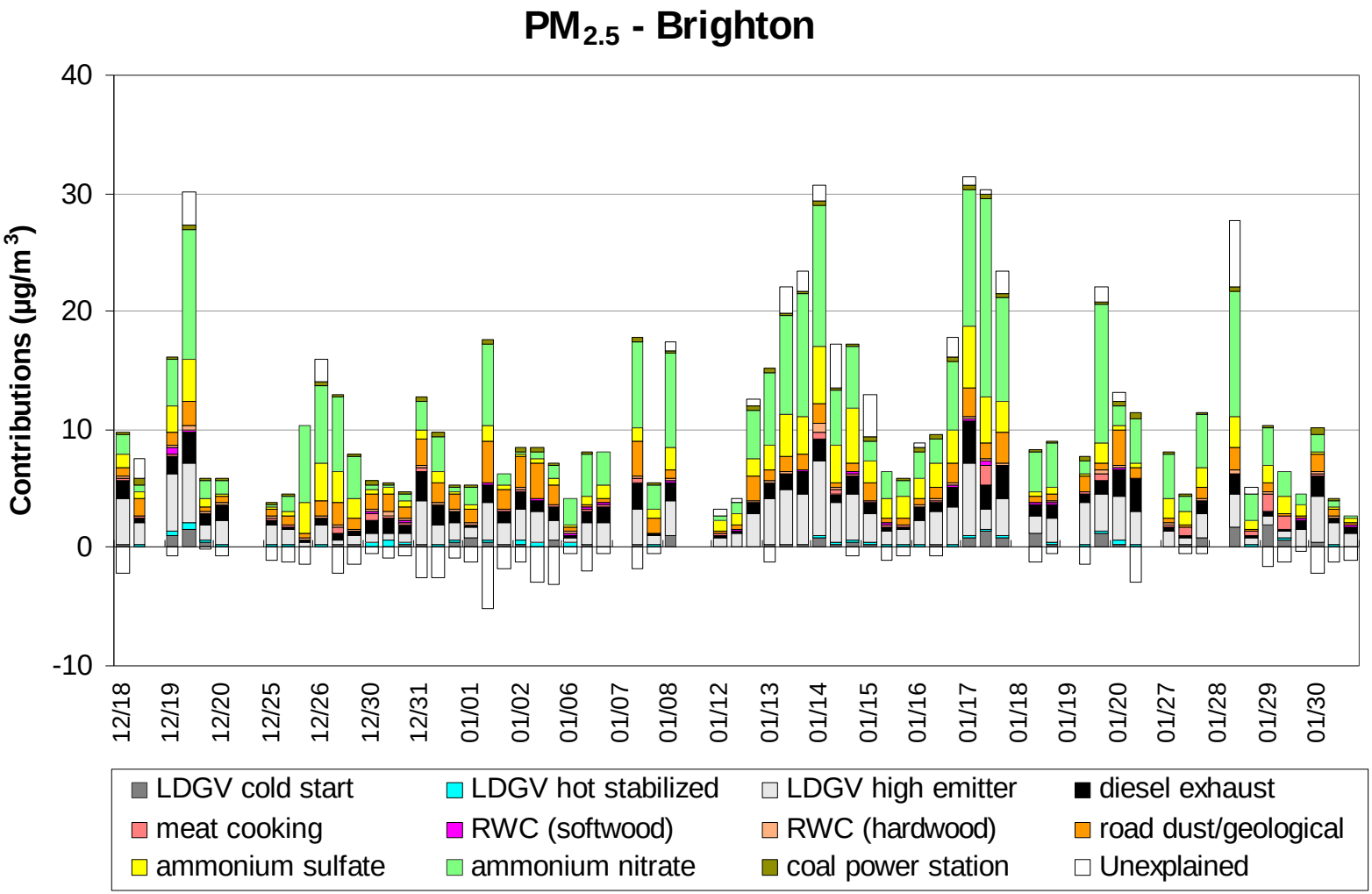

Figure 9.2-2. Time series of $PM_{2.5}$ source contributions at Brighton during Winter 1997 NFRAQS.

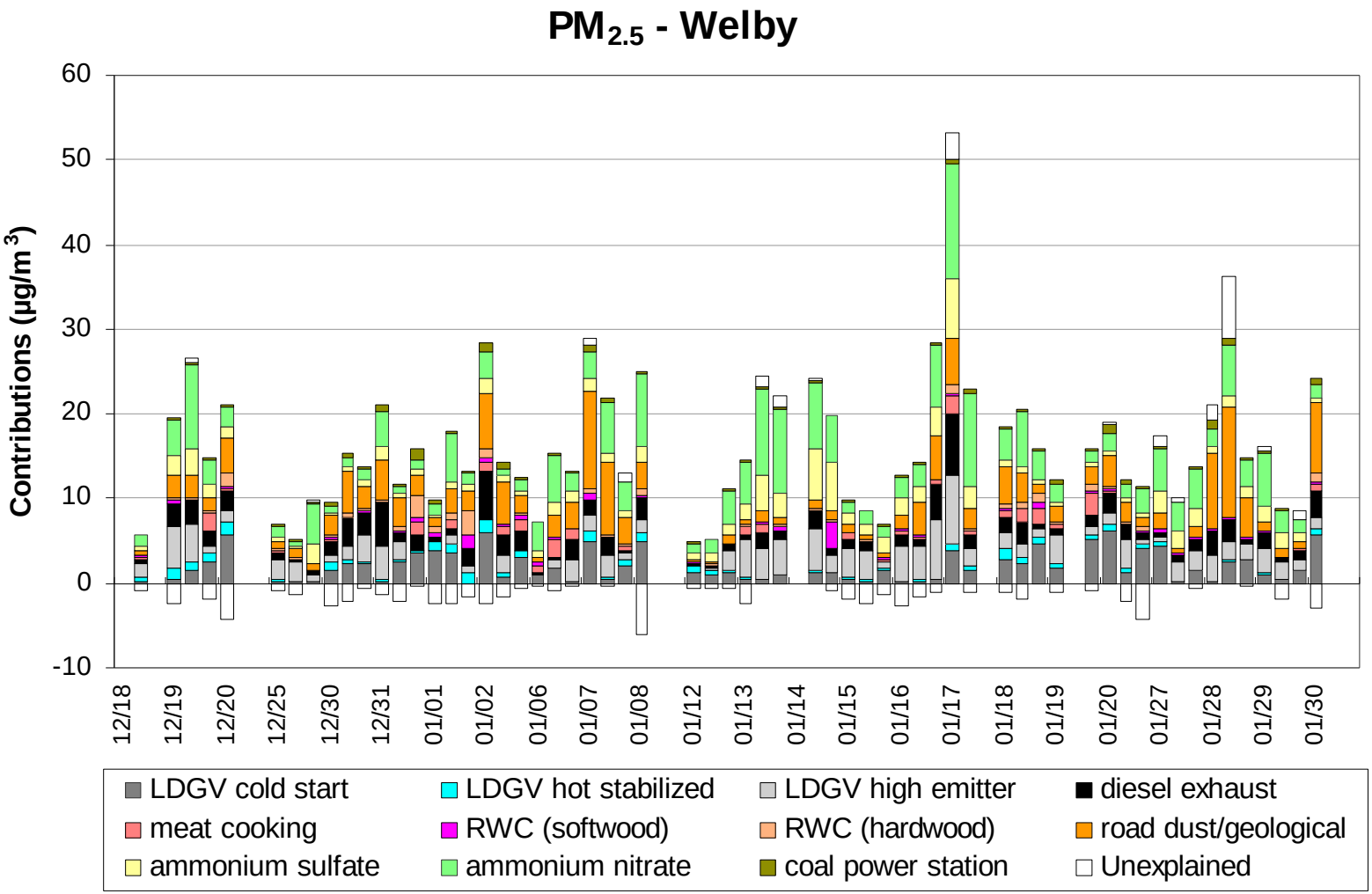

Figure 9.2-3. Time series of $PM_{2.5}$ source contributions at Welby during Winter 1997 NFRAQS.

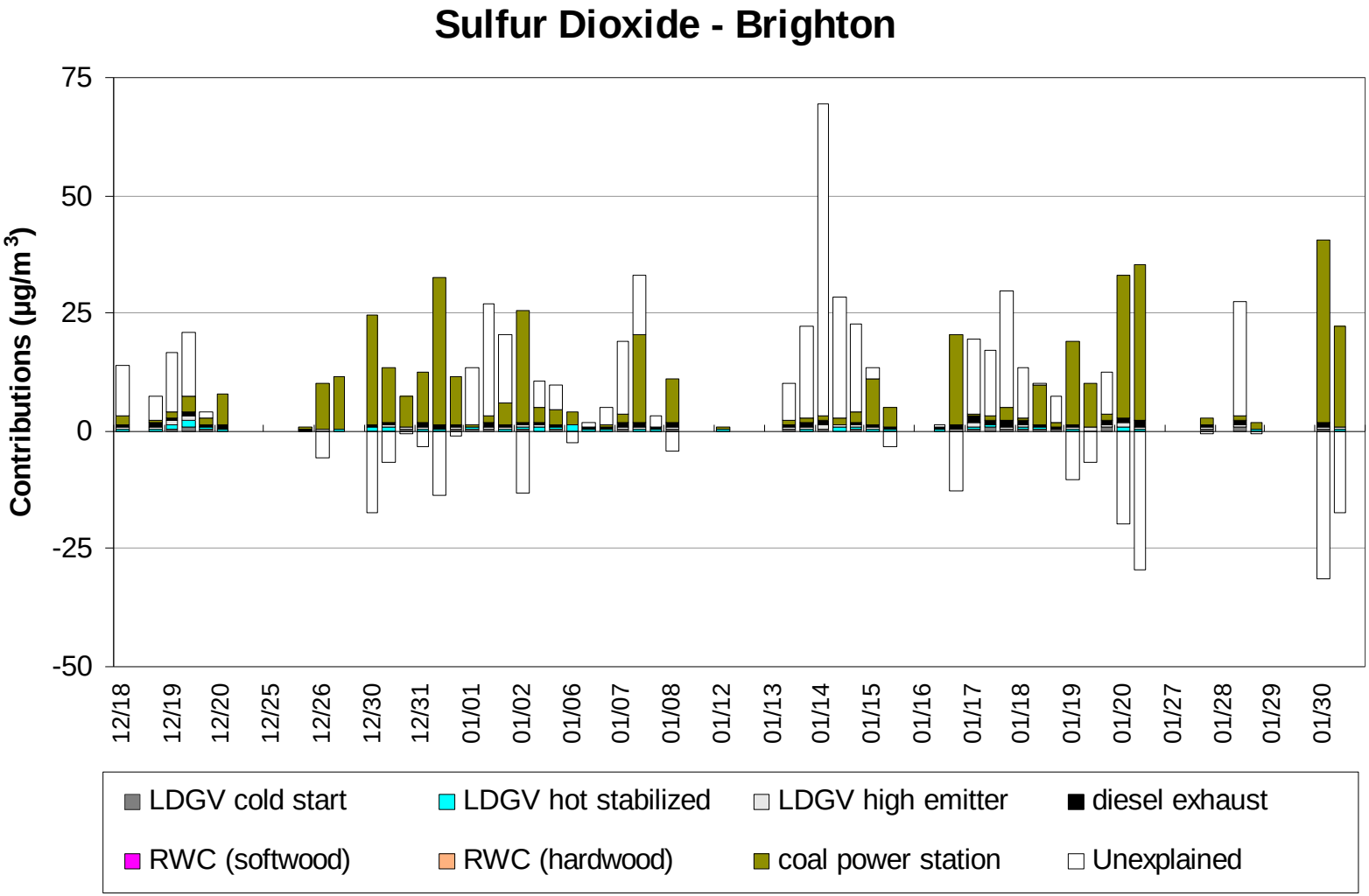

Figure 9.2-4. Time series of sulfur dioxide source contributions at Brighton during Winter 1997 NFRAQS.

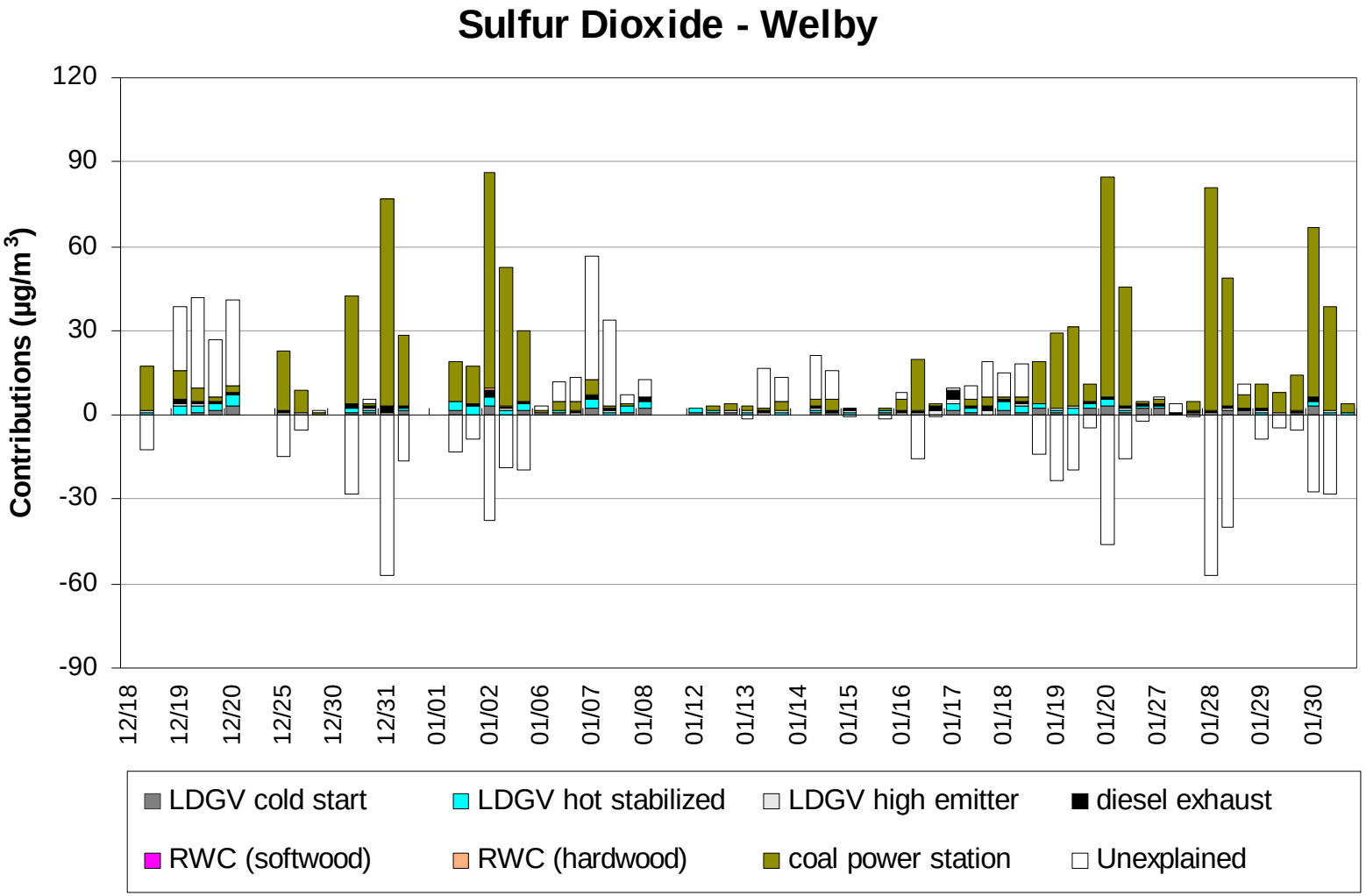

Figure 9.2-5. Time series of sulfur dioxide source contributions at Welby during Winter 1997 NFRAQS.

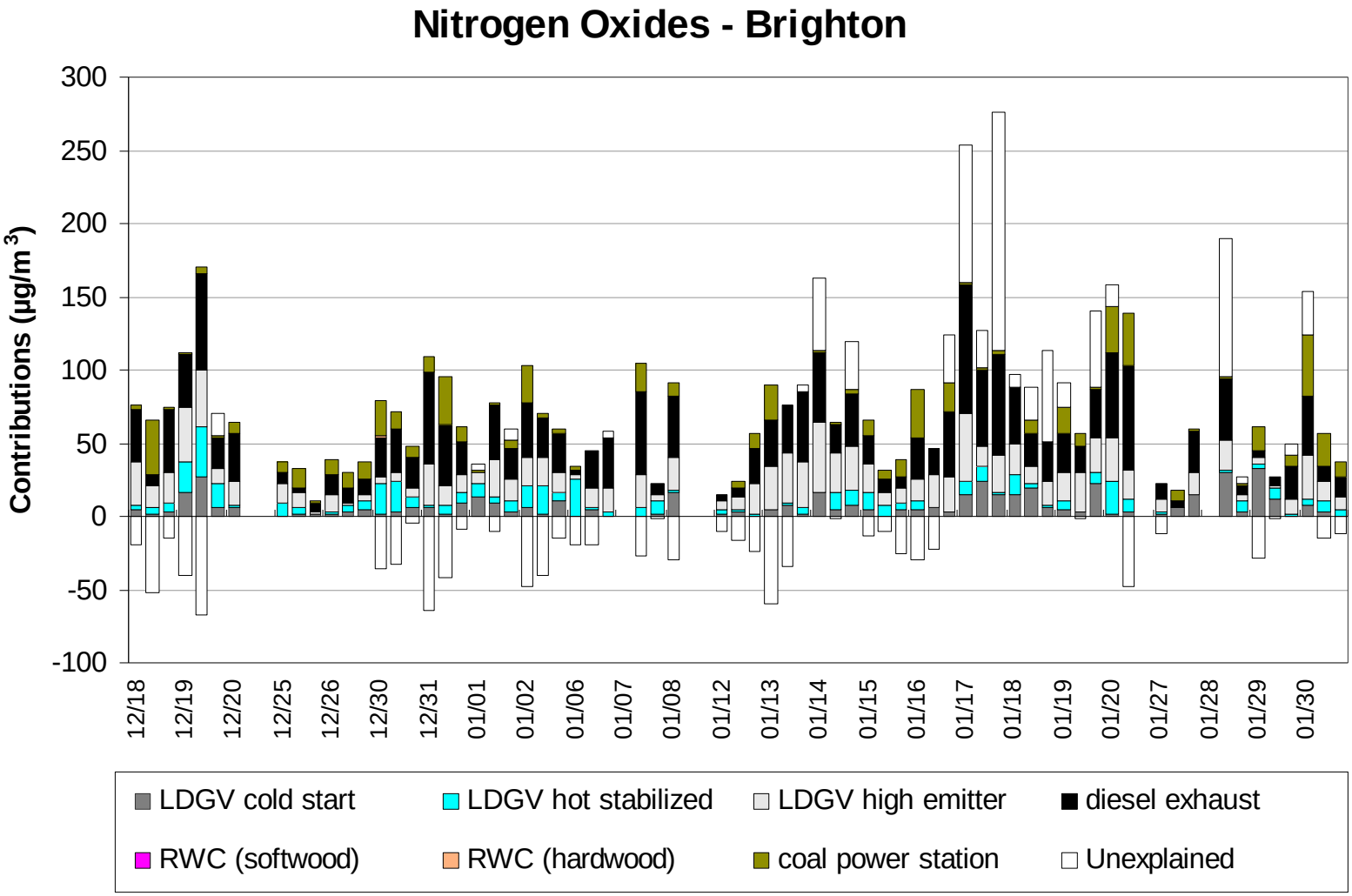

Figure 9.2-6. Time series of nitrogen oxide source contributions at Brighton during Winter 1997 NFRAQS.

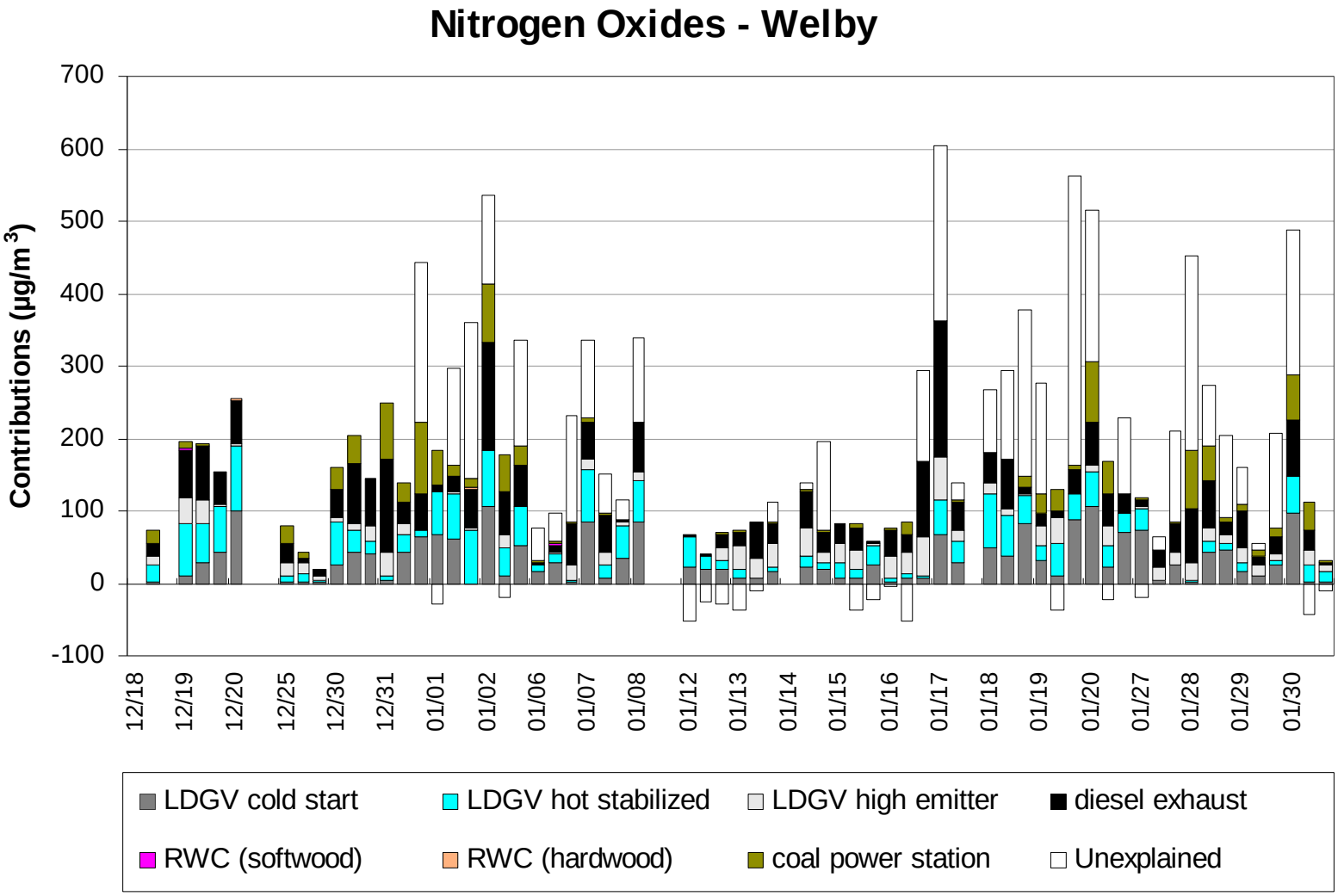

Figure 9.2-7. Time series of nitrogen oxide source contributions at Welby during Winter 1997 NFRAQS.

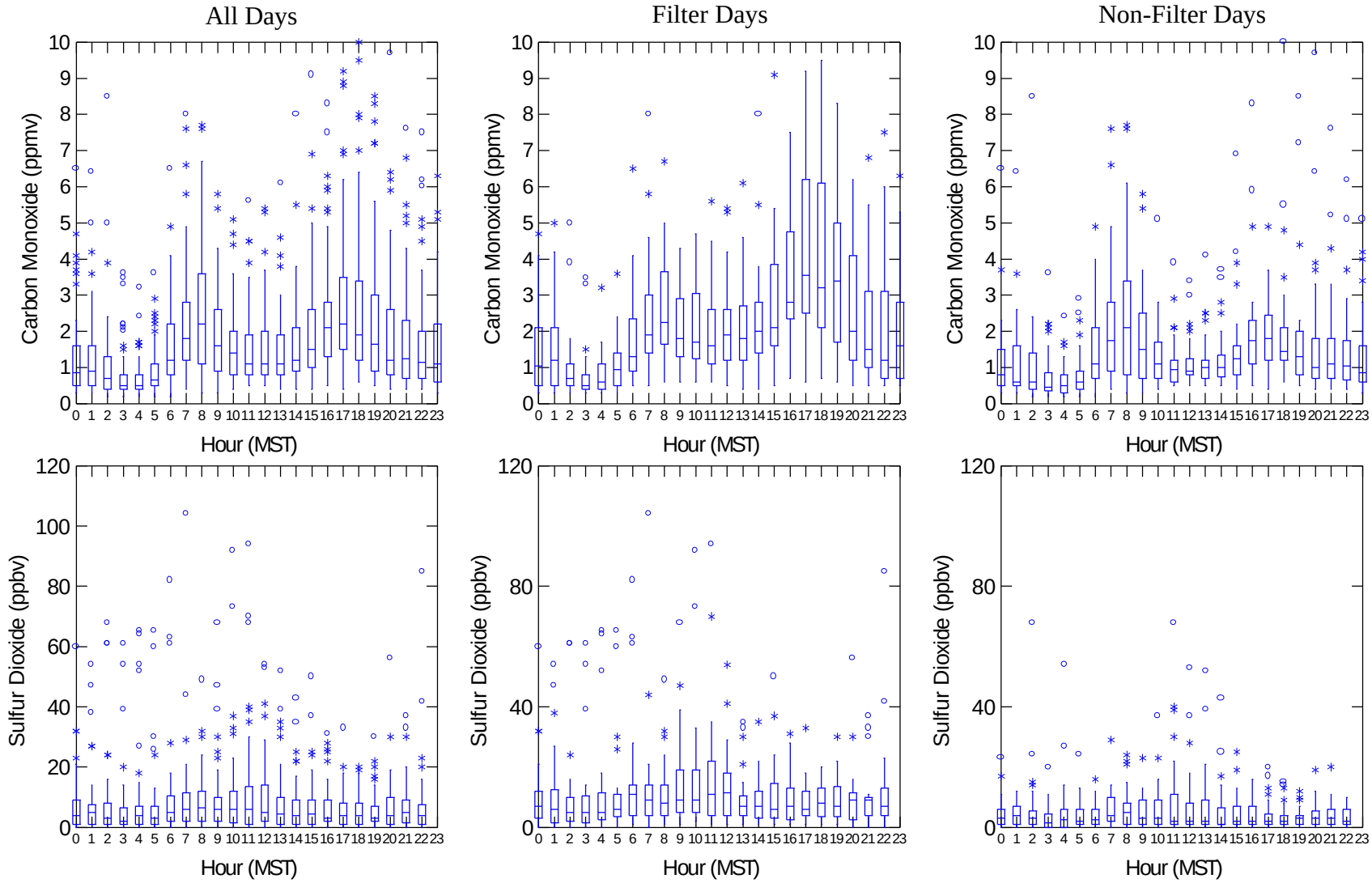

Figure 9.3-1. Diurnal variation of the CO and SO_2 concentrations at CAMP on (a) all days in the Winter 1997 field study, (b) days that filter samples were analyzed, and (c) days that filter samples were not analyzed.

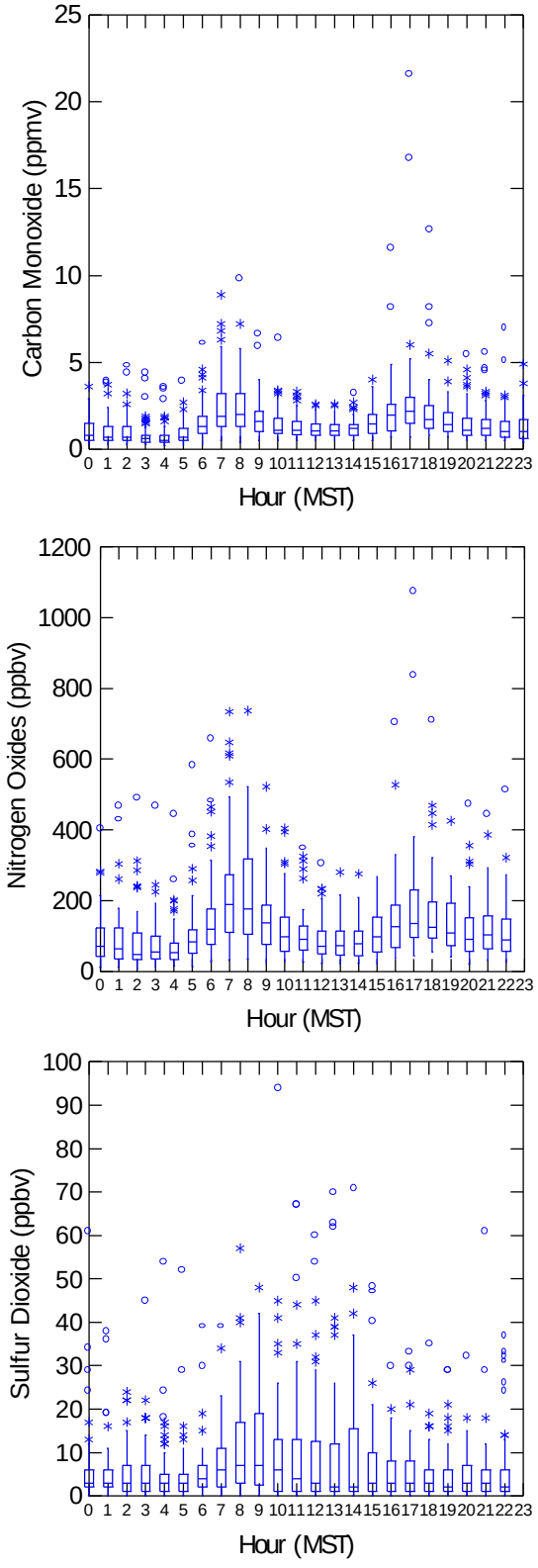

Figure 9.3-2. Diurnal variation of the concentrations of CO, NO_x, and SO_2 at CAMP during November 1996 and February 1997. This time period was selected because NO_x data were missing at CAMP during the Winter 1997 field study.

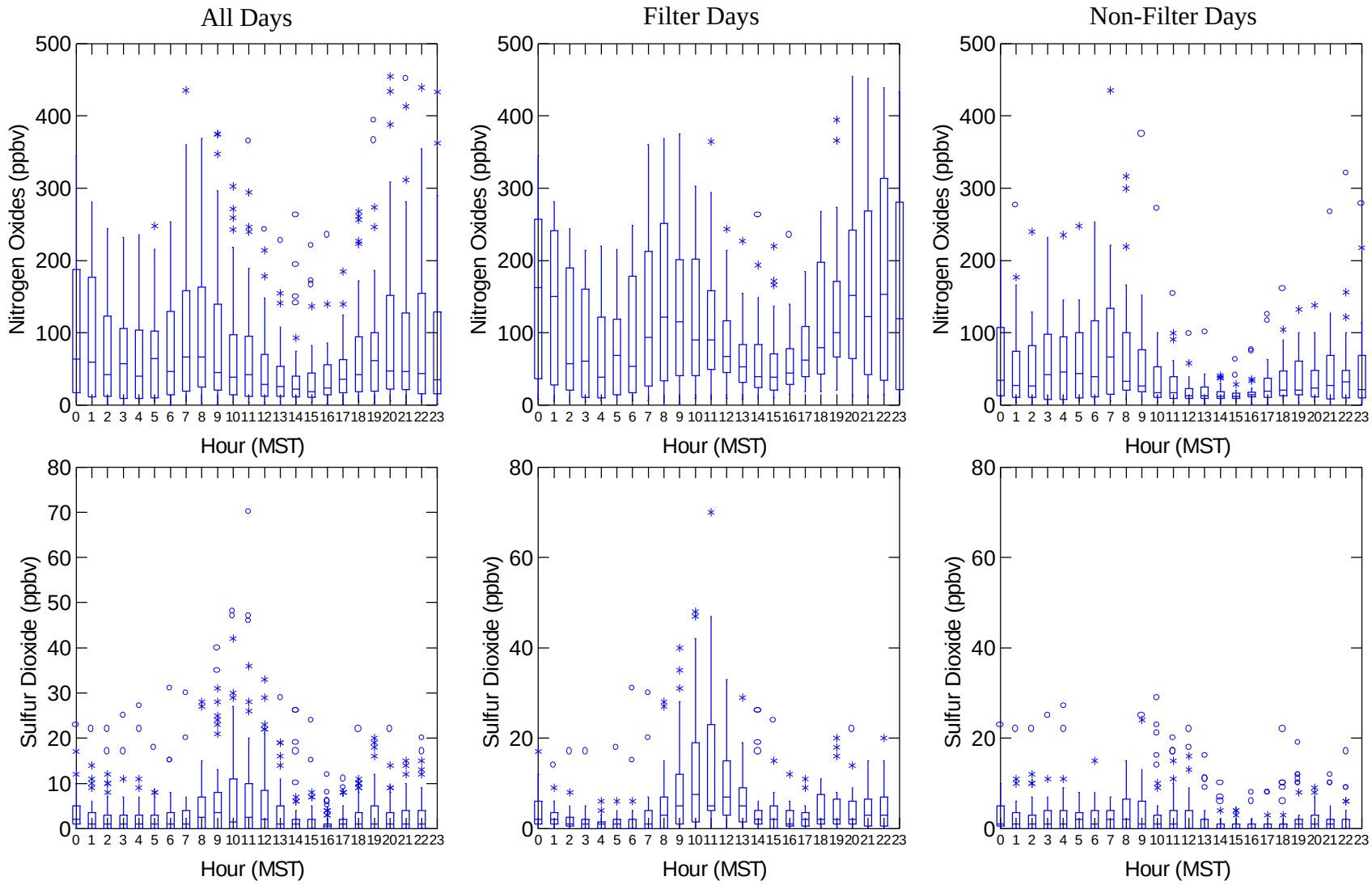

Figure 9.3-3. Diurnal variation of the NO_x and SO_2 concentrations at Welby on (a) all days in Winter 1997 field study, (b) days that filter samples were analyzed, and (c) days that filter samples were not analyzed.

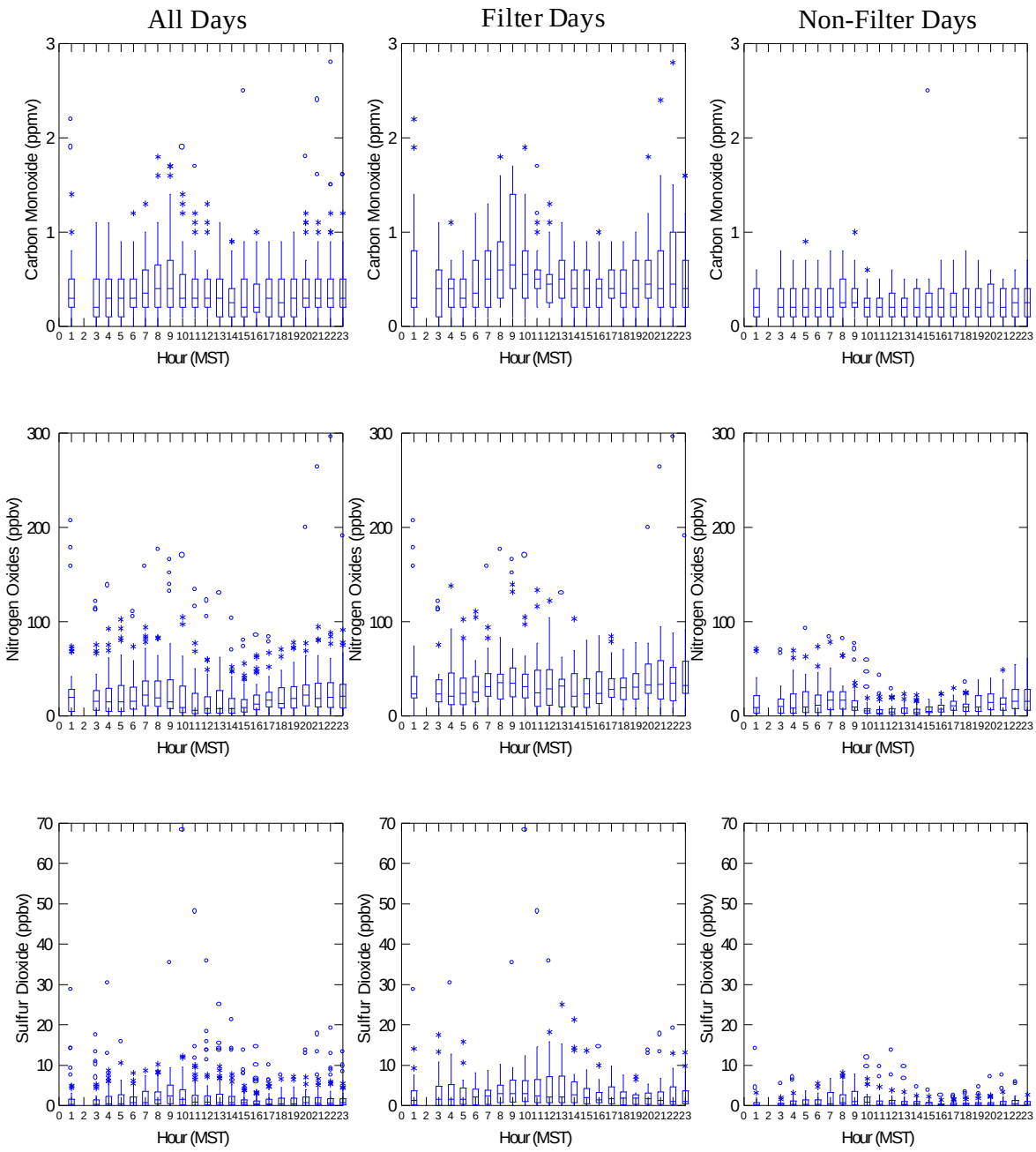

Figure 9.3-4. Diurnal variation of the CO, NO_x, and SO_2 concentrations at Brighton on (a) all days in the winter field study, (b) days that filter samples were analyzed, and (c) days that filter samples were not analyzed.

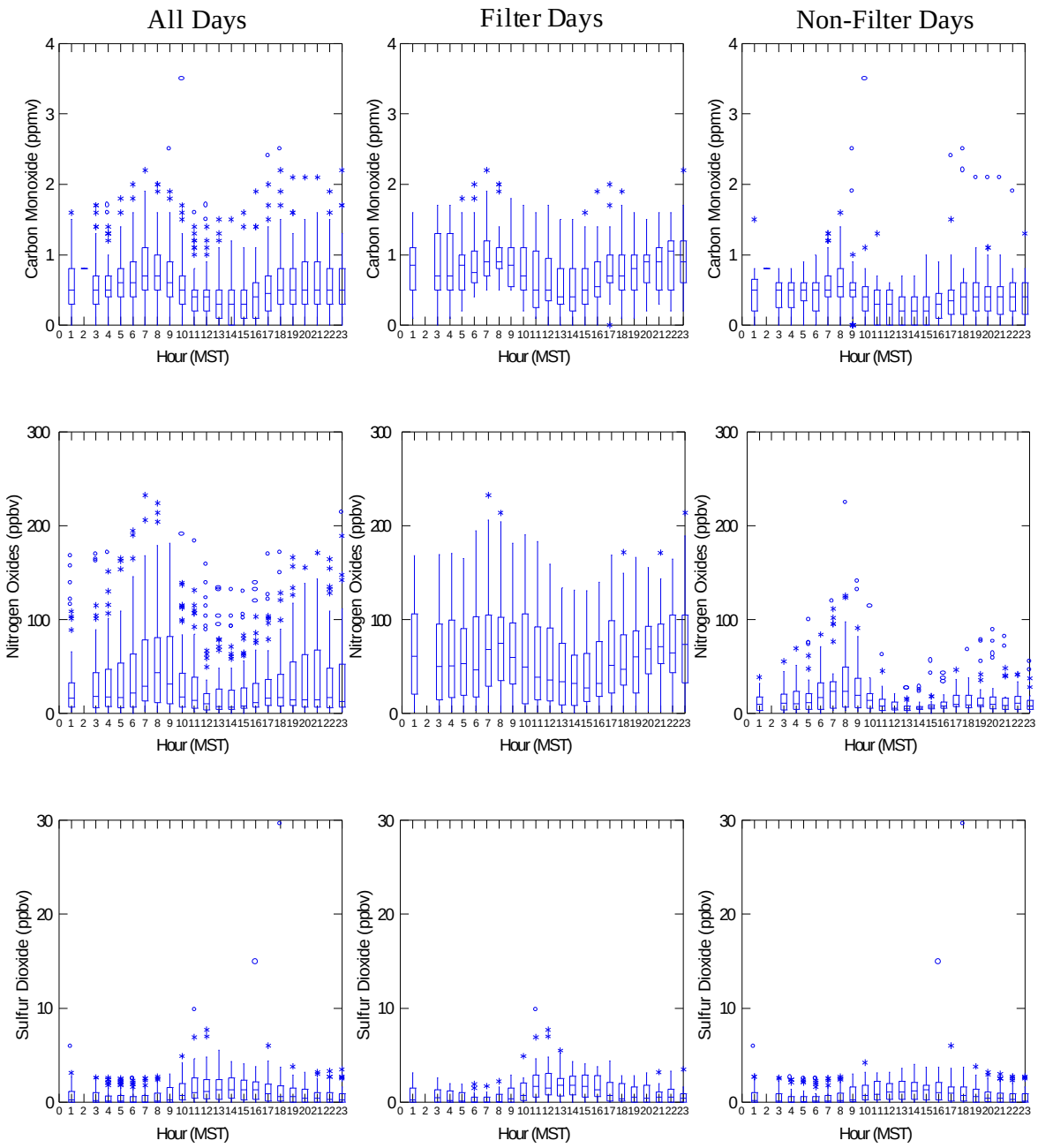

Figure 9.3-5. Diurnal variation of the CO, NO_x, and SO_2 concentrations at Evans on (a) all days in the winter field study, (b) days that filter samples were analyzed, and (c) days that filter samples were not analyzed.

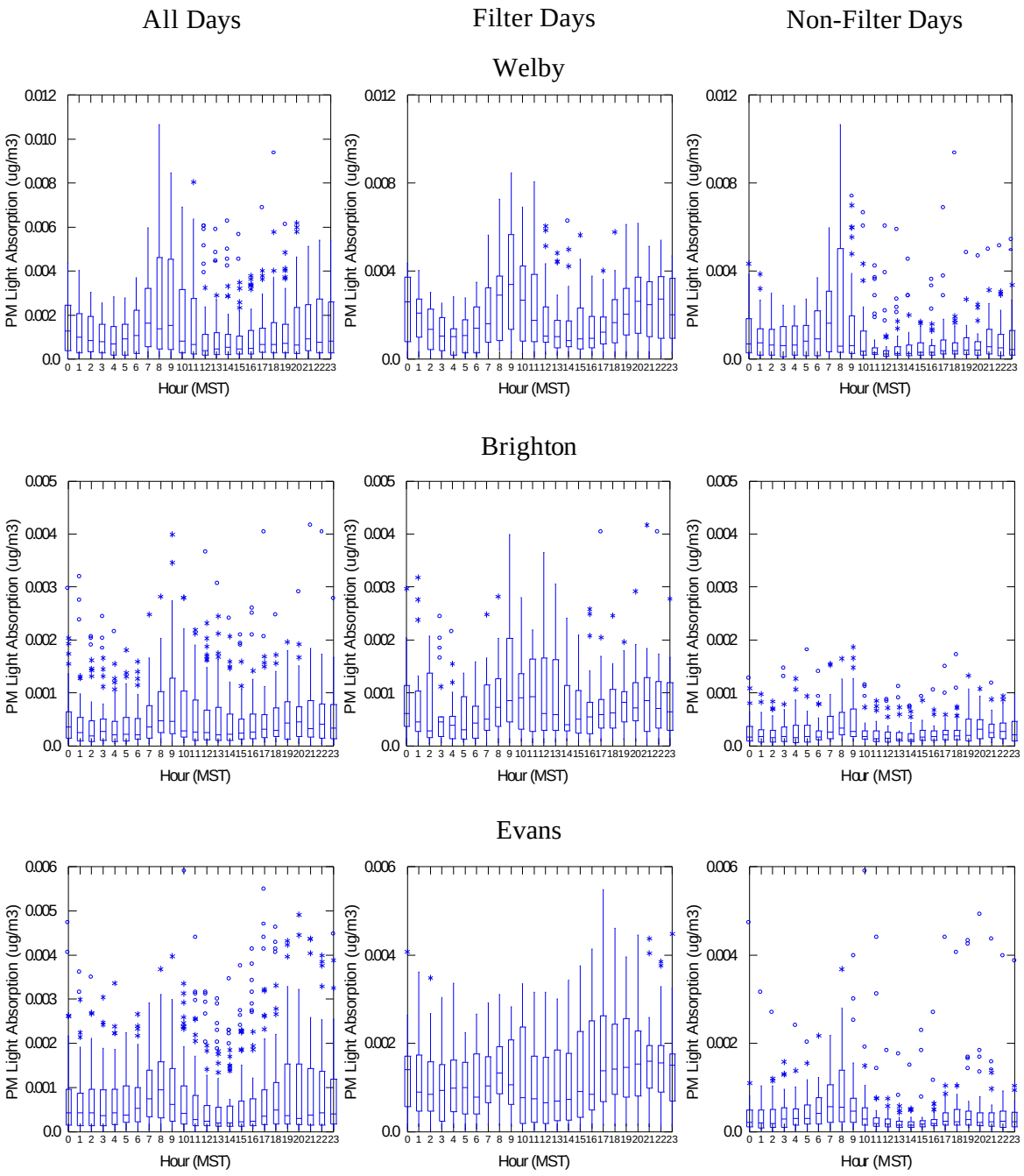

Figure 9.3-6. Diurnal variation of light absorption by particles at Welby, Brighton, and Evans on (a) all days in the winter field study, (b) days that filter samples were analyzed, and (c) days that filter samples were not analyzed.

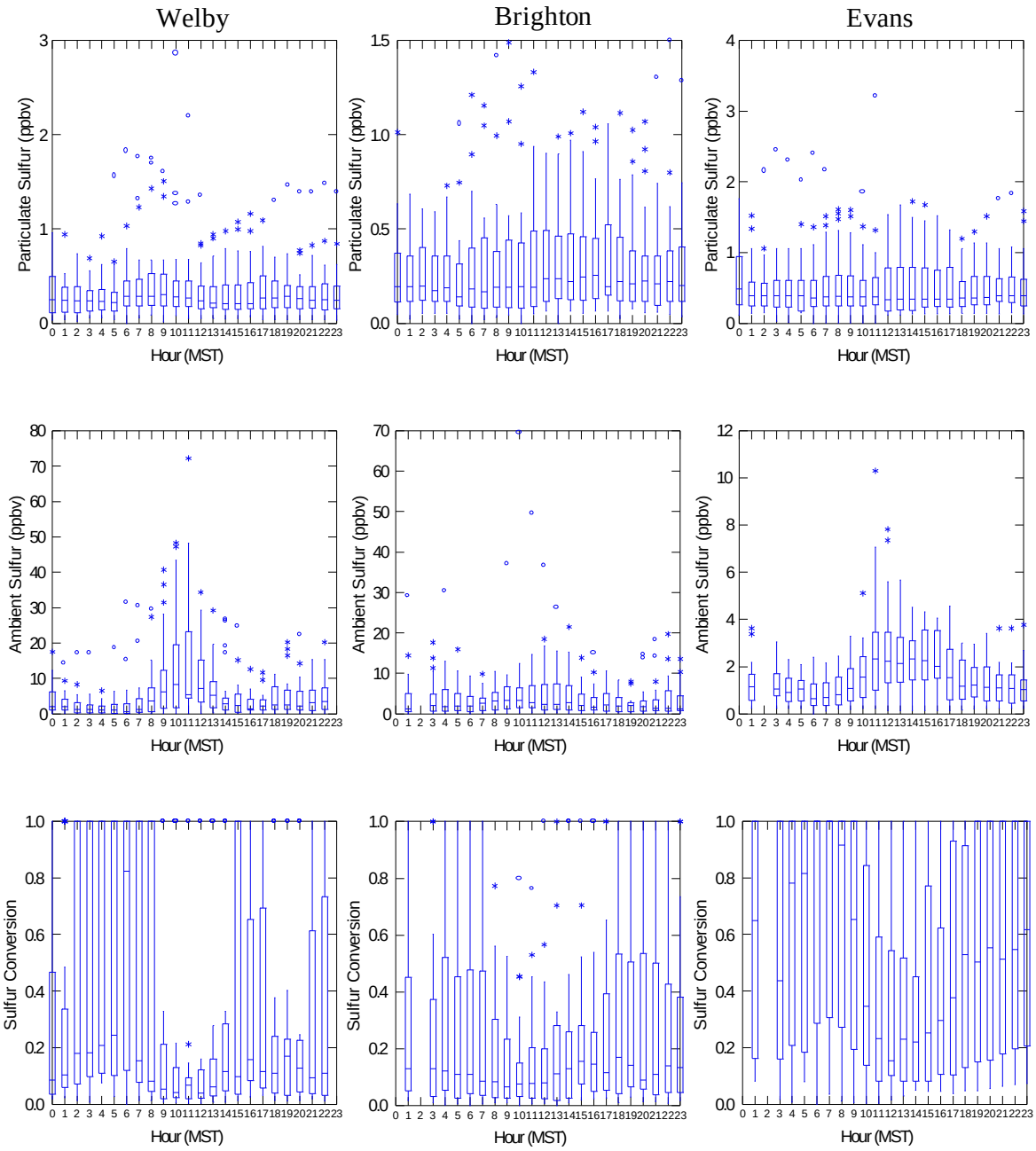

Figure 9.3-7. Diurnal variation of the hourly (a) particulate sulfur measured by the streaker sampler and PIXE analysis, (b) sum of particulate sulfur and SO_2 (labeled ambient sulfur), and (c) fraction of the ambient sulfur converted to particulate sulfur (labeled sulfur conversion) at Welby, Brighton, and Evans.

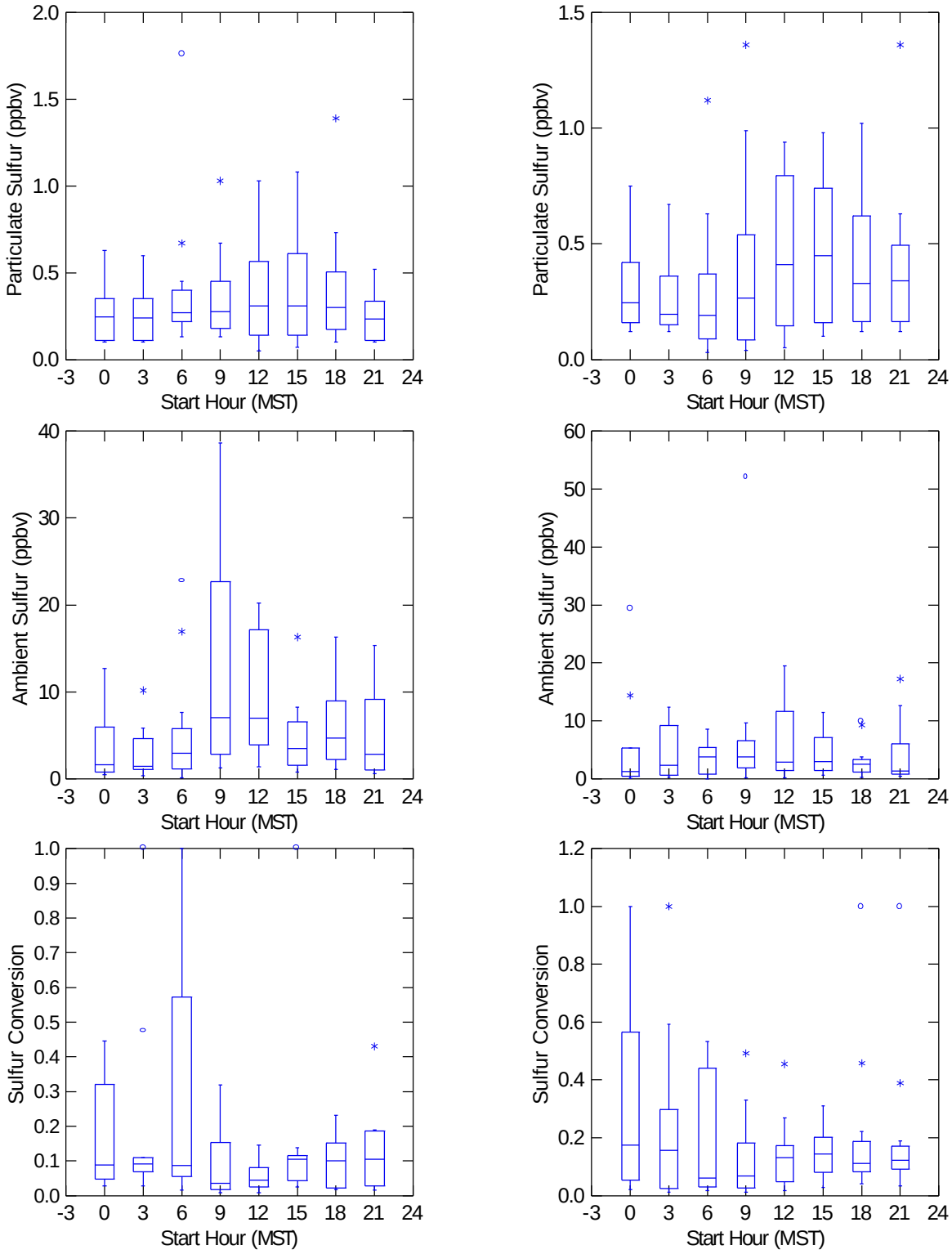

Figure 9.3-8. Diurnal variation of the 3-hour average of (a) particulate sulfur, (b) the sum of particulate sulfur and SO_2 (labeled ambient sulfur), and (c) the fraction of the ambient sulfur converted to particulate sulfur (labeled sulfur conversion) calculated from the hourly data at Welby and Brighton.

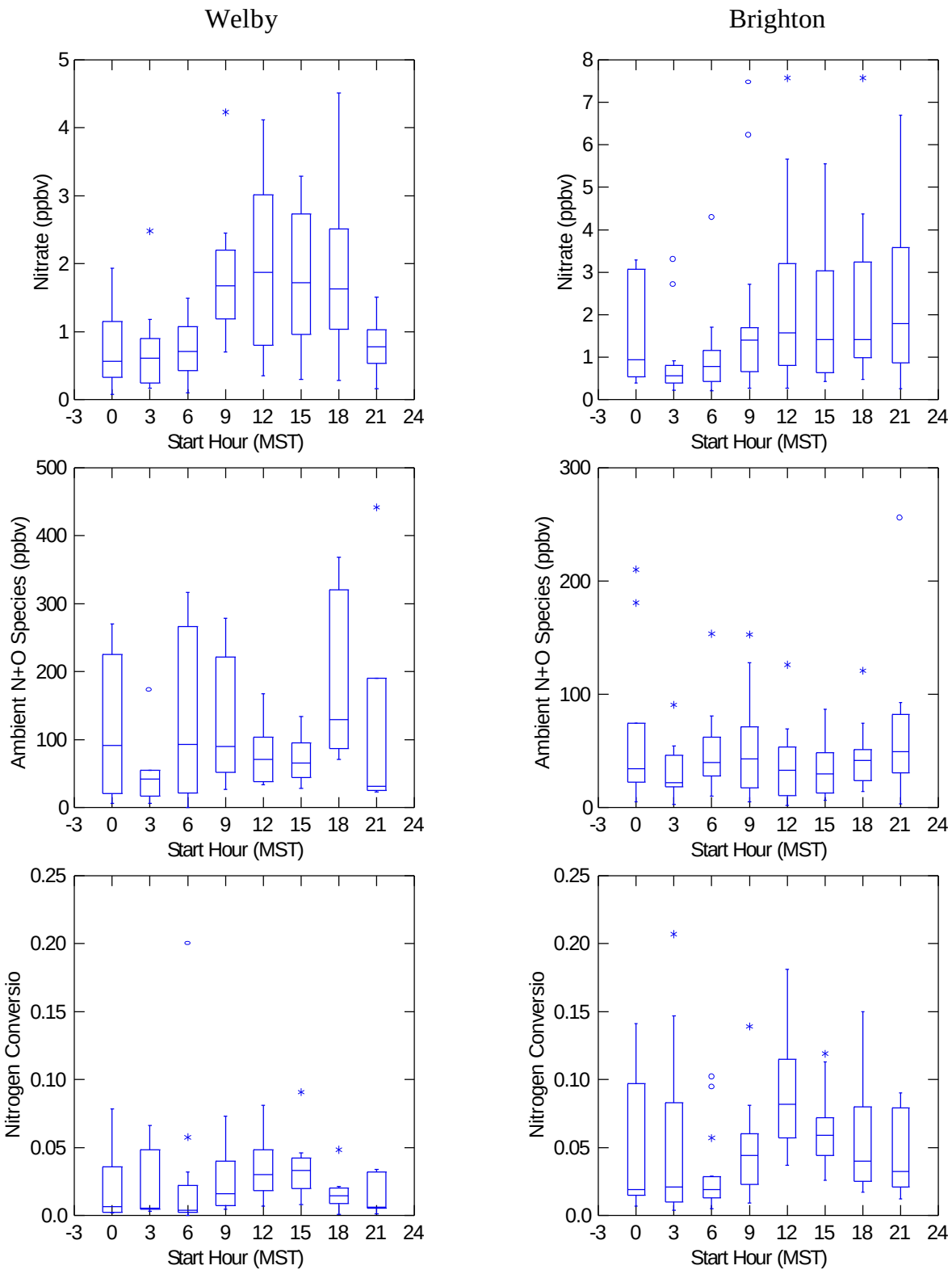

Figure 9.3-9. Diurnal variation of the 3-hour average (a) sum of nitric acid and particulate nitrate (labeled Nitrate), (b) sum of the NO_x, nitric acid, and particulate nitrate (labeled ambient N+O species), and (c) fraction of these species converted to particulate nitrate plus nitric acid (labeled nitrogen conversion) at Welby and Brighton.

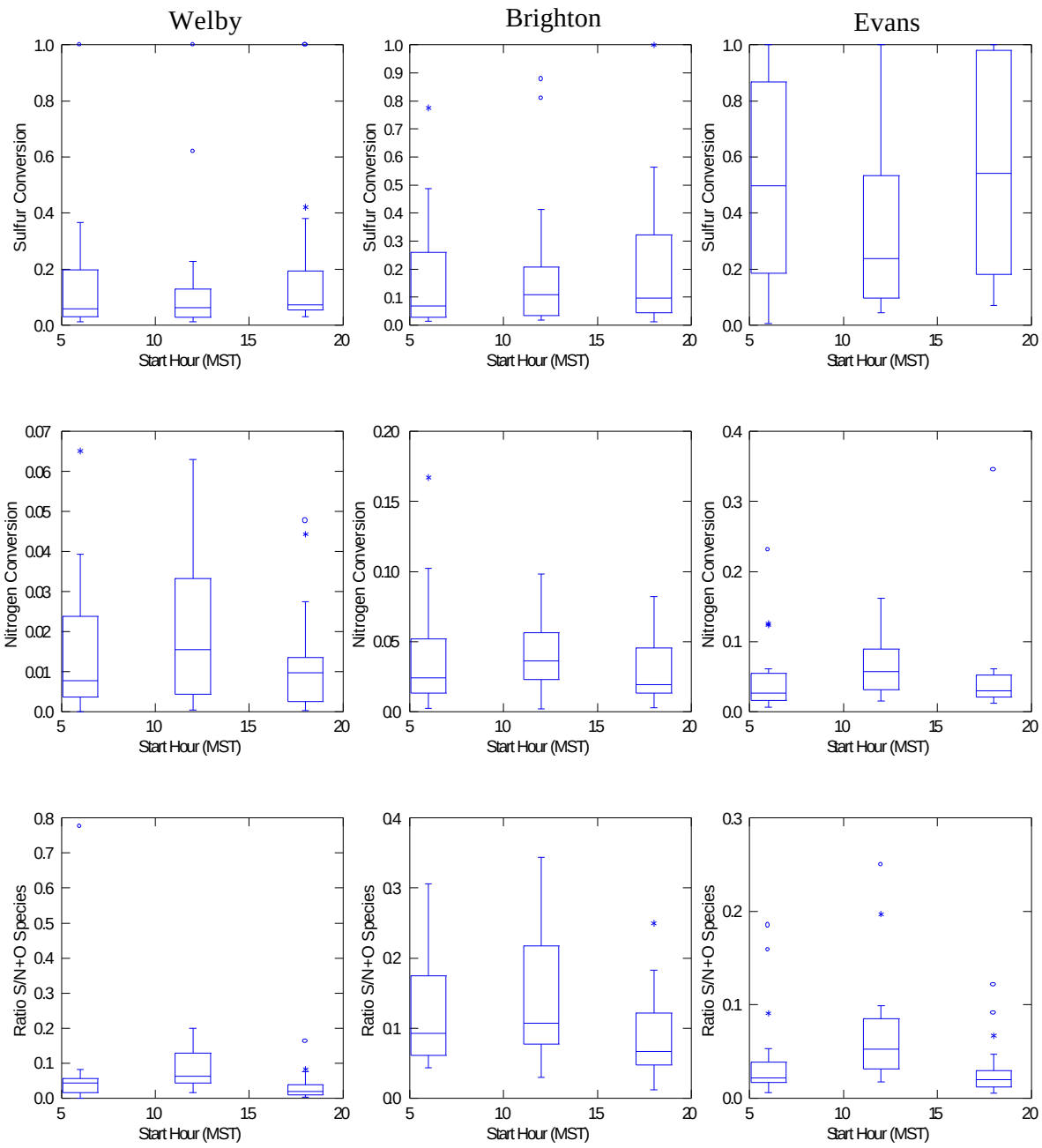

Figure 9.3-10. Diurnal variation of the sulfur conversion, nitrogen conversion, and the ratio of S to "N+O" species measured during the 6- and 12-hour filter sampling periods at Welby, Brighton, and Evans.

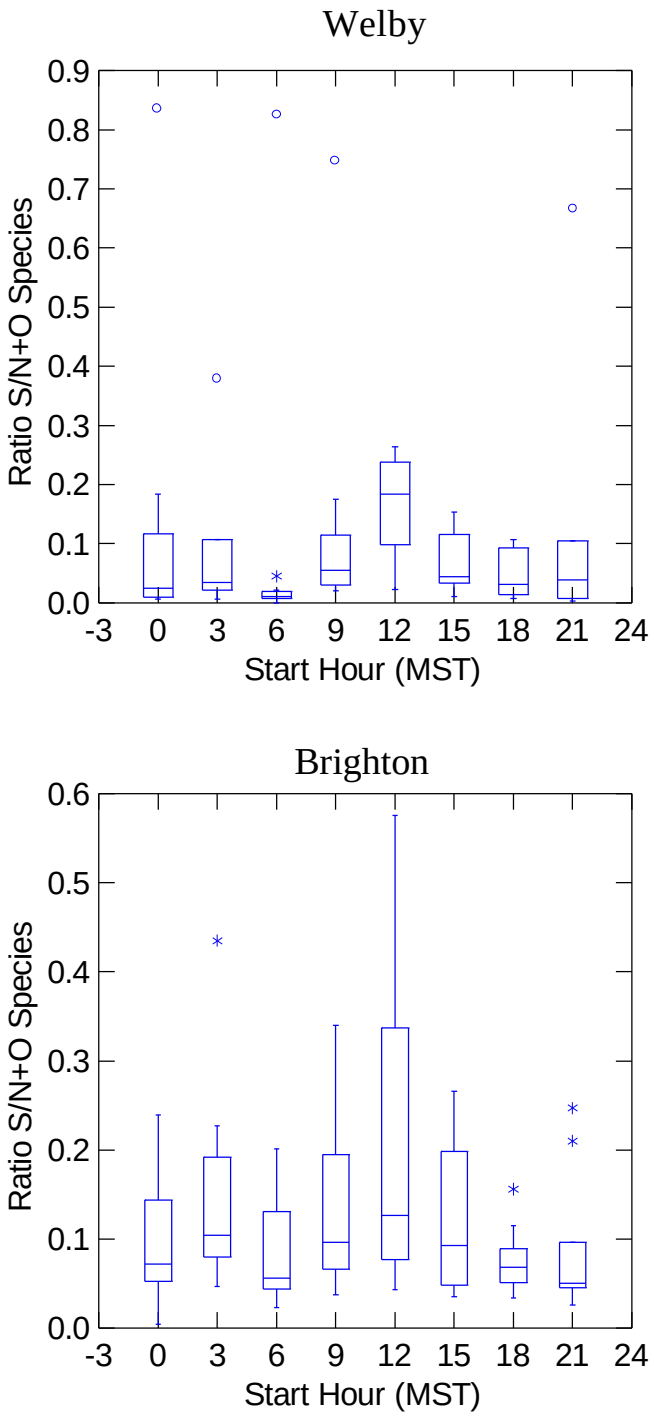

Figure 9.4-1. Diurnal variation of the 3-hour average ratio of measured sulfur species to N+O species. Measured sulfur species are SO_2 and particulate sulfur. Measured N+O species are NO_x, nitric acid, and particulate nitrate.

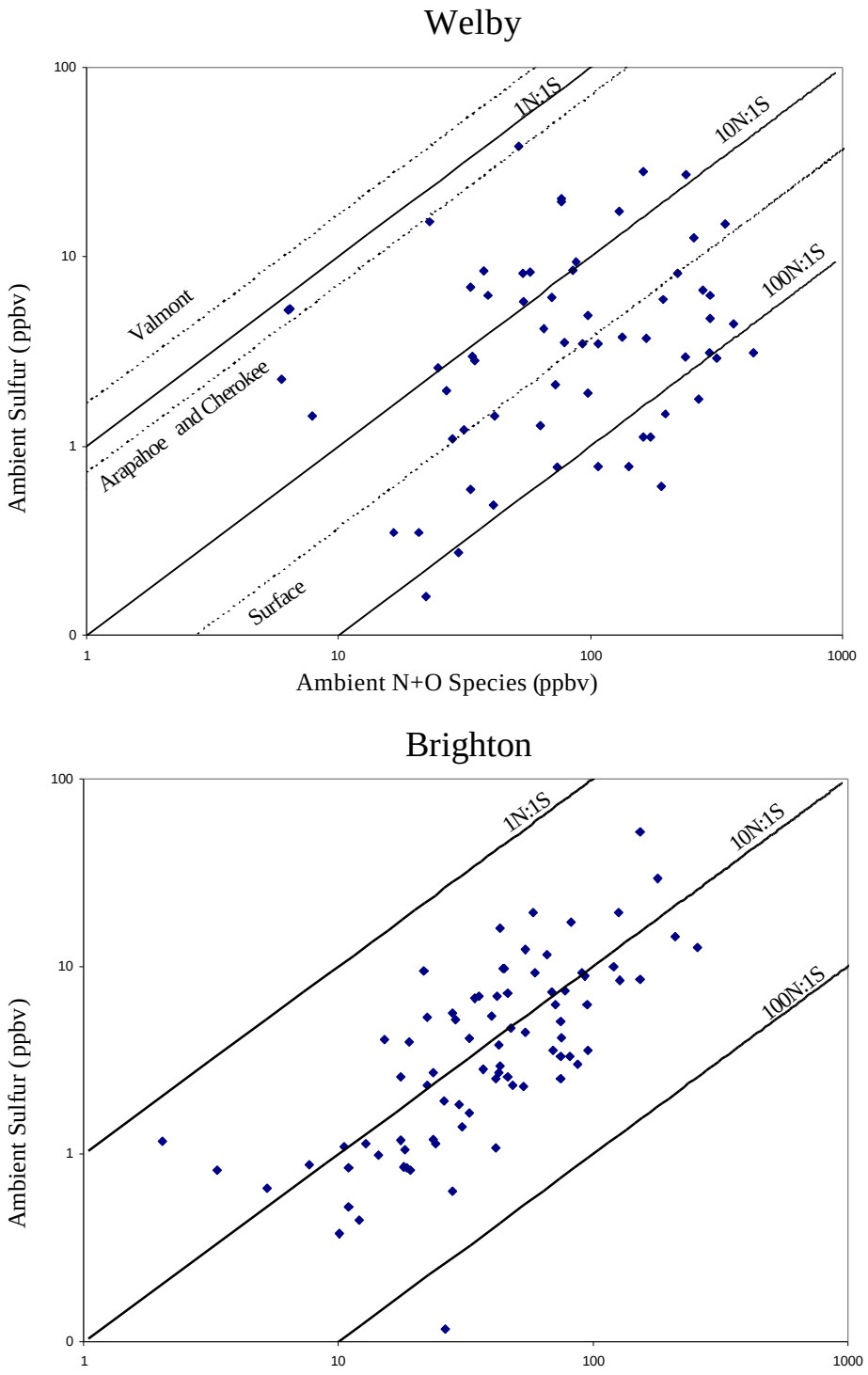

Figure 9.4-2. Ratios of ambient sulfur (SO_2 and particulate sulfur) to ambient N+O species (NO_x, nitric acid, and particulate nitrate) measured with 3-hour time resolution at Welby and Brighton.